8-1-2011

Selection of desiccant equipment at altitude

Kenneth Jacobs

SELECTION OF DESICCANT EQUIPMENT AT ALTITUDE

By

Kenneth Jacobs

A Thesis
Submitted to the Faculty of
Mississippi State University
in Partial Fulfillment of the Requirements
for the Degree of Master of Science
in Mechanical Engineering
in the Department of Mechanical Engineering

Mississippi State, Mississippi

August 2011

SELECTION OF DESICCANT EQUIPMENT AT ALTITUDE

By

Kenneth Jacobs

Approved:

Nelson Fumo
Assistant Research Professor
of Mechanical Engineering
(Major Professor)

Pedro Mago
Associate Professor
of Mechanical Engineering
(Committee Member)

Rogelio Luck
Profess of Mechanical Engineering
(Committee Member)

David Marcum
Professor of Mechanical Engineering
Graduate Coordinator in the
College of Mechanical Engineering

Sarah A. Rajala
Dean of the Bagley College of
Engineering

Name: Kenneth Jacobs

Date of Degree: August 6, 2011

Institution: Mississippi State University

Major Field: Mechanical Engineering

Major Professor: Dr. Nelson Fumo

Title of Study: SELECTION OF DESICCANT EQUIPMENT AT ALTITUDE

Pages in Study: 165

Candidate for Degree of Master of Science

ASHRAE Standard 139 provides parameters which are used in the desiccant industry to calculate the performance of a desiccant dehumidifier. This performance can be obtained from any manufacturer by means of performance curves or selection software. However, these performance parameters are generally rated at sea-level conditions.

Although some manufacturers provide a means for estimating the performance at altitude based on sea-level conditions, there is no set methodology that is accepted by all. The scope of this project involves investigating how the performance parameters are affected by altitude and develop a general methodology that can be applied to any desiccant wheel. Mississippi State University and the National Renewable Energy Laboratory both conducted tests and compared the results. It was found that, by keeping mass flow rate, inlet temperature, and inlet humidity ratio constant between sea-level and altitude, the pressure drop through the wheel was influenced the most by altitude.

Key words: altitude, desiccant, dehumidifier, performance

DEDICATION

I would like to dedicate this research to Jack “Baby J” Howard Martin, 2008-2011.

ACKNOWLEDGEMENTS

The author expresses his sincere gratitude to the many people whose guidance made it possible to achieve this much. Special thanks go to Swiss for being the biggest spoon of them all.

TABLE OF CONTENTS

LIST OF TABLES

LIST OF FIGURES

LIST OF NOMENCLATURE

English Symbols

A	Area, *[ft^2]*
C_1	Coefficient related to laminar flow through the channel
$C_{k,t}$	Coefficient related to entrance and exit losses
c_p	Specific heat of air, *[BTU/lbm °F]*
D_h	Hydraulic diameter, *[ft]*
f	Friction factor
F	Constant based on flow regime and channel geometry
G	Humidity ratio, *[Gr/lbm]*
h_{fg}	Specific enthalpy of evaporation, *[BTU/lbm]*
K	Entrance and exit losses
L	Depth of the wheel
$\dot{m}$	Mass flow rate, *[lbm/min]*
MRC	Moisture Removal Capacity, *[lbm/hr]*
N	Fan speed, *[rpm]*
NTU	Number of transfer units
p_{atm}	Atmospheric pressure, *[psi]*
p_{ws}	Saturation pressure of water vapor at a given temperature, *[psi]*

Q Regeneration heat energy, *[BTU/hr]*

$Q_{\Delta G}$ Heat produced by dehumidification, *[BTU/min]*

R_{da} Gas constant for dry air, 53.35 *[ft lbf/lbm °R]*

Re Reynolds number

RSHI Regeneration Specific Heat Input, *[BTU/hr]*

SCFM Standard volumetric flow rate, *[cfm]*

SFPM Standard velocity, *[fpm]*

T Absolute Temperature, *[°R]*

T_{db} Dry-bulb temperature, *[°F]*

T_{dp} Dew-point temperature, *[°F]*

T_{wb} Wet-bulb temperature, *[°F]*

V Face velocity, *[fpm]*

$\dot{V}$ Volumetric flow rate, *[cfm]*

w Humidity ratio, *[lbm/lbm]*

w_s Saturation humidity ratio, *[lbm/lbm]*

Z Altitude, *[ft]*

Greek Symbols

ΔGPP Grain depression, *[Gr/lbm]*

ΔP Pressure drop, *[in WC]*

Δp_w Change in partial pressure of water vapor, *[psi]*

μ Dynamic viscosity of air, *[lbm/s ft]*

ρ Density of moist air, *[lbm/ft^3]*

ϕ	Relative humidity

Subscripts

0	Sea-level
f	Fan
h	Heat
I	Inlet
m	Mass
O	Outlet
P	Process
R	Regeneration
z	Altitude

CHAPTER I

INTRODUCTION

Background

Integrated energy systems combine different technologies in order to provide energy services to a site. The electricity is provided by a power generation unit, which can be anything from an internal combustion engine to fuel cells [1]. Integrated energy systems take advantage of thermally activated technologies that use heat to power systems including heating, cooling, humidity control, and low grade electrical power. Benefits from using integrated energy systems include cost savings, increased efficiency, reduced carbon and other pollutant emissions, and improved indoor air quality [1]. The thermally activated technologies are essential to the energy and cost saving benefits of an integrated energy system by reducing seasonal peak demands [2].

One type of thermally activated technology is a desiccant dehumidification system. Desiccant dehumidification systems are composed of two key steps: the dehumidification of the process air, and the regeneration of the desiccant [3, Chapter 23]. According to a study by Houghton, *et al*. [4], desiccant systems can reduce the total residential power demand by more than 25% in areas with high humidity. Another way to take advantage of the efficiency of desiccant cooling is with a hybrid cooling system, which is a vapor compression system combined with a desiccant system. Howell and

Peterson [5] estimate that this hybrid system can reduce power demand by up to 25%, and also reduce the evaporation and condensation area up to 34%. It should be noted that, although desiccant systems generally provide higher efficiencies than vapor compression system, there can be some constraints on the working range for the desiccant systems. Panaras, *et al*. [6] have performed a methodology of how to define these achievable working conditions based on temperature and relative humidity.

A desiccant dehumidifier can either be composed of a solid or a liquid desiccant. Liquid desiccants work by absorption, which changes the state of the desiccant as it absorbs moisture. A solid desiccant uses the process of adsorption, which does not alter the chemical state of the desiccant, but merely adds additional mass to the desiccant from the water vapor that is adsorbed [7, Chapter 32].

Desiccant dehumidification can be used for a wide variety of applications, including breweries, candy manufacturing, corrosion control, electronics manufacturing, food storage and packaging, hospitals, ice rinks, libraries, and residences. These applications generally involve thermal comfort, but also include places where moisture in the air can lead to safety and efficiency issues [8]. The correct selection of equipment is essential to the proper dehumidification of the specific location. Some companies provide selection software to aide customers. Other companies provide technical resources on different scenarios where dehumidification may be necessary, with examples for each scenario on how to size the necessary equipment. All companies will provide the ratings of their equipment based on specific design conditions.

Hamed, *et al.* [9] have performed experiments on a liquid desiccant system, examining how different parameters affect the performance. These parameters include process and regeneration air velocity, rotational speed of the desiccant wheel, regeneration air temperature, process and regeneration air relative humidity, bed length, and regeneration air temperature. Out of these parameters, only some are affected by altitude due to the variation in density and humidity ratio. Pesarant and Heiden [10] have performed simulations testing the affect of altitude on a desiccant cooling system coupled with a direct/indirect evaporative cooler. They found that the performance of the desiccant dehumidifier decreased with decreasing ambient pressure, but the performance of the evaporative cooler increased with decreasing ambient pressure.

The National Renewable Energy Laboratory has performed limited tests to investigate the effect of altitude on the performance of a desiccant system. The tests concluded that the NTU's and inlet humidity ratios were kept constant between altitude and sea-level, the difference in performance between the two locations will be negligible. However, these tests were performed using mechanical means to set the pressures. Therefore, empirical data at two actual altitudes is required in order to fully understand how altitude affects the moisture capacity of the desiccant [11].

Objectives of the Project

The objective of this study is to develop a general methodology for all to use regarding how to select a desiccant dehumidifier for use at altitude. The project consists of different tasks which lead to the testing of a desiccant dehumidifier at set conditions at two different locations: Mississippi State University, Mississippi State, Mississippi

(elevation 330 feet) and the National Renewable Energy Laboratory, Golden, Colorado (elevation 5,850 feet).

The testing conditions were decided based on information gathered from manufactures as to how they have handled the selection process at altitude in the past, as well as information regarding the concept behind the adsorption process of a desiccant. By analyzing the results of the tests, the methodology was developed. This methodology allows design engineers and manufacturers to take a desiccant dehumidifier with a known rating at standard conditions, select a location at altitude, and use the methodology to acquire the predicted performance at that altitude.

When rating and selecting a desiccant dehumidifier, there are four figures of merit that should be examined. These are:

- Moisture Removal Capacity
- Regeneration Specific Heat Input
- Pressure Drop through the wheel
- Process air stream temperature rise

This project will examine how these four characteristics are affected by a change in altitude.

Usefulness of the Project

The task of acquiring manufacturer information as to how selection at altitude was handled in the past showed how useful the end result of the project will be. The standard industry practice in the past has been to simply add a safety factor to the sea-level performance based on the difference in air density between altitude and sea-level.

However, this can lead to over sizing of the equipment. ASHRAE estimates that more than $5 million worth of U.S. desiccant systems selected for use over 2000 feet are oversized, representing $15 million worldwide [11]. It was found that of the few manufacturers that have selection software available to the public, only two incorporated a change in altitude. Upon contacting the manufactures requesting information on their selection at altitude, two replied with software not available to the public. However, these four softwares differ in how altitude is considered, and there is not a general agreement as to which method is favorable, and most laboratories do not have the facilities to vary ambient pressure, leaving the validation of the different methodologies incomplete [12]. For example, Rotor Source considers altitude only by changing the pressure drop through the wheel, where Desiccant Rotors International incorporates a more in depth mathematical model to change the heat and mass transfer effects of the desiccant process. Therefore, the end result of this project will try to be a common tool that can be adopted by the industry in order to standardize the prediction of performance of solid desiccant systems at altitude.

CHAPTER II

SOLID DESICCANT DEHUMIDIFIER

Desiccants

A sorbent is a material that has the capacity to absorb gases or liquids. A desiccant is a type of sorbent that has a particular attraction to water. This attraction is quantified by the ASHRAE Handbook – Fundamentals, stating that "a commercial desiccant takes up between 10 and 1100% of its dry weight in water vapor" [7, Chapter 32]. This characteristic makes desiccants a prime candidate for use in the dehumidification of air.

A desiccant absorbs moisture due to the difference in vapor pressure between the desiccant and the air. If the vapor pressure at the surface of the desiccant is lower than that of the surrounding air, the desiccant will absorb moisture. If the vapor pressure at the surface of the desiccant is higher than that of the surrounding air, the desiccant will expel moisture [7, Chapter 32]. When expressed in terms of relative humidity of the surrounding air, it has been shown that the adsorption capacity of the desiccant increases with increasing relative humidity [10, 13].

The desiccant cycle is explained in Figure 2.1. Starting at State 1, the desiccant has a lower equilibrium vapor pressure than that of the surrounding air. As the desiccant absorbs moisture its equilibrium vapor pressure increases. It should be noted that vapor

pressure is a function of only temperature. Since energy is required for the condensation of water vapor from the air to the desiccant, the temperature of the desiccant rises.

This rise in temperature causes the equilibrium vapor pressure of the desiccant to also rise, leading to State 2. Once the equilibrium vapor pressure of the desiccant reaches the same vapor pressure of the surrounding air the desiccant and air are in equilibrium and the sorption process stops. The desiccant must then be heated so that the equilibrium vapor pressure of the desiccant is now higher than that of the surrounding air. This causes the sorption process to work in reverse, evaporating the condensed water from the desiccant back into the air. The desiccant is cooled by the reverse effects of the latent heat of evaporation, and the desiccant cycle repeats. This cycle is explained in more depth in the next section, Desiccant Dehumidification.

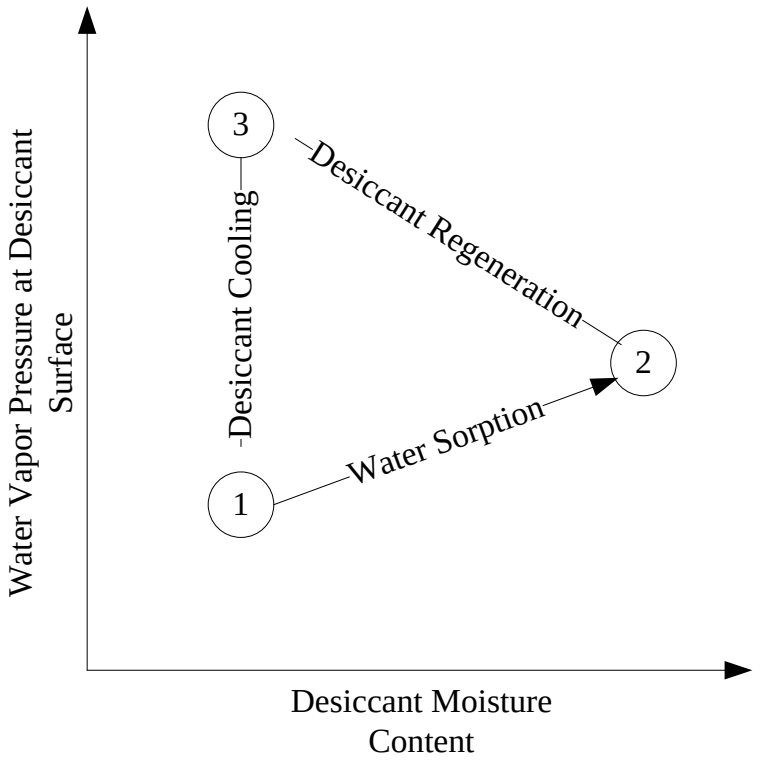

Figure 2.1

Desiccant Cycle as a Function of Desiccant Moisture Content and Water Vapor Pressure at Surface.

Desiccant Dehumidification

A desiccant dehumidifier is split into two air streams: process and regeneration. The process air stream is the stream that is being dehumidified. The regeneration air stream utilizes some sort of heating device (solar energy, waste heat, natural gas, electric heater, etc.) to regenerate the desiccant so that continuous operation can occur. Figure 2.2 shows a schematic of a desiccant rotary wheel utilizing a 75-25 (process-regeneration) split.

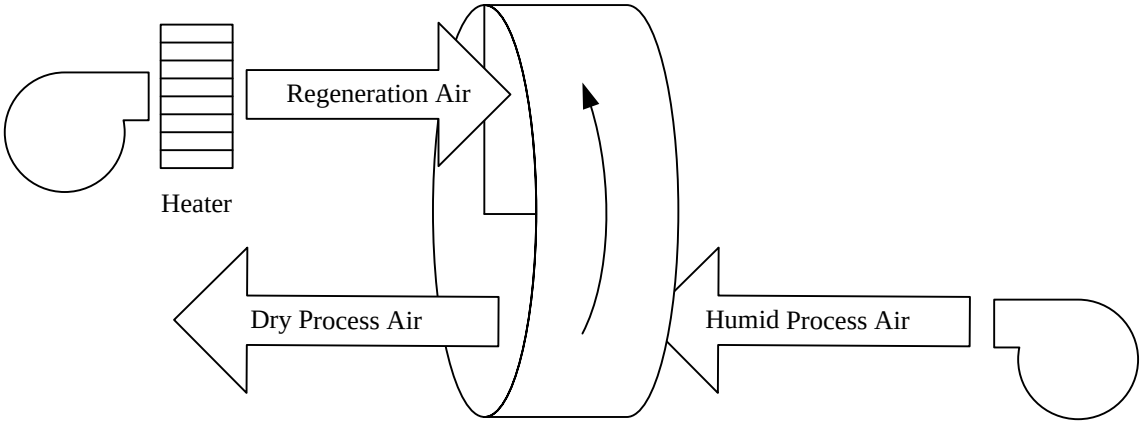

Figure 2.2

Schematic of a Solid Desiccant Dehumidifier with a 75-25 Wheel Split.

Figures of Merit

When rating a dehumidifier, the main figure of merit is the moisture removal capacity (MRC). MRC for standard conditions is defined as the rate at which moisture is removed from the process air stream, and is defined in Equation (2.1) [14]:

$$MRC = [Scfm_P(60 \cdot 0.075)(G_i - G_o)]/7000 \quad (2.1)$$

where:

$Scfm_P$ = Standard volumetric flow rate of process air, *[cfm]*

60 = Conversion from minutes to hours

0.075 = Standard density of air, *[lbm/ft^3]*

G_i = Inlet humidity ratio, *[Gr/lbm]*

G_o = Outlet humidity ratio, *[Gr/lbm]*

7000 = Conversion from Gr/lbm to lbm/lbm

Another figure of merit is the regeneration specific heat input (RSHI) [14]. The RSHI shows the amount of heat energy applied to regeneration per mass of moisture removed from the process air stream, and is defined in Equation (2.2):

$$RSHI = \frac{Q}{MRC} \tag{2.2}$$

where:

Q = Regeneration heat energy, *[BTU/hr]*

CHAPTER III

LITERATURE REVIEW

After an extensive literature search in the field of desiccant dehumidification at altitude, very few studies have been performed empirically [10, 15], while a handful of models have been numerically developed [12, 16, 17]. This Chapter examines these different studies, while referencing other relevant research which examines different key design features that can be extrapolated to altitude.

Solid Desiccant Dehumidifiers at Altitude

Recalling that Equations (2.1) and (2.2) are both related to performance at standard conditions, the question arises as to what happens to these figures when the desiccant dehumidification unit in question is taken to a higher altitude. According to industry standards, a desiccant system is selected based on the process inlet dry-bulb temperature and humidity ratio and the face velocity through the wheel [3, Chapter 23]. By examining Equation (2.1) it can be seen that MRC is a function of two of these design parameters: face velocity and inlet humidity ratio.

Pesaran and Heiden [10] state that the performance of a desiccant dehumidifier related to the number of heat transfer units (NTU_h) and the number of mass transfer units (NTU_m). NTU_h is a function of geometric properties, mass flow rate, Nusselt number, and the specific heat of air. For a specific unit the geometric properties will remain

constant with altitude. The change in specific heat of air can be considered negligible below 10,000 feet [10, 18], and the Nusselt number, which is a function of the heat transfer coefficient, is independent of density for fully developed laminar flow, and therefore constant with altitude [10]. Therefore, in order to keep NTU_h constant, the mass flow rate must also remain a constant. Pesaran and Heiden also conclude that, similar to the change in viscosity due to altitude, NTU_m is not affected by pressure.

Pesaran and Heiden [10] also state: "The moisture capacity [of a desiccant] depends on [total] pressure at a fixed humidity ratio." Their study shows that the moisture capacity of a desiccant is inversely proportional to the total pressure, meaning that, for a fixed humidity ratio, the moisture capacity of the desiccant decreases with increasing altitude.

This statement is reflected in models by Harshe, *et al.* [17], which show that the water content of a desiccant is a function of wheel speed, geometric properties of the desiccant, and air humidity ratio (which all stay constant with altitude), as well as a mass transfer coefficient and the equilibrium humidity at the surface of the desiccant. If the mass transfer coefficient decreases with altitude, the moisture content of the desiccant also declines. The equilibrium humidity at the surface of the desiccant has been discussed as being a function of humidity ratio, and therefore declines with altitude as well. This shows that, for a given mass flow rate and inlet humidity ratio, the outlet humidity ratio will increase with altitude, decreasing the grain depression and in turn decreasing the MRC.

This decrease in the moisture capacity is also shown in numerical models by Ruivo, *et al.* [16], which states that for a constant inlet temperature and humidity ratio, the pressure will decrease the relative humidity of the process and regeneration airflows. By examining a sorption isotherm for any arbitrary solid desiccant, it can be seen that the adsorbed water content of the desiccant will decrease with decreasing relative humidity [10, 12], decreasing the mass transfer rate.

By applying these concepts to the two figures of merit previously discussed (MRC, RSHI) it can be seen that for a fixed inlet temperature, inlet humidity ratio, and mass flow rate, the MRC will decline with altitude due to the change in relative humidity (vapor pressure). The RSHI will change inversely proportional to the MRC due to the definition of RSHI shown in Equation (2.2). The energy used for regeneration heat is assumed to remain constant due to the nature of the selection process, which assumes constant inlet temperatures and mass flow rates. Therefore, with the change in the specific heat of air being negligible below 10,000 feet, and the method of regeneration heating being the same, the energy consumption of the regeneration will not change.

However, research by Slayzak, *et al.* [15] shows that the MRC will remain a constant at different atmospheric pressures when using constant inlet humidity ratios and mass flow rates. This discrepancy between the previously discussed studies could be due to the nature of the experiment, which varied the pressure in the test loop by keeping it sealed from the atmosphere and manually altering the pressure.

Another important design parameter that can be affected by altitude is the pressure drop through the wheel. The fan laws state that for a constant mass flow rate

and wheel face area, the face velocity of the air must increase with decreasing air density [19]. Harshe, *et al.* [17] present a general equation for pressure drop in their mathematical models, shown in Equation (3.1):

$$\Delta P = \frac{2 f \rho V^2 L}{D_h} + K \frac{1}{2} \rho V^2 \tag{3.1}$$

where:

ΔP = Pressure drop through the wheel

f = Friction factor

V = Face velocity

D_h = Hydraulic diameter

L = Depth of the wheel

K = Entrance and exit losses

This equation is similar in form to the pressure drop equation used in various other applications relating to the flow of air through a channel [10, 15, 20, 21], differing in the fact that some studies neglect entrance and exit losses (variable *K* in Equation (3.1)). Also, experimental data by Tretiak and Abdallah [22] show that pressure drop through a packed bed is a second order polynomial as a function of Reynolds number.

The friction factor can be calculated using Equation (3.2) [17]. Simulations by Niu and Zhang [23] show that F depends on geometric properties of the channel. Reynolds number is easily calculated using Equation (3.3) [7, Chapter 3].

$$f = \frac{F}{Re} \tag{3.2}$$

where:

F = Constant based on flow regime and channel geometry

Re = Reynolds number

$$Re = \frac{\rho V D_h}{\mu} = \frac{\dot{m} D_h}{\mu A} \tag{3.3}$$

where:

μ = Dynamic viscosity

Belady [21] points out that many of the variables in Equation (3.1) will remain constant with altitude (e.g. terms related to geometry). Therefore, these variables can be combined into constant coefficients if the effect of altitude is to be evaluated, allowing for easy evaluation of how altitude affects the pressure drop.

Industry Practices Incorporating Altitude

Many desiccant dehumidifier companies include general selection process and/or software available to the public. Of these companies, NovelAire [24] and RotorSource [25] are the only two that take altitude into consideration. Investigation of the NovelAire software found that, with increasing altitude, the pressure drops and process outlet humidity ratio increases and the process outlet temperature decreases. Investigation of the RotorSource software shows that the pressure drop is the only variable that is altered with a change in altitude.

Once contacted two other companies, Munters [26] and Desiccant Rotors International [27], gave insight into their preferred method. It was explained that Munters assumes "the effect of elevation on the moisture removal of the desiccant wheels…is minimal as long as you are working in humidity units of grains per pound of dry air" [28]. It was also explained that Munters has proprietary software which allows for the input of different barometric pressures. With this information, it internally

converts the standard flow rate to the actual flow rate (keeping the mass flow rate constant), then uses the actual flow rate for calculations. It was seen in the software that, with increasing altitude, the pressure drops and process outlet humidity ratio increases, and the process outlet temperature decreases, similar to that seen in the NovelAire software.

By investigating the DRI software, and also having some knowledge of the numerical model used to create it [17], it was found that this software accounts for altitude in different ways. This is done by giving the user the option to choose a constant mass or constant velocity process. The method investigated here was the constant mass, as it is the industry standard being evaluated in this research. It was found that the standard velocity was converted to actual velocity, which accounts for the increase in pressure drops.

CHAPTER IV

UNCERTAINTY ANALYSIS

The uncertainty associated with the measured variables has been considered through the accuracy of the measurement systems. This is particularly the case for the inlet conditions. However, for other parameters of interest, such as the pressure drop through the wheel (process and regeneration) and the process outlet temperature, additional analysis is required because their results are a function of other variables. This is also the case for the most important variable to be considered, the moisture removal capacity, which is computed as a function of other variables. For this analysis the Taylor Series Method for propagation of uncertainties was applied to obtain the equations describing how the uncertainties of the independent variables define the uncertainties of the resulting variables. In this Chapter the equations obtained from the application of the Taylor Series Method are presented and the results to this analysis for the actual data acquired from the tests can be found in Chapter VI. The mathematical solution of the uncertainty analysis was made in Mathcad code, which is presented in Appendix A.

Overview of the Taylor Series Method

The method used for the uncertainty analysis is the Taylor Series Method for propagation of uncertainties [29, 30, 31]. For example, the data reduction equation for an

experimental result Y is shown in Equation (4.1), where Y is a function of n measured variables X_n:

$$Y = Y(X_1, X_2, \dots, X_n) \tag{4.1}$$

Using the Taylor Series Method, the uncertainty in Y is given by Equation (4.2):

$$U_Y^2 = \left(\frac{\partial Y}{\partial X_1} U_{X_1}\right)^2 + \left(\frac{\partial Y}{\partial X_2} U_{X_2}\right)^2 + \cdots + \left(\frac{\partial Y}{\partial X_n} U_{X_n}\right)^2 \tag{4.2}$$

where:

U_Y = uncertainty in Y

U_{X_n} = Uncertainties in the measured variables X_n

Uncertainty in MRC

The main figure of merit used to determine the performance of a desiccant dehumidifier is the MRC. From Equation (3.1), the MRC can be rewritten as Equation (4.3):

$$MRC = \frac{60}{7000} \dot{m}\, \Delta GPP_P \tag{4.3}$$

where:

$\dot{m}$ = Mass flow rate of the process air stream, *[lbm/min]*

ΔGPP_P = Grain depression through the process side of the desiccant wheel, defined as $G_{PI} - G_{PO}$, *[Gr/lbm]*

G_{PI} = Humidity ratio at the process inlet, *[Gr/lbm]*

G_{PO} = Humidity ratio at the process outlet, *[Gr/lbm]*

60 = Conversion between minutes and hours, *[min/hr]*

7000 = Conversion between grains and pounds, *[Gr/lbm]*

Using Equation (4.3) along with the Taylor Series Method of uncertainty analysis, Equation (4.4) can be used to find the uncertainty for the MRC.

$$U_{MRC} = \left[\left(\frac{\partial MRC}{\partial \dot{m}} U_{\dot{m}}\right)^2 + \left(\frac{\partial MRC}{\partial \Delta \mathrm{GPP}} U_{\Delta \mathrm{GPP}}\right)^2\right]^{1/2} \tag{4.4}$$

where:

U_{MRC} = Uncertainty for MRC

$U_{\dot{m}}$ = Uncertainty for mass flow rate

$U_{\Delta GPP}$ = Uncertainty for grain depression

Methods for Calculating Humidity Ratio

The first variable in Equation (4.3) that will be analyzed is the humidity ratio. There are three accepted methods for calculating the humidity ratio, each using different measured variables [29, 30]. They are:

- Dry-bulb temperature and relative humidity
- Dry-bulb temperature and dew-point temperature
- Dry-bulb temperature and wet-bulb temperature

The following sections outline how the humidity ratio can be calculated using these three methods.

Relative Humidity Method

This method uses the relative humidity, atmospheric pressure, and saturation vapor pressure (function of dry-bulb temperature) to calculate the humidity ratio using Equation (4.5) [7, Chapter 1]:

$$w = 0.621945 \frac{\phi\, p_{ws}}{p_{atm} - \phi\, p_{ws}} \quad (4.5)$$

where:

w = Humidity ratio, *[lbm/lbm]*

ϕ = Relative humidity

p_{ws} = Saturation pressure of water vapor at a given temperature, *[psi]*

p_{atm} = Atmospheric pressure, *[psi]*

Applying the Taylor Series Method to Equation (4.5), the uncertainty in humidity ratio for the relative humidity method can be estimated as:

$$U_w = \left[\left(\frac{\partial w}{\partial \phi} U_\phi\right)^2 + \left(\frac{\partial w}{\partial p_{ws}} U_{p_{ws}}\right)^2 + \left(\frac{\partial w}{\partial p_{atm}} U_{p_{atm}}\right)^2\right]^{1/2} \quad (4.6)$$

where:

U_w = Uncertainty in humidity ratio

U_ϕ = Uncertainty in relative humidity

$U_{p_{ws}}$ = Uncertainty in saturation pressure of water vapor

$U_{p_{atm}}$ = Uncertainty in atmospheric pressure

Wet-Bulb Temperature Method

This method takes humidity ratio as a function of dry- and wet-bulb temperatures, and the saturation humidity ratio. The saturation humidity ratio is calculated using Equation (4.5), taking $\phi = 1$ and the saturation pressure of water vapor using the wet-bulb temperature. This can be seen in Equation (4.7) [7, Chapter 1]:

$$w = \frac{(1093 - 0.556\, T_{wb}) w_s - 0.240(T_{db} - T_{wb})}{1093 + 0.444 T_{db} - T_{wb}} \quad (4.7)$$

where:

T_{wb} = Wet-bulb temperature, *[°F]*

w_s = Saturation humidity ratio, *[lbm/lbm]*

T_{db} = Dry-bulb temperature, *[°F]*

Applying the Taylor Series Method to Equation (4.7), the uncertainty for humidity ratio for the wet-bulb temperature method can be estimated as:

$$U_w = \left[\left(\frac{\partial w}{\partial T_{wb}} U_{T_{wb}}\right)^2 + \left(\frac{\partial w}{\partial w_s} U_{w_s}\right)^2 + \left(\frac{\partial w}{\partial T_{db}} U_{T_{db}}\right)^2\right]^{1/2} \quad (4.8)$$

where:

$U_{T_{wb}}$ = Uncertainty in wet-bulb temperature

U_{w_s} = Uncertainty in saturation humidity ratio

$U_{T_{db}}$ = Uncertainty in dry-bulb temperature

Dew-Point Temperature Method

This method uses the same equations as the wet-bulb temperature method, but replaces all measured temperatures (dry- and wet-bulb) with the dew-point temperature.

Equations Used to Calculate MRC

From the three methods previously outlined, MSU took the relative humidity approach while NREL took the dew-point temperature approach. The following equations show how the measured variables are used to calculate the dependent variables needed to find the MRC.

For both methods the saturation pressure of water vapor must be found using Equation (4.9) [7, Chapter 1]:

$$p_{ws} = \exp\left(C_1/T + C_2T + C_3T + C_4T^2 + C_5T^3 + C_6T^4 + C_7\ln\left(T\right)\right) \quad (4.9)$$

where:

C_1 = −1.021 416 5 E+04

C_2 = −4.893 242 8 E+00

C_3 = −5.376 579 4 E−03

C_4 = 1.920 237 7 E−07

C_5 = 3.557 583 2 E−10

C_6 = −9.034 468 8 E−14

C_7 = 4.163 501 9 E+00

T = Absolute temperature, *[°R]*

Next the humidity ratio is calculated using Equation (4.5) or Equation (4.7), depending on the method used. With the atmospheric pressure, dry-bulb temperature, and humidity ratio known, the density of the moist air can now be calculated. This is done using Equation (4.10) [7, Chapter 1]:

$$\rho = \frac{p_{atm}}{R_{da}\,T}\frac{1+w}{1+1.608\,w} \quad (4.10)$$

where:

ρ = Density of moist air, *[lbm/ft^3]*

R_{da} = Gas constant for dry air, 53.35 *[ft lbf/lbm°R]*

Applying the Taylor Series Method to Equation (4.10), the uncertainty for density can be estimated as:

$$U_\rho = \left[\left(\frac{\partial w}{\partial p_{atm}} U_{p_{atm}}\right)^2 + \left(\frac{\partial w}{\partial w} U_w\right)^2 + \left(\frac{\partial w}{\partial T} U_T\right)^2\right]^{1/2} \quad (4.11)$$

where:

U_ρ = Uncertainty in density

U_T = Uncertainty in absolute temperature

It should be noted that it is assumed there is no uncertainty involved with the gas constant.

By measuring the volumetric flow rate, the mass flow rate can be calculated using the previously calculated density. The mass flow rate is found using Equation (4.12):

$$\dot{m} = \rho \dot{V} \quad (4.12)$$

where:

$\dot{m}$ = Mass flow rate, *[lbm/min]*

$\dot{V}$ = Volumetric flow rate, *[cfm]*

The uncertainty for the mass flow rate is estimated using the Taylor Series Method as:

$$U_{\dot{m}} = \left[\left(\frac{\partial w}{\partial \rho} U_\rho\right)^2 + \left(\frac{\partial w}{\partial \dot{V}} U_{\dot{V}}\right)^2\right]^{1/2} \quad (4.13)$$

where:

$U_{\dot{V}}$ = Uncertainty in volumetric flow rate

Once the mass flow rate and the humidity ratios are known, Equation (4.3) can be used to calculate the MRC. Using the instrument accuracies for each location, the Taylor Series Method can be applied to each of these equations to find the uncertainty involved with the MRC in Equation (4.4).

Uncertainty in Pressure Drop through the Wheel

Since the pressure drop through the wheel has an uncertainty involved with it based on the mass flow rate (velocity and density), the pressure drop equation shown in Equation (3.1) must be evaluated. Since the coefficients in the equation include some unknown geometric parameters, the Methodology for pressure drop in Chapter VIII proposes a more general equation based solely on the velocity and density, which are parameters that change with altitude. By combining the variables that do not change with altitude, Equation (3.1) can be simplified to Equation (4.14).

$$\Delta P = C_l \, V + C_{k,t} \, \rho \, V^2 \tag{4.14}$$

where:

C_l = Coefficient related to laminar flow through the channel

$C_{k,t}$ = Coefficient related to entrance and exit losses

These variables are functions of viscosity and geometry of the channels in the desiccant wheel, and therefore vary with each analysis. Since the variables associated with geometry are unknown, they are estimated using the proposed methodology in Chapter VIII as constant coefficients. Analyzing the uncertainty in these variables would be quite laborious in order to consider the exact uncertainties for pressure drop in each test. However, analysis of some cases showed that the uncertainty for the pressure drop can be conservatively approximated as equal to the percentage uncertainty of the mass flow rate.

Uncertainty in Process Outlet Temperature

The process outlet temperature cannot be exactly defined because the temperature is the result of heat and mass transfer processes that are not know. However, if it is assumed that the temperature will depend strongly on the mass transfer, the latent heat released to the air due to the dehumidification of the air stream can be defined using Equation (4.15).

$$Q_{\Delta G} = \dot{m}\, \Delta GPP_P h_{fg} \tag{4.15}$$

where:

$Q_{\Delta G}$ = Heat produced by dehumidification, *[BTU/min]*

h_{fg} = Specific enthalpy of evaporation, *[BTU/lbm]*

The uncertainty for the heat rate is estimated using the Taylor Series Method as:

$$U_{Q_{\Delta G}} = \left[\left(\frac{\partial Q_{\Delta G}}{\partial \dot{m}} U_{\dot{m}}\right)^2 + \left(\frac{\partial Q_{\Delta G}}{\partial \Delta GPP_P} U_{\Delta GPP_P}\right)^2\right]^{1/2} \tag{4.16}$$

where:

$U_{Q_{\Delta G}}$ = Uncertainty in heat rate

Once the uncertainty for the heat rate is known, Equation (4.17) can be used to find the estimated process outlet temperature.

$$T_{PO} = \frac{Q_{\Delta G}}{\dot{m}\, c_p} + T_{PI} \tag{4.17}$$

where:

T_{PO} = Process outlet temperature, *[°F]*

c_p = Specific heat of air, *[BTU/lbm°F]*

T_{PI} = Process inlet temperature, *[°F]*

The uncertainty for the process outlet temperature can be estimated using the Taylor Series Method as:

$$U_{T_{PO}} = \left[\left(\frac{\partial T_{PO}}{\partial Q_{\Delta G}} U_{Q_{\Delta G}}\right)^2 + \left(\frac{\partial T_{PO}}{\partial \dot{m}} U_{\dot{m}}\right)^2 + \left(\frac{\partial T_{PO}}{\partial T_{PI}} U_{T_{PI}}\right)^2\right]^{1/2} \qquad (4.18)$$

where:

$U_{T_{PO}}$ = Uncertainty in process outlet temperature

$U_{T_{PI}}$ = Uncertainty in process inlet temperature

CHAPTER V

EXPERIMENTAL SETUP

Instrumentation

In order to perform the testing, several measurement stations were needed to acquire the inlet and outlet conditions of both process and regeneration air streams. The method for calculating humidity ratio was used by MSU, therefore four humidity probes were used. These probes measured relative humidity as well as dry-bulb temperature so that the humidity ratio could be calculated. Since the maximum constant-state temperature for these probes was 160°F, an RTD was placed after the natural gas burner to measure the heated regeneration temperature. The flow rates were measured using four multi-point self-averaging flow sensors which were coupled with additional flow straighteners to conform as much as possible to ASHRAE Standard 139 [14]. Several pressure transducers were used to measure the differential pressures for the flow meters as well as the pressure drop through the wheel. All of these measurement systems were connected to a data acquisition system so that the data could be recorded. Table 5.1 shows a more comprehensive view of the instrumentation used, while Table 5.2 presents the DAQ devices.

Table 5.1

Instrumentation Used.

	Instrument		Measured Variable		
Description	**Make**	**Model**		**Quantity**	**Accuracy**
Temp/RH Probe	Vaisala	HMP233	T, RH	4	±0.18°F, ±1% RH
RTD	Omega	PR-20	T	1	±0.27°F
Flow Meter	Air Monitor Corporation	LO-flo	Velocity	4	±2% of actual flow
Pressure Transducer	Omega	PX653	ΔP	6	±0.5% FS

Table 5.2

DAQ Equipment Used.

Description	**Model**
USB Chassis	NI cDAQ-9174
RTD Input Module	NI 9217
Terminal Block	BNC-2095
Analog Input Module	SCXI-1100

Test Loop

Figure 5.1 shows a schematic of the test loop used. The schematic outlines where the previously mentioned instruments were placed for measurements. The humidifiers correspond to steam produced by two boilers. The three fans in each flow stream were used to set the differential pressure between the process outlet and regeneration inlet chambers to zero while at the same time maintaining the appropriate mass flow rate. The test cassette used had an estimated effective face area of 0.415 ft^2 for both the process and regeneration sides.

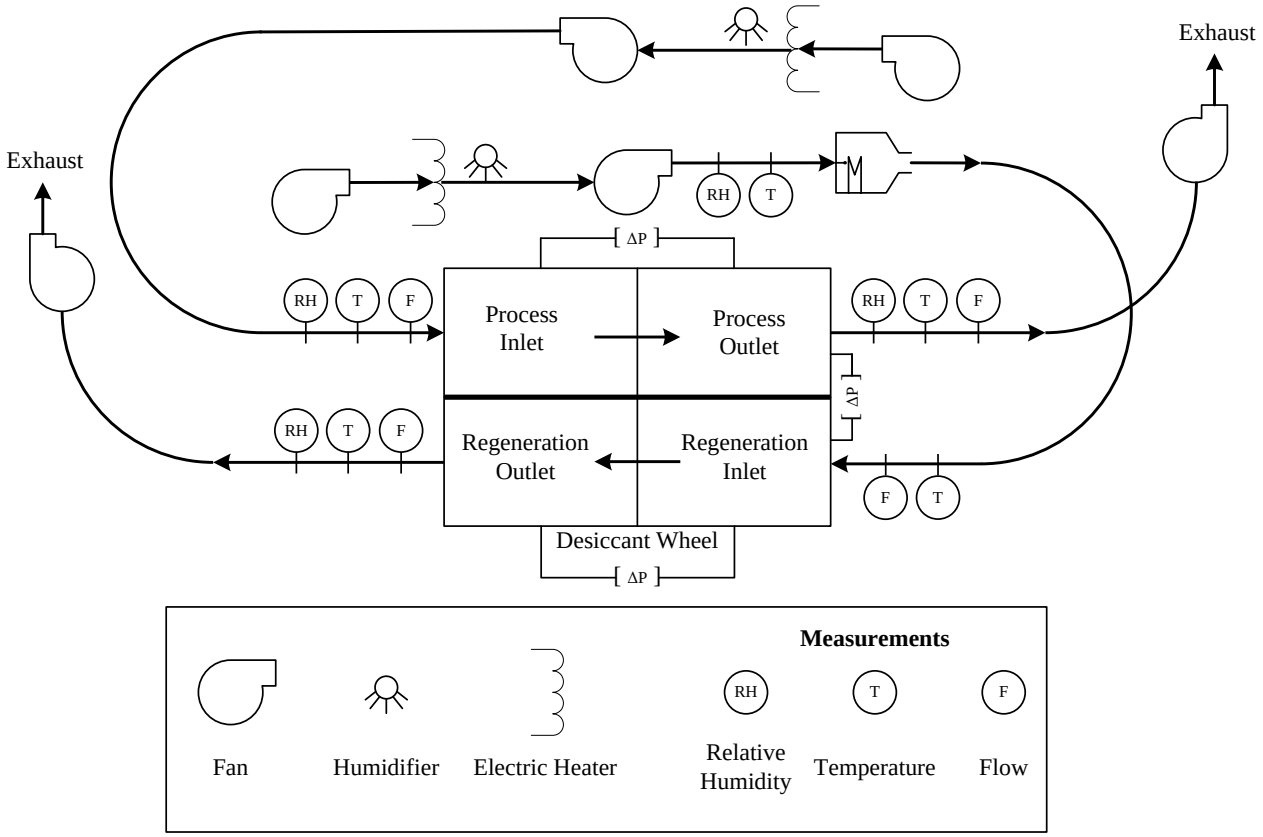

Figure 5.1

Schematic of Test Loop.

Figures 5.2 through 5.4 show photographs of the experimental setup at MSU; Figure 5.5 shows a photograph of the experimental setup at NREL.

Figure 5.2

Photograph #1 of MSU's Experimental Setup.

Figure 5.3

Photograph #2 of MSU's Experimental Setup.

Figure 5.4

Photograph #3 of MSU's Experimental Setup.

Figure 5.5

Photograph of NREL's Experimental Setup.

Method of Tests

The testing procedure was done under the requirements of ASHRAE Standard 139. These requirements state that the tests must be performed under steady-state conditions, which have been held for at least fifteen minutes. The standard also states that the mass flow rates must be calculated using the air flow at the flow meter, and also the density calculated at the flow meter by the temperature and humidity probes.

One important consideration that was taken was the pressure differential between the different test chambers. In order to maintain the required balances (see Chapter VI), the pressure differential between the Process Outlet and Regeneration Inlet chambers was

set to zero. This assured that no mixing of the air occurred between the process out and regeneration inlet air streams, leading to false readings of the actual process outlet and regeneration inlet conditions and flow rates. Also, the pressure differential between the Process Inlet and the atmosphere was set to be equal-but-opposite of the pressure differential between the Regeneration Outlet and the atmosphere. This ensured that the system was properly balanced, allowing for minimal leakage between the different chambers of the desiccant apparatus and the atmosphere.

CHAPTER VI

TEST RESULTS

Test Conditions

After careful deliberation over the conditions to be tested, a set of fifteen tests was decided on. These tests cover three mass flow rates, three temperatures, and five humidity ratios. The range of these temperatures and humidity ratios covers the general range that a dehumidifier would be used in. The flow rates were decided on based on the capacities of the testing apparatuses. The flow rate for Tests C were set so that there would be a set of matching face velocities between both locations (MSU-C matches velocity at NREL-B, NREL-C matches velocity at MSU-A). The face velocities were also set so that the regeneration stream was half that of the process stream for each test. These conditions are outlined in Table 6.1. As explained in Chapter V, the differential pressure between the Process Outlet and Regeneration Inlet chambers was set to zero. Therefore, the process outlet flow rate was used as the design condition mass flow rate to ensure that this flow rate was the actual value crossing the desiccant wheel.

Based on previous experiences, it was agreed that the mass flow rates and humidity ratios were kept constant for each test at both locations. In computing the humidity ratios in Table 6.1, the barometric pressure at each location was calculated using Equation (6.1) [7, Chapter 1]:

$$p_{atm} = 14.696(1 - 6.8754 \times 10^{-6}\, Z)^{5.2559} \quad (6.1)$$

where:

p_{atm} = Atmospheric pressure at altitude, *[psi]*

Z = Altitude, *[ft]*

Since the actual barometric pressure was used to calculate the humidity ratios during the tests, the relative humidity (MSU) and dew-point temperature (NREL) were adjusted accordingly so that the resulting humidity ratios were the same for both locations, as defined in the test conditions.

Table 6.1

Test Conditions for (a) MSU.

Test		SFPM	SCFM	T_{db}	Relative Humidity	Humidity Ratio	Mass Flow
		[ft/min]	*[ft^3/min]*	*[°F]*	*[%]*	*[Gr/lbm]*	*[lbm/min]*
1A	**P**	600	249.0	75.0	60.0	79	18.7
	R	300	124.5	200.0	3.63	129	9.3
2A	**P**	600	249.0	75.0	70.0	92	18.7
	R	300	124.5	200.0	3.63	129	9.3
3A	**P**	600	249.0	75.0	80.0	106	18.7
	R	300	124.5	200.0	3.63	129	9.3
4A	**P**	600	249.0	65.0	98.0	92	18.7
	R	300	124.5	200.0	3.63	129	9.3
5A	**P**	600	249.0	55.0	98.0	64	18.7
	R	300	124.5	200.0	3.63	129	9.3
1B	**P**	400	166.0	75.0	60.0	79	12.5
	R	200	83.0	200.0	3.63	129	6.2
2B	**P**	400	166.0	75.0	70.0	92	12.5
	R	200	83.0	200.0	3.63	129	6.2
3B	**P**	400	166.0	75.0	80.0	106	12.5
	R	200	83.0	200.0	3.63	129	6.2
4B	**P**	400	166.0	65.0	98.0	92	12.5
	R	200	83.0	200.0	3.63	129	6.2
5B	**P**	400	166.0	55.0	98.0	64	12.5
	R	200	83.0	200.0	3.63	129	6.2
1C	**P**	488	202.5	75.0	60.0	79	15.2
	R	244	101.3	200.0	3.63	129	7.6
2C	**P**	488	202.5	75.0	70.0	92	15.2
	R	244	101.3	200.0	3.63	129	7.6
3C	**P**	488	202.5	75.0	80.0	106	15.2
	R	244	101.3	200.0	3.63	129	7.6
4C	**P**	488	202.5	65.0	98.0	92	15.2
	R	244	101.3	200.0	3.63	129	7.6
5C	**P**	488	202.5	55.0	98.0	64	15.2
	R	244	101.3	200.0	3.63	129	7.6

Table 6.1 (continued)

(b) NREL.

Test		SFPM	SCFM	T_{db}	Relative Humidity	Humidity Ratio	Mass
		[ft/min]	*[ft^3/min]*	*[°F]*	*[%]*	*[Gr/lbm]*	*[lbm/min]*
1A	**P**	600	249.0	75.0	49.4	79	18.7
	R	300	124.5	200.0	3.63	159	9.3
2A	**P**	600	249.0	75.0	57.4	92	18.7
	R	300	124.5	200.0	3.63	159	9.3
3A	**P**	600	249.0	75.0	65.9	106	18.7
	R	300	124.5	200.0	3.63	159	9.3
4A	**P**	600	249.0	65.0	80.7	92	18.7
	R	300	124.5	200.0	3.63	159	9.3
5A	**P**	600	249.0	55.0	80.7	64	18.7
	R	300	124.5	200.0	3.63	159	9.3
1B	**P**	400	166.0	75.0	49.4	79	12.5
	R	200	83.0	200.0	3.63	159	6.2
2B	**P**	400	166.0	75.0	57.4	92	12.5
	R	200	83.0	200.0	3.63	159	6.2
3B	**P**	400	166.0	75.0	65.9	106	12.5
	R	200	83.0	200.0	3.63	159	6.2
4B	**P**	400	166.0	65.0	80.7	92	12.5
	R	200	83.0	200.0	3.63	159	6.2
5B	**P**	400	166.0	55.0	80.7	64	12.5
	R	200	83.0	200.0	3.63	159	6.2
1C	**P**	492	204.2	75.0	49.4	79	15.3
	R	246	102.1	200.0	3.63	159	7.7
2C	**P**	492	204.2	75.0	57.4	92	15.3
	R	246	102.1	200.0	3.63	159	7.7
3C	**P**	492	204.2	75.0	65.9	106	15.3
	R	246	102.1	200.0	3.63	159	7.7
4C	**P**	492	204.2	65.0	80.7	92	15.3
	R	246	102.1	200.0	3.63	159	7.7
5C	**P**	492	204.2	55.0	80.7	64	15.3
	R	246	102.1	200.0	3.63	159	7.7

Experimental Results

Outlined below are the resulting data from the previously outlined test conditions. This data shows the set inlet conditions for the process and regeneration air streams, as well as the resulting outlet conditions for both air streams (process and regeneration). Tables 6.2 and 6.3 outline the results from MSU for the process and regeneration air streams, respectively. Tables 6.4 and 6.5 outline the results from NREL for the process and regeneration air streams, respectively. IP and SI units are presented for the results because IP units were preferred at MSU, while SI units were preferred at NREL.

Table 6.2

MSU Test Results for Process Air Stream (a) (IP).

Test	Process In			Process Out			Process
	Mass	**T_{db}**	**W**	**Mass**	**T_{db}**	**W**	**ΔP**
	[lbm/min]	*[°F]*	*[Gr/lbm]*	*[lbm/min]*	*[°F]*	*[Gr/lbm]*	*[in WC]*
1A	20.9	75.0	79	18.7	103.4	46	0.566
2A	20.7	74.9	92	18.6	105.8	55	0.571
3A	20.5	75.1	105	18.6	107.9	64	0.577
4A	20.7	65.1	91	18.6	100.3	49	0.574
5A	20.9	55.1	63	18.7	87.4	29	0.547
1B	13.9	75.0	78	12.5	107.9	38	0.382
2B	13.8	75.0	92	12.4	111.0	46	0.376
3B	14.1	75.0	107	12.5	112.9	57	0.390
4B	13.8	65.0	91	12.5	107.6	41	0.380
5B	13.8	55.2	63	12.4	94.0	21	0.374
1C	16.9	75.1	79	15.2	106.4	42	0.467
2C	16.9	75.0	92	15.2	108.3	51	0.464
3C	16.9	74.9	106	15.2	110.6	59	0.483
4C	17.0	65.0	92	15.2	103.9	45	0.464
5C	16.8	55.2	63	15.3	90.8	24	0.456

Table 6.2 (continued)

(b) (SI).

Test	Process In			Process Out		
	Mass	**T_{db}**	**W**	**Mass**	**T_{db}**	**W**
	[kg/s]	*[°C]*	*[kg/kg]*	*[kg/s]*	*[°C]*	*[kg/kg]*
1A	0.158	23.9	0.0113	0.142	39.7	0.0066
2A	0.156	23.8	0.0131	0.141	41.0	0.0078
3A	0.155	23.9	0.0150	0.141	42.2	0.0092
4A	0.157	18.4	0.0130	0.141	37.9	0.0070
5A	0.158	12.9	0.0091	0.142	30.8	0.0041
1B	0.105	23.9	0.0112	0.095	42.2	0.0054
2B	0.104	23.9	0.0131	0.094	43.9	0.0066
3B	0.106	23.9	0.0152	0.095	45.0	0.0082
4B	0.105	18.3	0.0131	0.094	42.0	0.0059
5B	0.104	12.9	0.0090	0.094	34.5	0.0030
1C	0.128	23.9	0.0112	0.115	41.4	0.0060
2C	0.128	23.9	0.0131	0.115	42.4	0.0072
3C	0.128	23.9	0.0151	0.115	43.7	0.0085
4C	0.128	18.4	0.0131	0.115	39.9	0.0064
5C	0.127	12.9	0.0090	0.115	32.7	0.0034

Table 6.3

MSU Test Results for Regeneration Air Stream (a) (IP).

Test	Regeneration In			Regeneration Out			Regen
	Mass	**T_{db}**	**W**	**Mass**	**T_{db}**	**W**	**ΔP**
	[lbm/min]	*[°F]*	*[Gr/lbm]*	*[lbm/min]*	*[°F]*	*[Gr/lbm]*	*[in WC]*
1A	9.3	199.7	130	10.9	134.7	182	0.384
2A	9.3	200.1	129	10.8	131.4	190	0.383
3A	9.4	199.8	128	10.9	128.1	198	0.387
4A	9.4	199.3	129	11.0	125.8	198	0.378
5A	9.3	199.8	130	10.9	129.7	184	0.386
1B	6.3	199.9	128	7.6	123.6	185	0.261
2B	6.2	199.2	128	7.4	120.8	193	0.253
3B	6.3	199.8	128	7.6	117.2	205	0.257
4B	6.2	200.1	128	7.4	113.0	202	0.255
5B	6.3	200.6	128	7.5	114.4	186	0.256
1C	7.6	200.0	128	9.0	131.5	173	0.313
2C	7.6	199.8	128	9.0	128.5	191	0.314
3C	7.6	200.3	128	9.0	124.2	201	0.312
4C	7.6	200.0	128	8.9	117.8	202	0.308
5C	7.6	200.0	128	9.0	120.0	187	0.311

Table 6.3 (continued)

(b) (SI).

Test	Regeneration In			Regeneration Out		
	Mass	**T_{db}**	**W**	**Mass**	**T_{db}**	**W**
	[kg/s]	*[°C]*	*[kg/kg]*	*[kg/s]*	*[°C]*	*[kg/kg]*
1A	0.071	93.2	0.0186	0.082	57.0	0.0260
2A	0.070	93.4	0.0184	0.081	55.2	0.0272
3A	0.071	93.2	0.0182	0.083	53.4	0.0283
4A	0.071	93.0	0.0184	0.083	52.1	0.0282
5A	0.071	93.2	0.0186	0.083	54.3	0.0262
1B	0.048	93.3	0.0183	0.057	50.9	0.0264
2B	0.047	92.9	0.0183	0.056	49.3	0.0276
3B	0.047	93.2	0.0182	0.058	47.4	0.0292
4B	0.047	93.4	0.0184	0.056	45.0	0.0289
5B	0.047	93.7	0.0183	0.056	45.8	0.0265
1C	0.057	93.3	0.0183	0.068	55.3	0.0247
2C	0.057	93.2	0.0183	0.068	53.6	0.0273
3C	0.057	93.5	0.0183	0.068	51.2	0.0287
4C	0.057	93.3	0.0182	0.067	47.6	0.0288
5C	0.057	93.3	0.0183	0.068	48.9	0.0267

Table 6.4

NREL Test Results for Process Air Stream (a) (IP).

Test	Process In			Process Out			Process
	Mass	**T_{db}**	**W**	**Mass**	**T_{db}**	**W**	**ΔP**
	[lbm/min]	*[°F]*	*[Gr/lbm]*	*[lbm/min]*	*[°F]*	*[Gr/lbm]*	*[in WC]*
1A	20.8	75.0	79	18.7	103.1	48	0.69
2A	20.8	75.0	92	18.7	105.5	57	0.71
3A	20.8	75.0	106	18.7	107.6	67	0.71
4A	20.8	65.0	92	18.7	99.3	52	0.67
5A	20.8	55.0	64	18.7	87.0	29	0.66
1B	13.9	75.0	79	12.5	110.5	41	0.47
2B	13.8	75.0	92	12.4	113.2	49	0.48
3B	13.8	75.0	106	12.4	115.6	59	0.48
4B	13.9	65.0	92	12.5	107.1	44	0.45
5B	13.8	55.1	65	12.4	94.9	23	0.41
1C	17.1	75.0	79	15.3	106.6	44	0.58
2C	17.1	75.0	92	15.3	109.0	53	0.58
3C	17.0	75.0	107	15.3	111.9	63	0.54
4C	17.0	65.0	92	15.3	103.3	48	0.56
5C	17.0	55.0	64	15.3	90.8	26	0.52

Table 6.4 (continued)

(b) (SI).

Test	Process In			Process Out		
	Mass	**T_{db}**	**W**	**Mass**	**T_{db}**	**W**
	[kg/s]	*[°C]*	*[kg/kg]*	*[kg/s]*	*[°C]*	*[kg/kg]*
1A	0.158	23.9	0.0113	0.141	39.5	0.0068
2A	0.157	23.9	0.0132	0.141	40.8	0.0081
3A	0.158	23.9	0.0152	0.141	42.0	0.0096
4A	0.158	18.3	0.0132	0.141	37.4	0.0074
5A	0.158	12.8	0.0091	0.141	30.5	0.0042
1B	0.105	23.9	0.0113	0.094	43.6	0.0058
2B	0.105	23.9	0.0131	0.094	45.1	0.0070
3B	0.104	23.9	0.0152	0.094	46.4	0.0084
4B	0.105	18.3	0.0132	0.094	41.7	0.0063
5B	0.105	12.8	0.0093	0.094	35.0	0.0033
1C	0.129	23.9	0.0113	0.116	41.4	0.0063
2C	0.129	23.9	0.0131	0.116	42.8	0.0076
3C	0.129	23.9	0.0153	0.116	44.4	0.0090
4C	0.129	18.3	0.0132	0.116	39.6	0.0069
5C	0.129	12.8	0.0092	0.116	32.7	0.0037

Table 6.5

NREL Test Results for Regeneration Air Stream (a) (IP).

Test	Regeneration In			Regeneration Out			Regen
	Mass	**T_{db}**	**W**	**Mass**	**T_{db}**	**W**	**ΔP**
	[lbm/min]	*[°F]*	*[Gr/lbm]*	*[lbm/min]*	*[°F]*	*[Gr/lbm]*	*[in WC]*
1A	9.3	200.0	160	10.9	140.0	199	0.47
2A	9.3	200.0	159	10.9	136.4	202	0.46
3A	9.3	200.0	159	10.9	132.7	209	0.46
4A	9.3	200.0	158	10.9	129.1	211	0.46
5A	9.3	200.0	159	10.9	132.6	200	0.46
1B	6.2	200.0	159	7.5	127.6	204	0.31
2B	6.2	200.0	159	7.5	123.6	212	0.30
3B	6.2	200.0	159	7.5	119.7	220	0.30
4B	6.2	200.0	159	7.4	115.9	221	0.29
5B	6.2	200.0	159	7.4	119.5	209	0.29
1C	7.7	200.0	159	9.1	134.1	200	0.38
2C	7.7	200.0	158	9.1	130.2	206	0.38
3C	7.7	200.0	159	9.0	126.1	217	0.37
4C	7.7	200.0	159	9.0	122.6	216	0.37
5C	7.7	200.0	159	9.0	126.3	205	0.37

Table 6.5 (continued)

(b) (SI).

Test	Regeneration In			Regeneration Out		
	Mass	**T_{db}**	**W**	**Mass**	**T_{db}**	**W**
	[kg/s]	*[°C]*	*[kg/kg]*	*[kg/s]*	*[°C]*	*[kg/kg]*
1A	0.071	93.3	0.0228	0.082	60.0	0.0284
2A	0.071	93.3	0.0227	0.082	58.0	0.0288
3A	0.071	93.3	0.0227	0.082	55.9	0.0298
4A	0.071	93.4	0.0226	0.082	53.9	0.0302
5A	0.071	93.3	0.0227	0.082	55.9	0.0286
1B	0.047	93.3	0.0228	0.057	53.1	0.0292
2B	0.047	93.3	0.0228	0.057	50.9	0.0303
3B	0.047	93.3	0.0227	0.057	48.7	0.0315
4B	0.047	93.3	0.0227	0.056	46.6	0.0316
5B	0.047	93.3	0.0227	0.056	48.6	0.0298
1C	0.058	93.3	0.0227	0.069	56.7	0.0285
2C	0.058	93.3	0.0226	0.069	54.5	0.0295
3C	0.058	93.3	0.0227	0.068	52.3	0.0309
4C	0.058	93.3	0.0227	0.068	50.3	0.0309
5C	0.058	93.3	0.0227	0.068	52.4	0.0293

Using this data, the MRC, Mass Balance, Moisture Balance, and Enthalpy Balance can be calculated. These calculations are shown in Tables 6.6 and 6.7 for MSU and NREL, respectively. SI units are abandoned here for simplicity since the industry standard for air conditioning applications uses IP units. Analyzing the balances for both locations shows that the numbers are within or very close to the limits recommended by ASHRAE Standard 139 – Method of Testing for Rating Desiccant Dehumidifiers Utilizing Heat for the Regeneration Process [14]. These requirements are shown in Table 6.8.

Table 6.6

Calculations of MRC, Mass Balance, Moisture Balance, and Enthalpy Balance for MSU.

Test	MRC	MRC	Mass Balance	Moisture Balance	Enthalpy Balance
	[lbm/hr]	*[kg/hr]*	---	---	---
1A	5.35	2.42	1.02	1.01	1.01
2A	5.95	2.70	1.02	1.01	1.00
3A	6.57	2.98	1.01	1.00	1.00
4A	6.75	3.06	1.02	1.01	1.00
5A	5.62	2.55	1.02	1.00	0.99
1B	4.33	1.9	1.01	1.01	1.01
2B	4.83	2.19	1.01	1.02	1.01
3B	5.28	2.41	1.01	1.01	1.00
4B	5.36	2.43	1.01	1.02	1.00
5B	4.49	2.04	1.01	1.02	1.01
1C	4.79	2.17	1.01	1.05	1.01
2C	5.33	2.42	1.01	1.01	1.00
3C	6.03	2.73	1.01	1.02	1.01
4C	6.11	2.77	1.02	1.02	1.00
5C	5.14	2.33	1.01	1.00	1.00

Table 6.7

Calculations of MRC, Mass Balance, Moisture Balance, and Enthalpy Balance for NREL.

Test	MRC	MRC	Mass Balance	Moisture Balance	Enthalpy Balance
	[lbm/hr]	*[kg/hr]*	---	---	---
1A	5.03	1.85	1.02	1.03	1.01
2A	5.64	2.06	1.02	1.04	1.01
3A	6.23	2.28	1.02	1.05	1.02
4A	6.42	2.07	1.02	1.04	1.01
5A	5.50	2.31	1.02	1.03	1.00
1B	4.09	2.56	1.01	1.02	0.99
2B	4.56	2.28	1.01	1.03	1.00
3B	5.02	2.59	1.01	1.03	1.00
4B	5.10	2.82	1.01	1.03	1.00
5B	4.44	2.31	1.01	1.03	0.99
1C	4.55	2.63	1.01	1.03	1.00
2C	5.10	2.91	1.01	1.04	1.01
3C	5.71	2.01	1.01	1.04	1.01
4C	5.79	2.28	1.02	1.04	1.00
5C	5.02	2.49	1.01	1.03	0.99

Table 6.8

System Balances Recommended by ASHRAE Standard 139.

Mass Balance	0.98 – 1.02
Moisture Balance	0.97 – 1.03

Uncertainties

When performing the uncertainty analysis as outlined in Chapter IV, the instrument accuracies given in Table 6.9 were used. The table presents instrument accuracies for the two locations, as well as the required accuracies according to ASHRAE Standard 139. It can be seen from this table that all of the instrument uncertainties fall within the required accuracies of the devices.

Table 6.9

Instrument Accuracies of NREL and MSU with Accuracies Required by ASHRAE Standard 139.

Measurement	MSU	NREL	ASHRAE
Mass Flow	±2.4% of reading	±2% of reading	±3% of reading
Dry-Bulb Temperature	±0.18°F (Humidity Probe) ±0.27°F (RTD)	±0.3°F	±0.5°F
Dew-Point Temperature	---	±0.3°F	±0.5°F
Relative Humidity	±1% RH	---	±3%
Pressure Measurements	±0.5% FS	---	±1%

By taking the test conditions as the nominal values, the uncertainties for the MRC of each test condition, as well as the uncertainties for each measured value used to calculate the MRC were found. These calculated uncertainties are outlined in Tables 6.10 and 6.11 for the process and regeneration streams at MSU, respectively; Tables 6.12 and 6.13 present the calculated uncertainties for the process and regeneration streams at NREL, respectively. It should be noted that the uncertainties used for temperature in the following calculations are the accuracies of the dry-bulb measurement systems provided in Table 6.9.

Table 6.10

Data Uncertainties for Process Stream at MSU.

Test	Mass Flow		Humidity Ratio In		Humidity Ratio Out		Grain Depression		MRC	
	[lbm/min]	*[%]*	*[Gr/lbm]*	*[%]*	*[Gr/lbm]*	*[%]*	*[Gr/lbm]*	*[%]*	*[lbm/hr]*	*[%]*
1A	0.39	2.1	1.4	1.8	3.2	6.9	3.5	10.5	0.57	10.7
2A	0.39	2.1	1.4	1.6	3.5	6.4	3.7	10.0	0.61	10.2
3A	0.39	2.1	1.5	1.4	3.7	5.8	4.0	9.7	0.65	9.9
4A	0.39	2.1	1.5	1.7	2.9	5.9	3.1	7.4	0.54	8.1
5A	0.39	2.1	1.1	1.7	1.9	6.8	2.1	6.0	0.37	6.7
1B	0.29	2.3	1.4	1.8	3.6	9.5	3.9	9.6	0.43	9.9
2B	0.29	2.3	1.4	1.6	4.0	8.6	4.2	9.4	0.46	9.7
3B	0.29	2.3	1.5	1.4	4.2	7.4	4.5	9.1	0.50	9.4
4B	0.29	2.3	1.6	1.7	3.6	8.8	3.8	7.6	0.44	8.3
5B	0.29	2.4	1.1	1.7	2.4	11.2	2.6	6.2	0.30	6.6
1C	0.33	2.2	1.4	1.8	3.5	8.4	4.1	10.9	0.50	10.4
2C	0.33	2.2	1.5	1.6	3.7	7.3	4.3	10.4	0.53	10.0
3C	0.33	2.2	1.5	1.4	4.0	6.7	4.5	9.8	0.57	9.5
4C	0.33	2.2	1.5	1.7	3.2	7.2	3.6	7.7	0.49	8.0
5C	0.33	2.2	1.1	1.7	2.1	9.2	2.4	6.1	0.33	6.5

Table 6.11

Data Uncertainties for Regeneration Stream at MSU.

Test	Mass Flow		Inlet Humidity Ratio	
	[lbm/min]	*[%]*	*[Gr/lbm]*	*[%]*
1A	0.22	2.0	2.8	2.5
2A	0.22	2.0	2.8	2.6
3A	0.22	2.0	2.9	2.7
4A	0.23	2.0	2.8	2.6
5A	0.22	2.0	2.7	2.5
1B	0.16	2.1	2.8	2.6
2B	0.16	2.1	3.0	2.7
3B	0.16	2.1	2.6	2.5
4B	0.16	2.1	2.2	2.0
5B	0.16	2.1	2.2	2.1
1C	0.18	2.1	3.2	2.9
2C	0.18	2.1	3.2	3.0
3C	0.19	2.1	2.6	2.4
4C	0.18	2.1	2.7	2.5
5C	0.19	2.0	1.7	1.6

Table 6.12

Data Uncertainties for Process Stream at NREL.

Test	Mass Flow		Humidity Ratio In		Humidity Ratio Out		Grain Depression		MRC	
	[lbm/min]	*[%]*	*[Gr/lbm]*	*[%]*	*[Gr/lbm]*	*[%]*	*[Gr/lbm]*	*[%]*	*[lbm/hr]*	*[%]*
1A	0.37	2.0	0.9	1.1	0.6	1.2	1.0	3.3	0.20	3.9
2A	0.37	2.0	1.0	1.1	0.7	1.2	1.2	3.4	0.22	3.9
3A	0.38	2.0	1.1	1.1	0.8	1.1	1.4	3.5	0.25	4.0
4A	0.38	2.0	1.0	1.1	0.6	1.2	1.2	2.9	0.23	3.5
5A	0.37	2.0	0.7	1.1	0.4	1.2	0.8	2.4	0.17	3.1
1B	0.25	2.0	0.9	1.1	0.5	1.2	1.0	2.6	0.14	3.3
2B	0.25	2.0	1.0	1.1	0.6	1.2	1.2	2.7	0.15	3.4
3B	0.25	2.0	1.1	1.1	0.7	1.1	1.3	2.8	0.17	3.5
4B	0.25	2.0	1.0	1.1	0.5	1.2	1.1	2.4	0.16	3.1
5B	0.25	2.0	0.7	1.1	0.3	1.3	0.8	2.0	0.12	2.8
1C	0.31	2.0	0.9	1.1	0.5	1.2	1.0	2.9	0.16	3.6
2C	0.31	2.0	1.0	1.1	0.6	1.2	1.2	3.0	0.19	3.6
3C	0.31	2.0	1.2	1.1	0.7	1.1	1.4	3.1	0.21	3.7
4C	0.31	2.0	1.0	1.1	0.6	1.2	1.2	2.6	0.19	3.3
5C	0.31	2.0	0.7	1.1	0.3	1.2	0.8	2.1	0.15	2.9

Table 6.13

Data Uncertainties for Regeneration Stream at NREL.

Test	Mass Flow		Inlet Humidity Ratio	
	[lbm/min]	*[%]*	*[Gr/lbm]*	*[%]*
1A	0.19	2.0	1.7	1.0
2A	0.19	2.0	1.7	1.0
3A	0.19	2.0	1.7	1.0
4A	0.19	2.0	1.6	1.0
5A	0.19	2.0	1.7	1.0
1B	0.12	2.0	1.7	1.0
2B	0.13	2.0	1.7	1.0
3B	0.13	2.0	1.7	1.0
4B	0.13	2.0	1.6	1.0
5B	0.12	2.0	1.7	1.0
1C	0.15	2.0	1.7	1.0
2C	0.15	2.0	1.6	1.0
3C	0.15	2.0	1.7	1.0
4C	0.15	2.0	1.6	1.0
5C	0.15	2.0	1.7	1.0

As explained in Chapter IV, the percentage uncertainty involved with the pressure drop through the wheel is estimated to be the same as the percentage uncertainty involved with the mass flow rate for both locations. Tables 6.14 and 6.15 show the uncertainties for the pressure drop through the wheel for MSU and NREL, respectively. Also, Chapter IV explains the method used to calculate the uncertainty involved with the process outlet temperatures. These uncertainties are shown in Table 6.16 for both locations.

Table 6.14

Wheel Pressure Drop Uncertainties for MSU.

Test	Process		Regeneration	
	[in WC]	*[%]*	*[in WC]*	*[%]*
1A	0.012	2.1	0.009	2.0
2A	0.012	2.1	0.009	2.0
3A	0.012	2.1	0.009	2.1
4A	0.012	2.1	0.009	2.0
5A	0.011	2.1	0.009	2.0
1B	0.009	2.3	0.007	2.0
2B	0.009	2.3	0.006	2.1
3B	0.009	2.3	0.006	2.1
4B	0.009	2.3	0.006	2.1
5B	0.009	2.4	0.006	2.1
1C	0.010	2.2	0.008	2.1
2C	0.010	2.2	0.008	2.1
3C	0.010	2.2	0.008	2.0
4C	0.010	2.2	0.008	2.1
5C	0.010	2.2	0.008	2.1

Table 6.15

Wheel Pressure Drop Uncertainties for NREL.

Test	Process		Regeneration	
	[in WC]	*[%]*	*[in WC]*	*[%]*
1A	0.014	2.0	0.009	2.0
2A	0.014	2.0	0.009	2.0
3A	0.014	2.0	0.009	2.0
4A	0.014	2.0	0.009	2.0
5A	0.013	2.0	0.009	2.0
1B	0.009	2.0	0.006	2.0
2B	0.010	2.0	0.006	2.0
3B	0.010	2.0	0.006	2.0
4B	0.009	2.0	0.006	2.0
5B	0.008	2.0	0.006	2.0
1C	0.012	2.0	0.008	2.0
2C	0.012	2.0	0.008	2.0
3C	0.011	2.0	0.007	2.0
4C	0.011	2.0	0.007	2.0
5C	0.010	2.0	0.007	2.0

Table 6.16

Process Outlet Temperature Uncertainties for MSU and NREL.

Test	MSU		NREL	
	[°F]	*[%]*	*[°F]*	*[%]*
1A	2.4	2.3	0.8	0.8
2A	2.3	2.2	0.9	0.9
3A	2.1	1.9	0.9	0.8
4A	2.6	2.6	0.9	0.9
5A	2.4	2.7	1.0	1.1
1B	2.3	2.1	1.0	0.9
2B	2.8	2.5	1.0	0.9
3B	2.6	2.3	1.1	1.0
4B	2.4	2.2	1.1	1.0
5B	2.5	2.7	1.2	1.3
1C	2.2	2.1	1.0	0.9
2C	2.0	1.8	1.0	0.9
3C	1.7	1.5	0.8	0.7
4C	1.6	1.5	0.8	0.8
5C	1.4	1.5	0.8	0.9

CHAPTER VII

ANALYSIS OF RESULTS

Moisture Removal Capacity

Since MRC is a function of mass flow rate and grain depression, and because mass flow rate was a controlled variable, it is important to present the results of the grain depression in order to explain the behavior of the MRC. Figures 7.1, 7.2, 7.3, 7.4, and 7.5 show the grain depression as a function of mass flow rate for tests 1, 2, 3, 4, and 5, respectively; while Figures 7.6, 7.7, and 7.8 show the grain depression as a function of process inlet humidity ratio, for tests 1A/2A/3A, 1B/2B/3B, and 1C/2C/3C, respectively. Therefore, it should be noticed that in each figure three points are plotted for each site; with the first set of figures (7.1 – 7.5) having points which correspond to the same process inlet temperature and humidity ratio tested for the three different mass flow rates, and the second set of figures (7.6 – 7.8) having points which correspond to the same process inlet temperature and mass flow rate tested for the three different humidity ratios.

From Figures 7.1, 7.2, 7.3, 7.4, and 7.5 it can be seen that the grain depression decreases with mass flow rate. This can be explained since, for lower velocities through the wheel, the air is dried more deeply because the air is in contact with the desiccant longer and can therefore come closer to equilibrium [3, Chapter 23], i.e. to the point of maximum possible dehumidification. On the other hand, Figures 7.6, 7.7, and 7.8

illustrate that the grain depression increases with inlet humidity ratio. This can be explained since, keeping all other inlet conditions constant, a higher humidity ratio implies a higher partial pressure differential between the air and the desiccant surface, leading to a larger capacity for dehumidification.

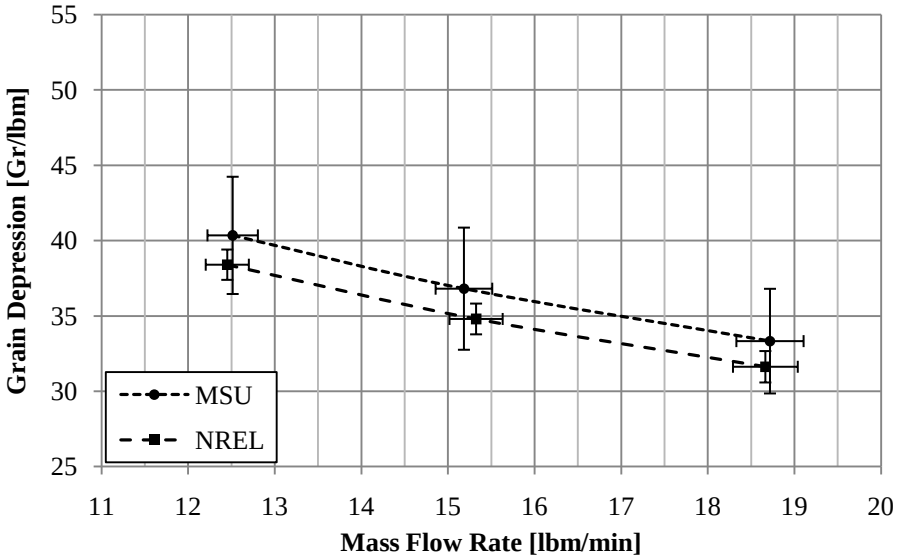

Figure 7.1

Grain Depression as a Function of Mass Flow Rate for Results of Tests 1A, 1B, and 1C at MSU and NREL.

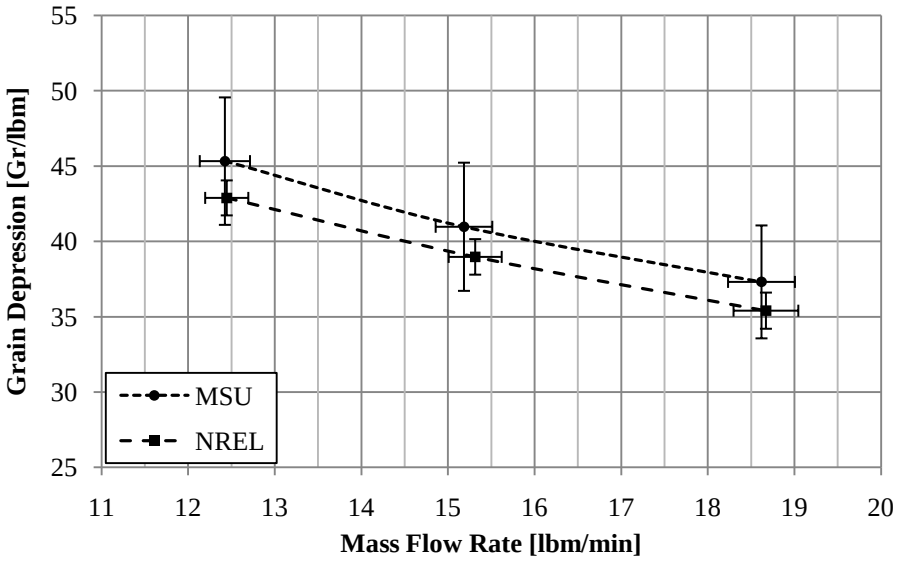

Figure 7.2

Grain Depression as a Function of Mass Flow Rate for Results of Tests 2A, 2B, and 2C at MSU and NREL.

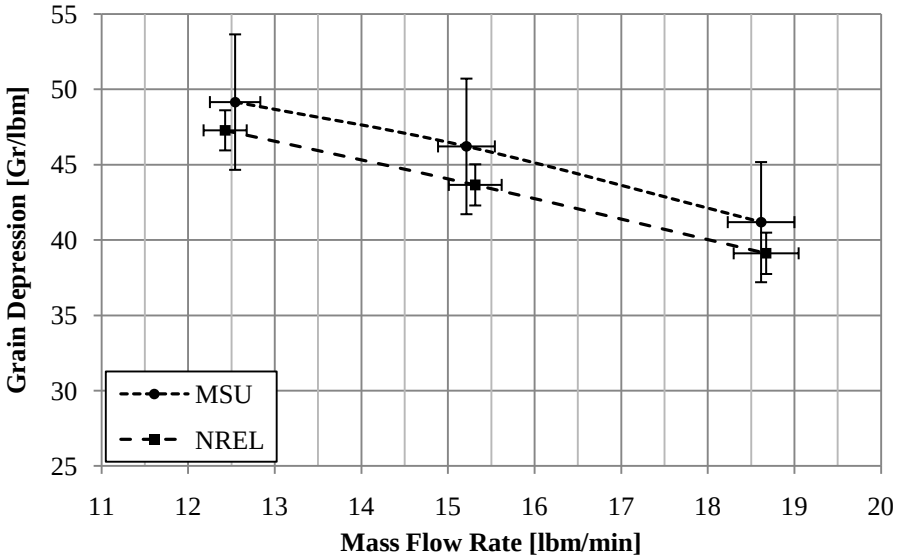

Figure 7.3

Grain Depression as a Function of Mass Flow Rate for Results of Tests 3A, 3B, and 3C at MSU and NREL.

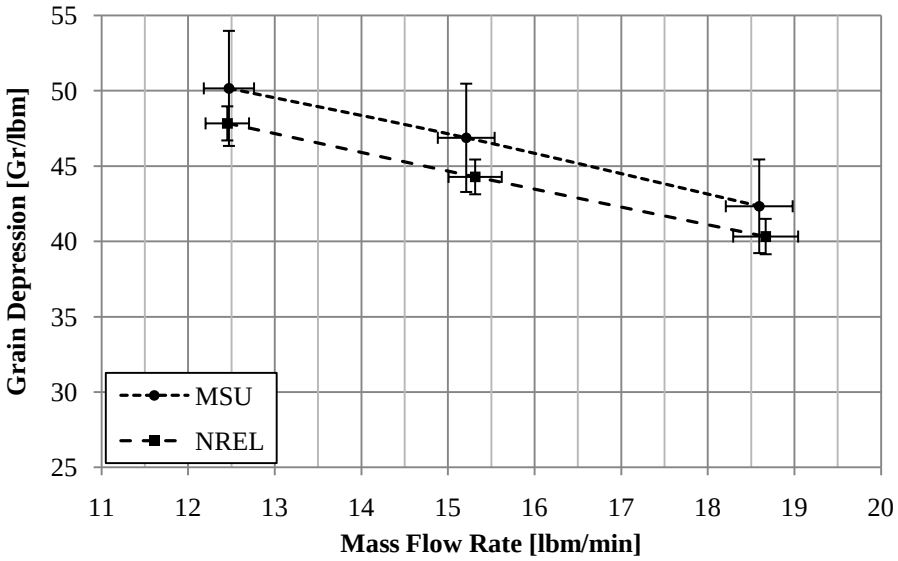

Figure 7.4

Grain Depression as a Function of Mass Flow Rate for Results of Tests 4A, 4B, and 4C at MSU and NREL.

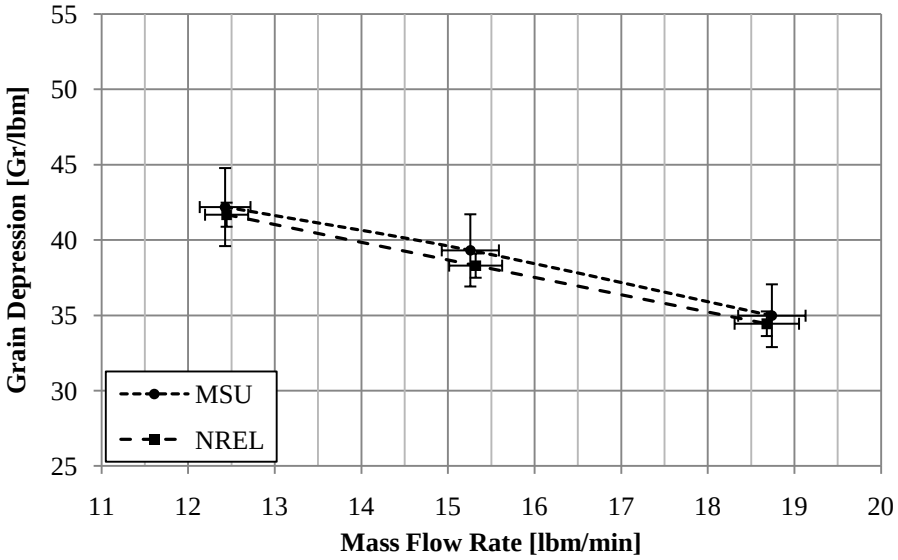

Figure 7.5

Grain Depression as a Function of Mass Flow Rate for Results of Tests 5A, 5B, and 5C at MSU and NREL.

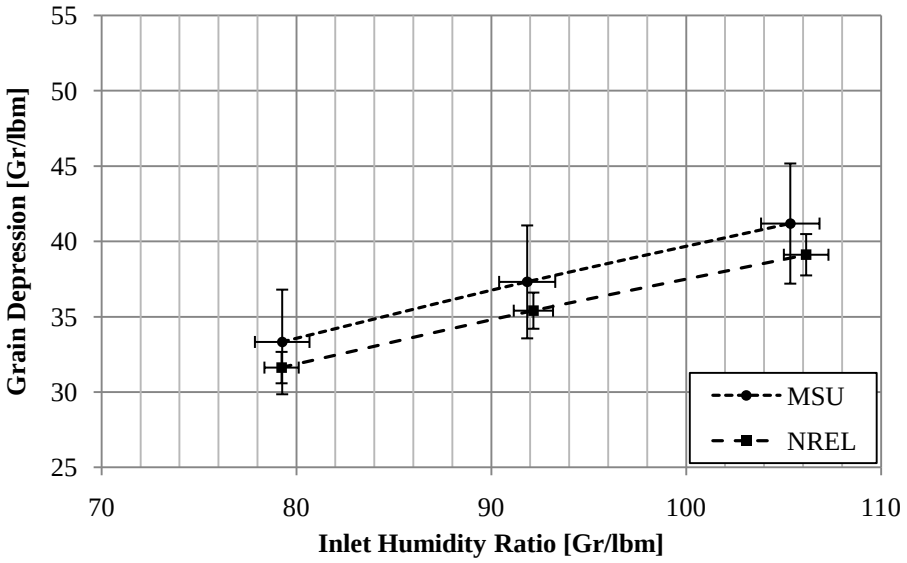

Figure 7.6

Grain Depression as a Function of Inlet Humidity Ratio for Results of Tests 1A, 2A, and 3A at MSU and NREL.

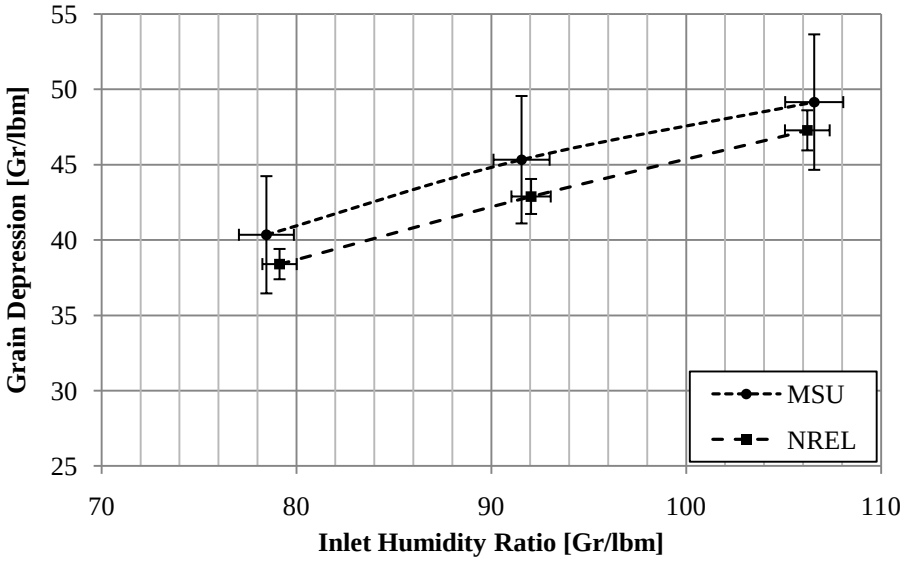

Figure 7.7

Grain Depression as a Function of Inlet Humidity Ratio for Results of Tests 1B, 2B, and 3B at MSU and NREL.

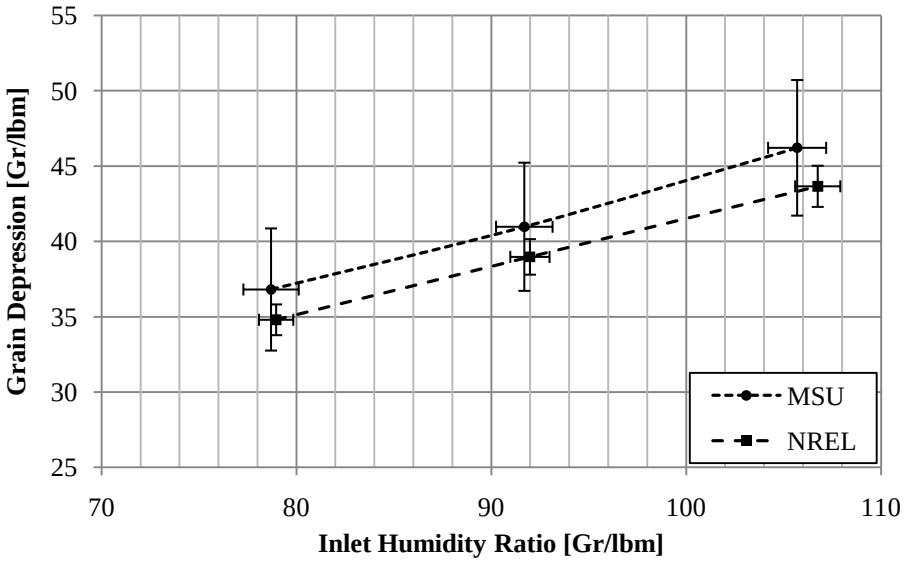

Figure 7.8

Grain Depression as a Function of Inlet Humidity Ratio for Results of Tests 1C, 2C, and 3C at MSU and NREL.

Figures 7.9, 7.10, 7.11, 7.12, and 7.13 show the MRC as a function of mass flow rate for tests 1, 2, 3, 4, and 5, respectively. These figures show that the MRC increases with the mass flow rate. By analyzing the equation for MRC, it seems that this behavior should be obvious. However, since the grain depression decreases with mass flow rate, the results show that the effect of the increase of mass flow rate on the MRC has a larger impact than the decrease of grain depression as a consequence of the increase in mass flow rate.

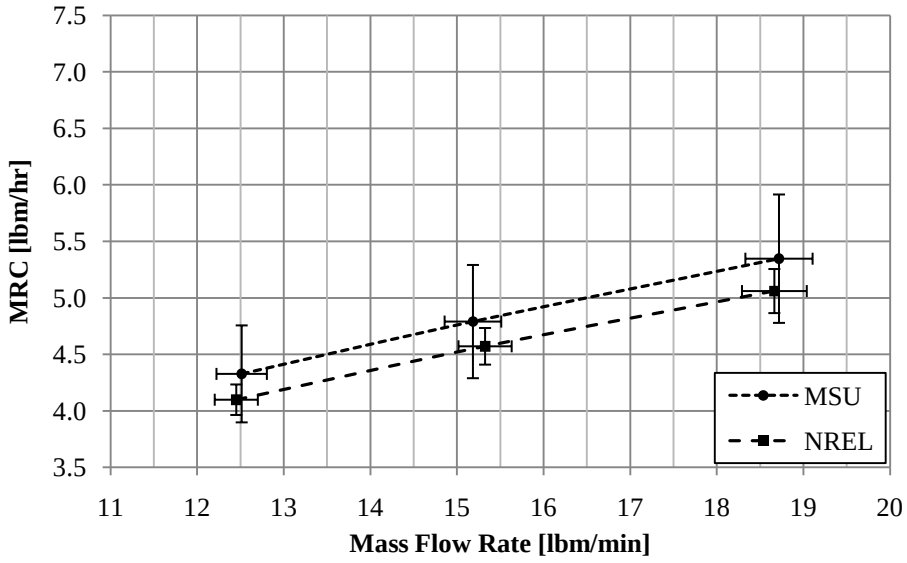

Figure 7.9

MRC as a Function of Mass Flow Rate for Results of Tests 1A, 1B, and 1C at MSU and NREL.

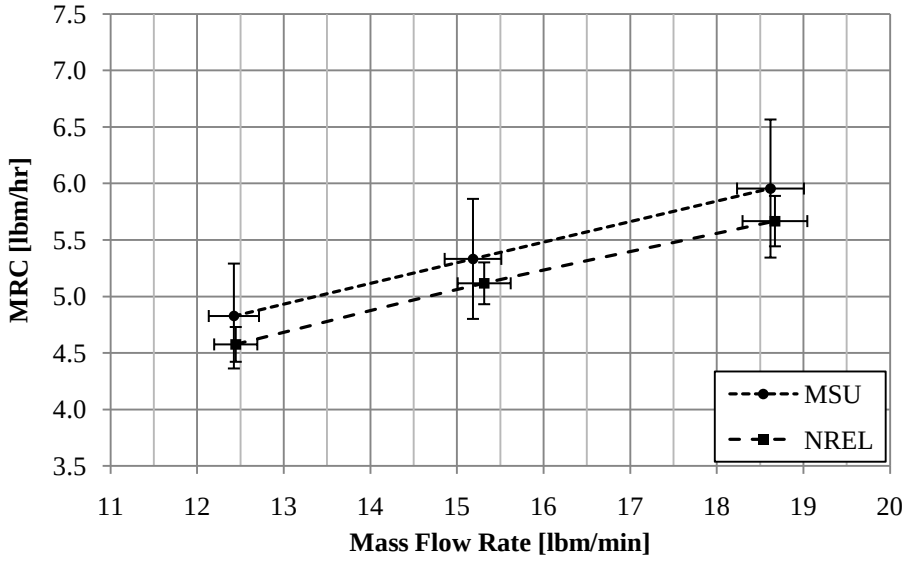

Figure 7.10

MRC as a Function of Mass Flow Rate for Results of Tests 2A, 2B, and 2C at MSU and NREL.

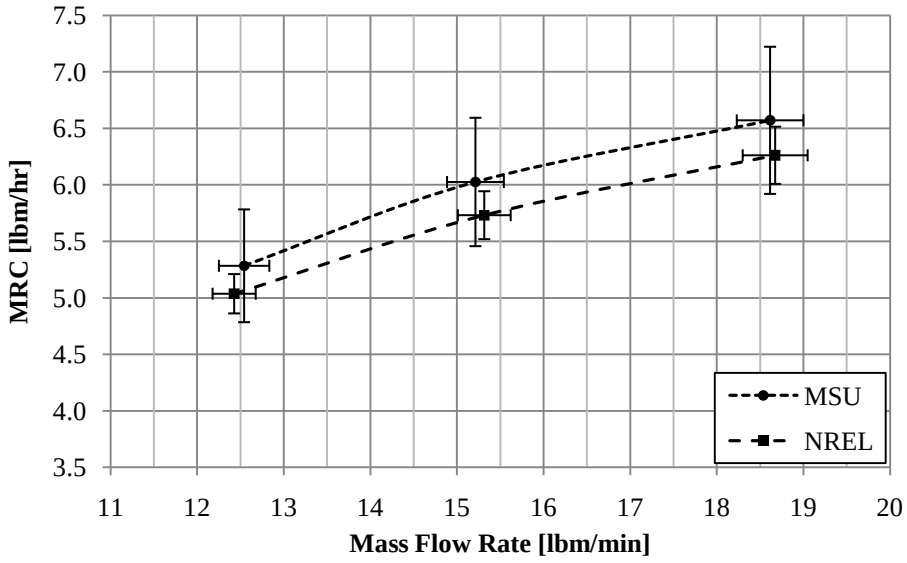

Figure 7.11

MRC as a Function of Mass Flow Rate for Results of Tests 3A, 3B, and 3C at MSU and NREL.

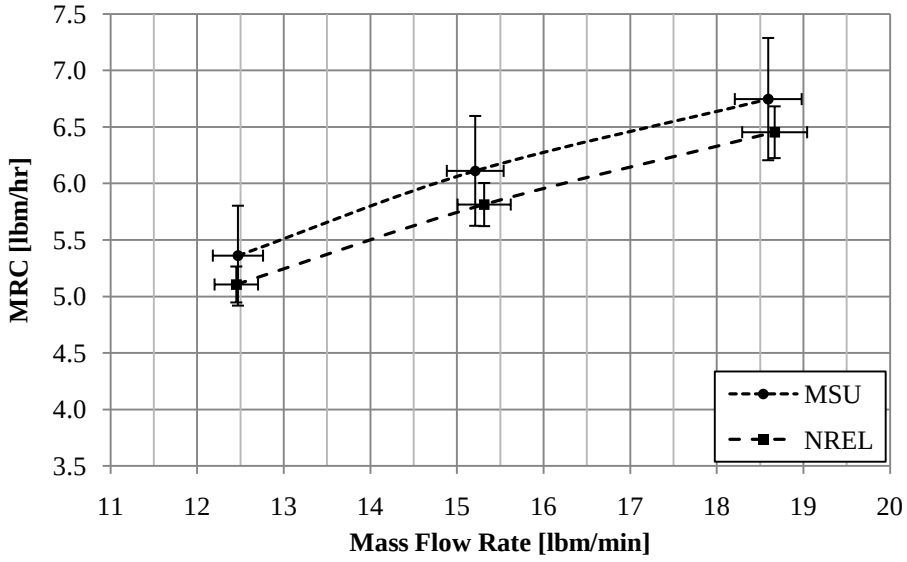

Figure 7.12

MRC as a Function of Mass Flow Rate for Results of Tests 4A, 4B, and 4C at MSU and NREL.

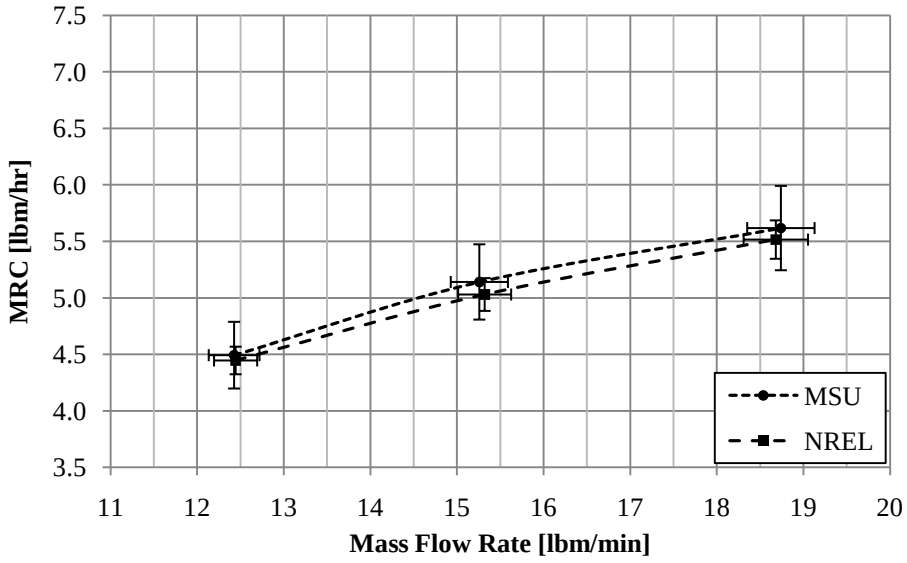

Figure 7.13

MRC as a Function of Mass Flow Rate for Results of Tests 5A, 5B, and 5C at MSU and NREL.

Figures 7.14, 7.15, and 7.16 show the MRC as a function of process inlet humidity ratio for mass flow rates of 18.7 lbm/hr (Test A), 12.5 lbm/hr (Test B), and 15.3 lbm/hr (Test C), respectively. These figures illustrate that the MRC increases with the humidity ratio. This behavior is explained by the fact that if the dry-bulb temperature is kept constant, a higher humidity means a higher partial pressure of water vapor, which is the driving force for desiccant dehumidification.

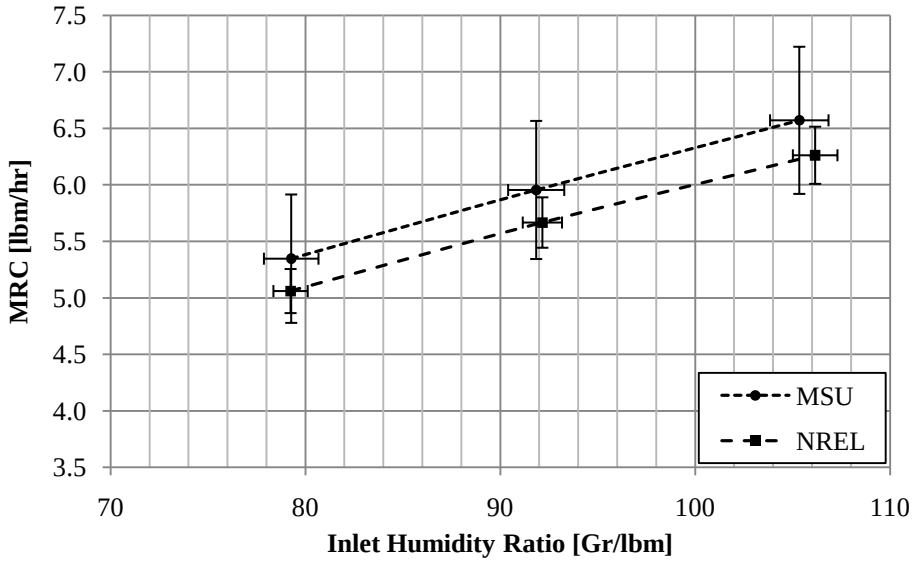

Figure 7.14

MRC as a Function of Inlet Humidity Ratio for Results of Tests 1A, 2A, and 3A at MSU and NREL.

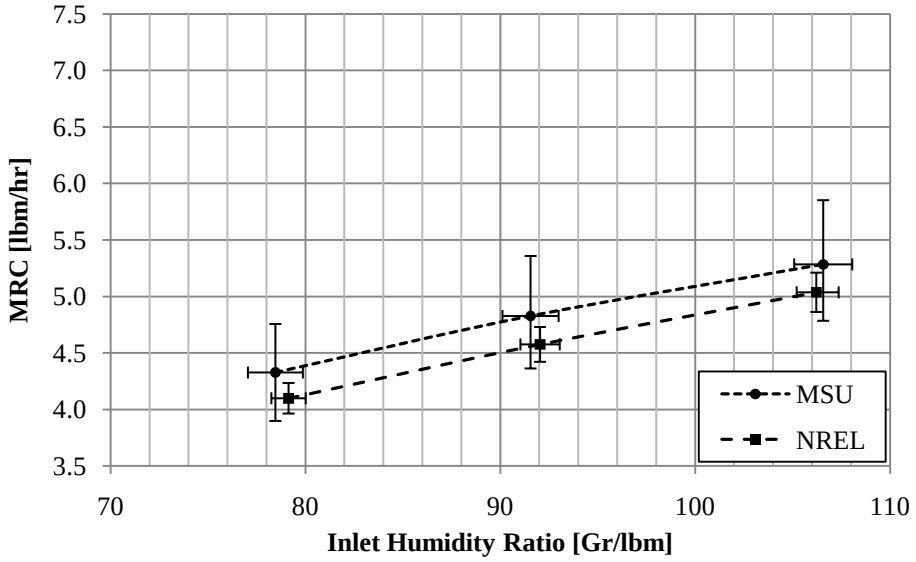

Figure 7.15

MRC as a Function of Inlet Humidity Ratio for Results of Tests 1B, 2B, and 3B at MSU and NREL.

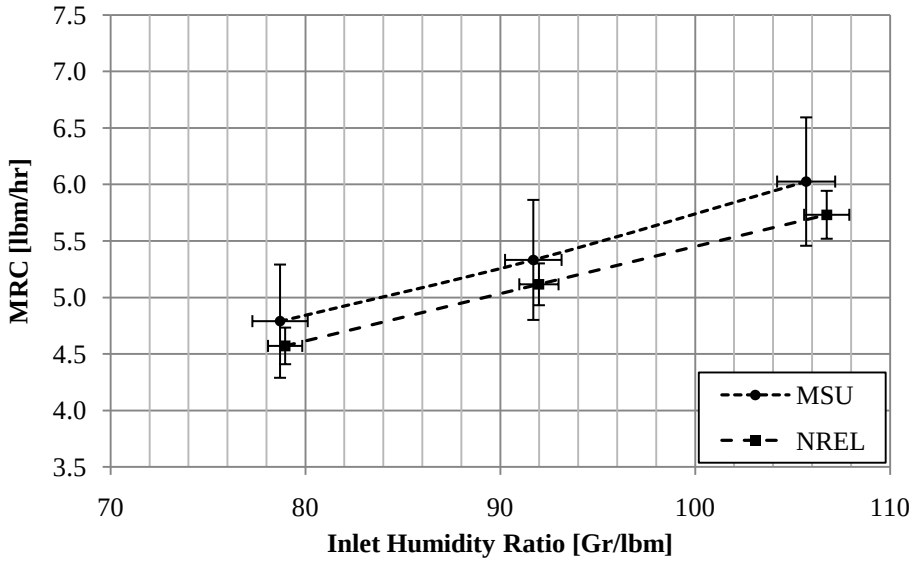

Figure 7.16

MRC as a Function of Inlet Humidity Ratio for Results of Tests 1C, 2C, and 3C at MSU and NREL.

Table 7.1 shows the comparison of the MRC at both locations, as well as the variation between the locations. It can be seen that the variation is about 5% for each test, with the exception of Tests 5A, 5B, and 5C, which have a lower variation. For the same mass flow rate (Tests A, B, and C), the variations are due to the effect of the inlet temperature and humidity ratio on the heat and mass transfer processes. It should be kept in mind that the effect of humidity ratio is actually due to the partial pressure of water vapor. If the mass flow rate, dry-bulb temperature, and humidity ratio are kept constant when comparing desiccant performance at altitude, by analyzing the equation for the MRC, it can be seen that the only variable producing a change in the MRC is the outlet humidity ratio, G_o. Therefore, the difference in inlet partial pressure of water vapor is

defining the variation in G_o and therefore in the MRC. To explain the lower variation in MRC of Tests 5A, 5B, and 5C with respect to the other tests, it is necessary to recall that the water capacity of a given desiccant decreases over altitude at a constant humidity ratio [10, 16]. This is the consequence of a lower partial pressure of water vapor (or relative humidity) at altitude for the same humidity ratio. As can be seen from the variation in inlet partial pressure of water vapor for the different tests (Table 7.2), the variation in partial pressure of Tests 5 is about 0.009 psi (19%) lower than Tests 1, 0.016 psi (29%) lower than Tests 2, 0.025 (39%) lower than Tests 3, and 0.015 (28%) than Tests 4.

Table 7.1

Comparison of MRC at MSU and NREL.

Test	MSU	NREL	Variation	
	[lbm/hr]		*[lbm/hr]*	*[%]*
1A	5.35	5.06	0.29	5.4
2A	5.95	5.67	0.29	4.8
3A	6.57	6.26	0.31	4.7
4A	6.75	6.45	0.29	4.3
5A	5.62	5.52	0.10	1.8
1B	4.33	4.10	0.23	5.3
2B	4.83	4.58	0.25	5.2
3B	5.28	5.04	0.25	4.7
4B	5.36	5.11	0.26	4.8
5B	4.49	4.45	0.05	1.0
1C	4.79	4.57	0.22	4.6
2C	5.33	5.12	0.22	4.1
3C	6.03	5.73	0.29	4.9
4C	6.11	5.81	0.30	4.9
5C	5.14	5.03	0.11	2.2

Table 7.2

Comparison of Process Inlet Partial Pressure of Water Vapor at MSU and NREL

Test	MSU	NREL	Variation
	[psi]		
1A	0.264	0.214	0.050
2A	0.302	0.248	0.054
3A	0.346	0.285	0.061
4A	0.303	0.248	0.055
5A	0.212	0.171	0.041
1B	0.260	0.214	0.046
2B	0.303	0.248	0.055
3B	0.350	0.286	0.064
4B	0.299	0.248	0.051
5B	0.211	0.174	0.037
1C	0.260	0.214	0.046
2C	0.302	0.248	0.054
3C	0.347	0.283	0.064
4C	0.301	0.248	0.053
5C	0.209	0.172	0.037

Pressure Drop through the Wheel

Recalling the discussion on pressure drop in Chapter III and Chapter IV, the pressure drop is a function of face velocity. Since mass flow rate is directly related to face velocity, the pressure drop is presented here as a function of mass flow rate. Besides, mass flow rate is a variable to be kept constant when comparing performance at different altitudes. Figures 7.17 through 7.21 present the pressure drop as a function of mass flow rate for the process streams at MSU and NREL. Figures 7.22 through 7.26 present the pressure drop as a function of mass flow rate for the regeneration streams at MSU and NREL.

Analysis of pressure drop (Figures 7.17 through 7.26) shows a constant trend between MSU and NREL: for a given mass flow rate, pressure drop at NREL is always higher than MSU. This can be explained since for the same mass flow rate, NREL will always have a higher velocity than MSU to compensate for the lower density at altitude. This higher velocity implies a higher pressure drop according to equations proposed to describe the pressure drop (e.g. Equation (3.1)). The other trend that can be noticed from the analysis of the figures is that, as mass flow rate increases, the difference in pressure drop between MSU and NREL also increases. This trend can also be explained through Equation (3.1). This equation shows that the pressure drop follows a second-order polynomial behavior with respect to the velocity. Although the second-order term is considerably smaller than the first-order term, with increasing velocity comes a larger variation due to the velocity-squared term. It should be noted that a point for NREL in Figure 7.19 breaks the trend of the apparent linear relationship between mass flow rate

and pressure drop. As this is the only outlying point, it can be said that this difference is due to uncertainties and should not be considered when evaluating the entire scope of the pressure drop.

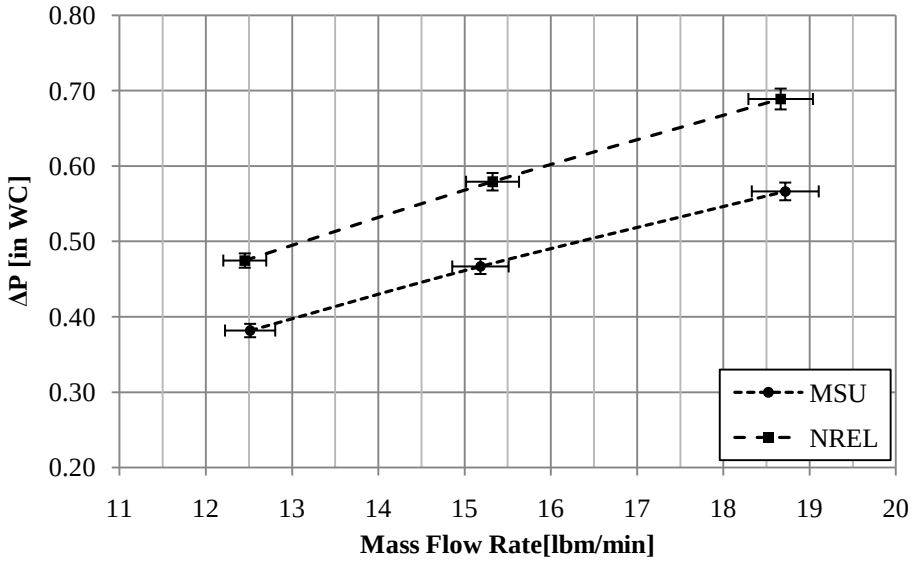

Figure 7.17

Plot of Pressure Drop versus Mass Flow Rate of the Process Stream for Tests 1A, 1B, and 1C at MSU and NREL.

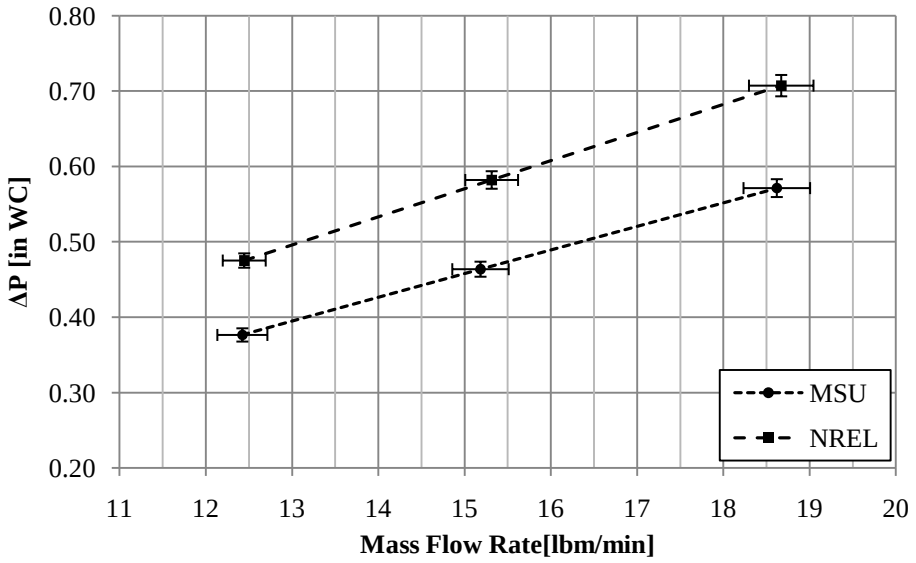

Figure 7.18

Plot of Pressure Drop versus Mass Flow Rate of the Process Stream for Tests 2A, 2B, and 2C at MSU and NREL.

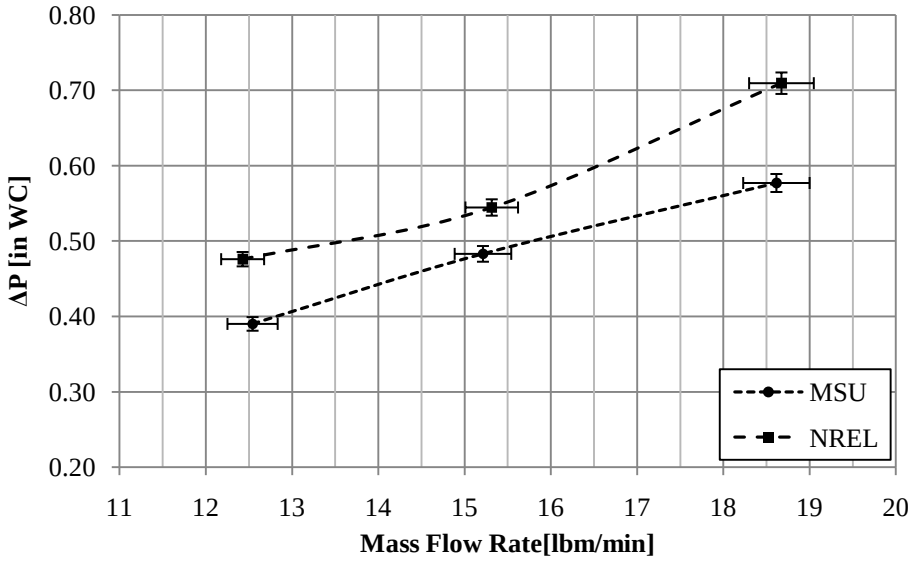

Figure 7.19

Plot of Pressure Drop versus Mass Flow Rate of the Process Stream for Tests 3A, 3B, and 3C at MSU and NREL.

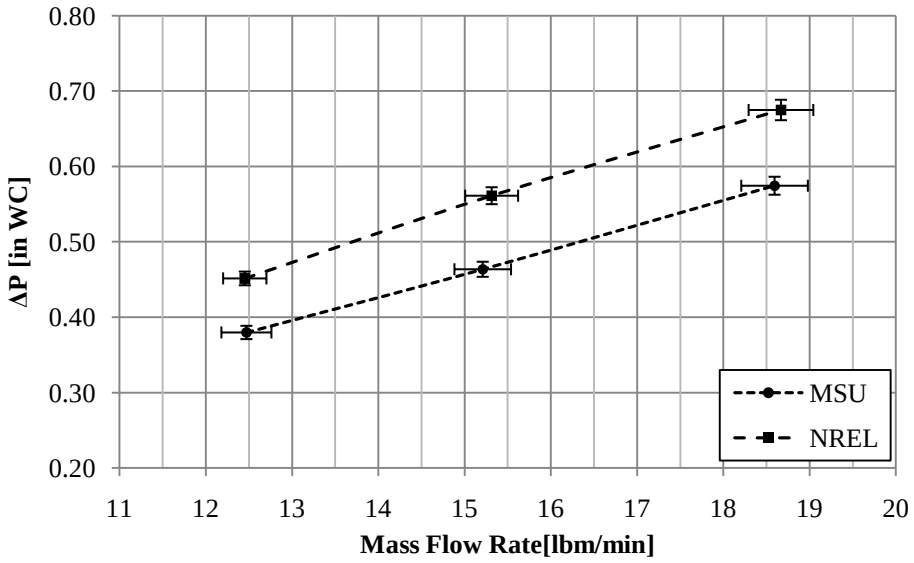

Figure 7.20

Plot of Pressure Drop versus Mass Flow Rate of the Process Stream for Tests 4A, 4B, and 4C at MSU and NREL.

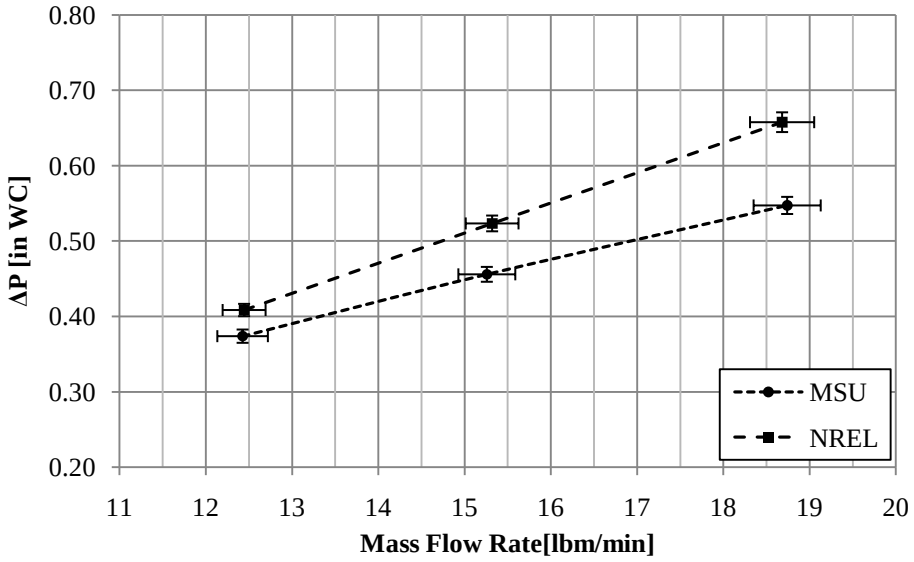

Figure 7.21

Plot of Pressure Drop versus Mass Flow Rate of the Process Stream for Tests 5A, 5B, and 5C at MSU and NREL.

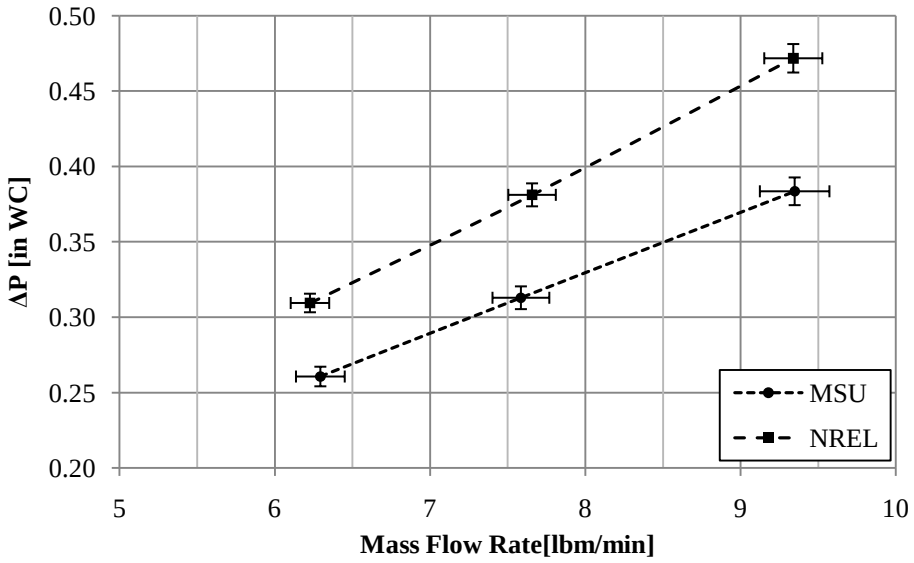

Figure 7.22

Plot of Pressure Drop versus Mass Flow Rate of the Regeneration Stream for Tests 1A, 1B, and 1C at MSU and NREL.

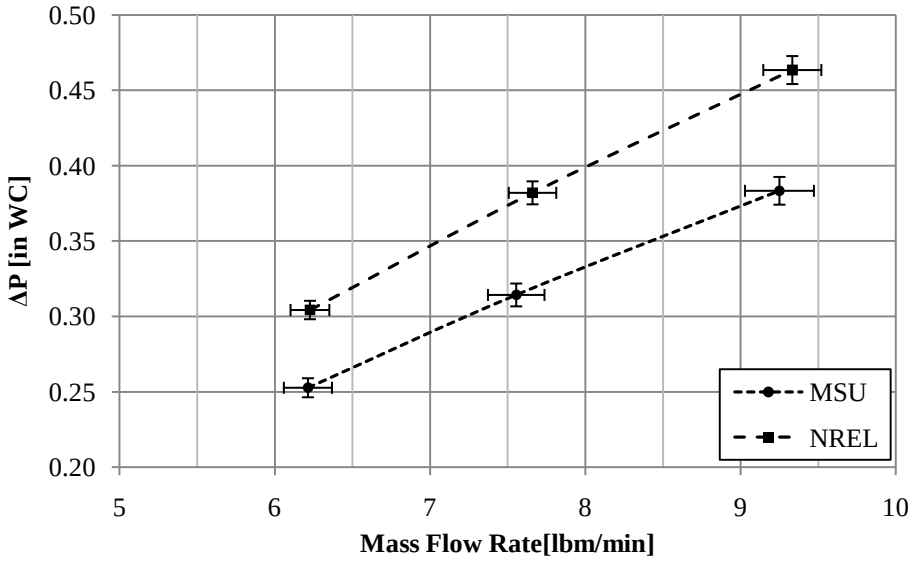

Figure 7.23

Plot of Pressure Drop versus Mass Flow Rate of the Regeneration Stream for Tests 2A, 2B, and 2C at MSU and NREL.

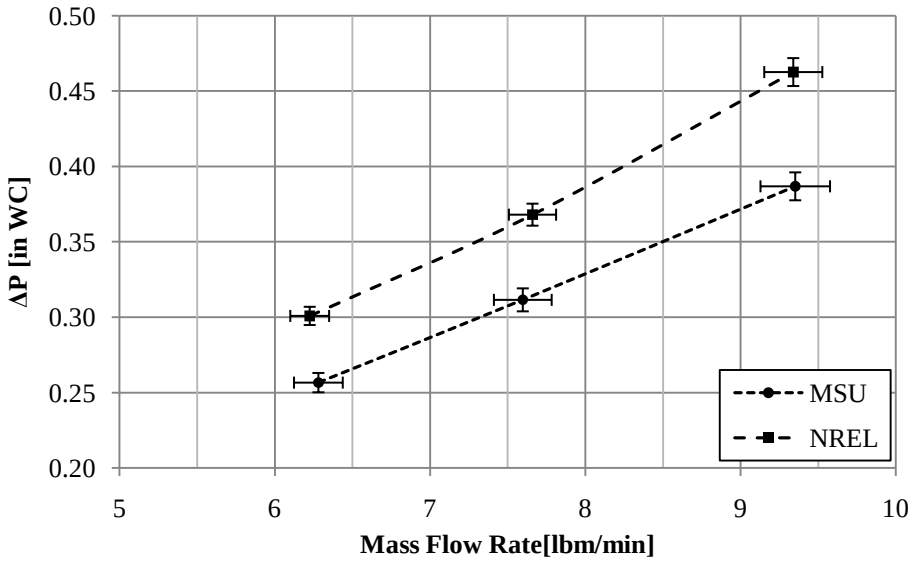

Figure 7.24

Plot of Pressure Drop versus Mass Flow Rate of the Regeneration Stream for Tests 3A, 3B, and 3C at MSU and NREL.

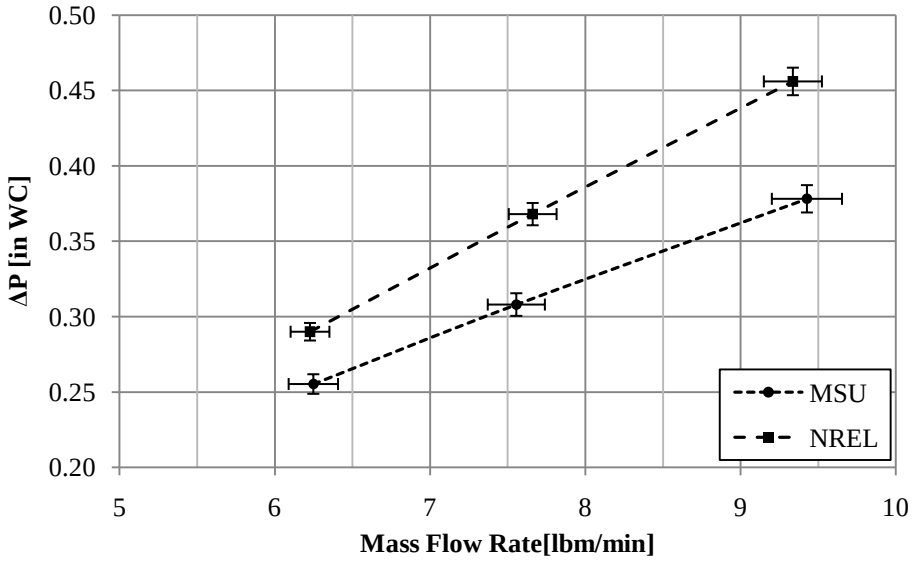

Figure 7.25

Plot of Pressure Drop versus Mass Flow Rate of the Regeneration Stream for Tests 4A, 4B, and 4C at MSU and NREL.

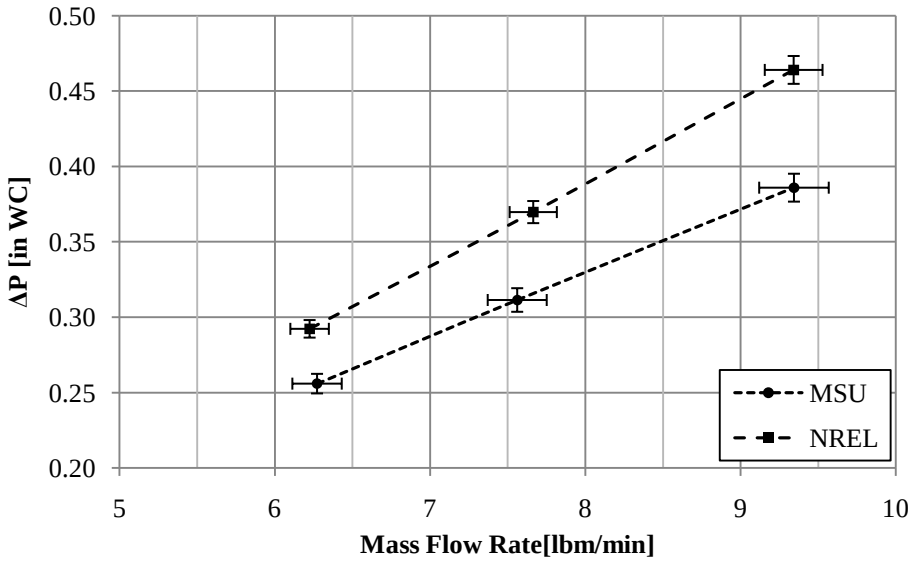

Figure 7.26

Plot of Pressure Drop versus Mass Flow Rate of the Regeneration Stream for Tests 5A, 5B, and 5C at MSU and NREL.

Process Outlet Temperature

As has been the trend, the process outlet temperature will be analyzed using mass flow rate. Figures 7.27 through 7.31 show the process outlet temperature as a function of mass flow rate for both locations. In these figures the uncertainty for the temperature is calculated using the method outlined in Chapter IV. Table 7.3 presents the variation in the process outlet temperature between the two sites.

From Figures 7.27 through 7.31 and Table 7.3, it can be seen that altitude has a lower impact on the process outlet temperatures than the MRC and the pressure drop. If it is said that the MRC summarizes the performance of the desiccant system, then a low variation in MRC between sites suggests that the variation in atmospheric pressure does not have a great impact on the heat and mass transfer processes, and therefore on the process temperature rise. Figures 7.27 through 7.31 illustrate that at lower flow rates the outlet temperature at altitude tends to be slightly higher, while at higher flow rates the temperature at altitude is lower, but with less magnitude than for the low flow rates. This may be a consequence of the higher influence of the mass transfer process in the overall performance; as seen from the grain depression behavior, the grain depression decreases with mass flow rate. Table 7.3 indicates that the maximum variation for the process outlet temperature is 2.4% with most of the variations below 1%.

By comparing the figures for the different tests and humidity conditions (Tests 1, 2, 3, 4, and 5), it can be seen that there is not a clear trend. Therefore the results show that the influence of this variable in the energy balance from the heat and mass transfer process [7, Chapter 6] is inconclusive without a mathematical model.

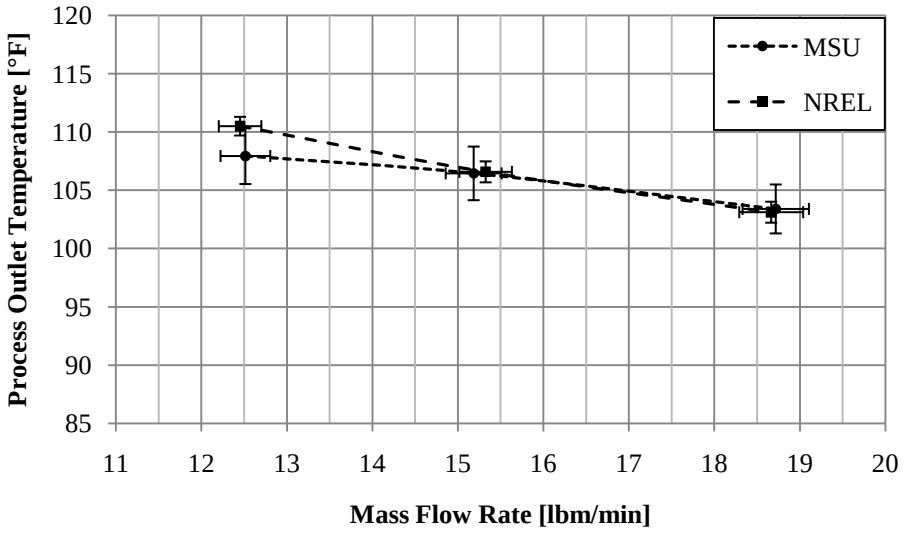

Figure 7.27

Process Outlet Temperature versus Mass Flow Rate of the Process Stream for Tests 1A, 1B, and 1C at MSU and NREL.

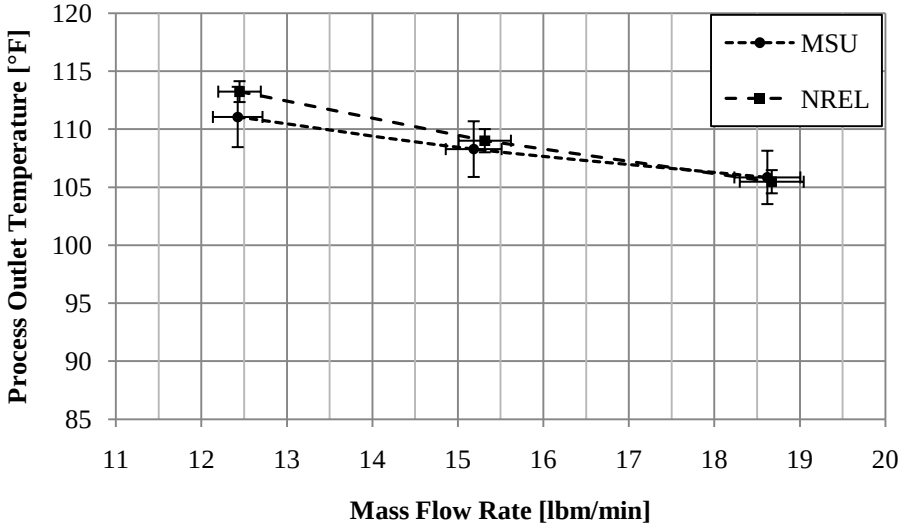

Figure 7.28

Process Outlet Temperature versus Mass Flow Rate of the Process Stream for Tests 2A, 2B, and 2C at MSU and NREL.

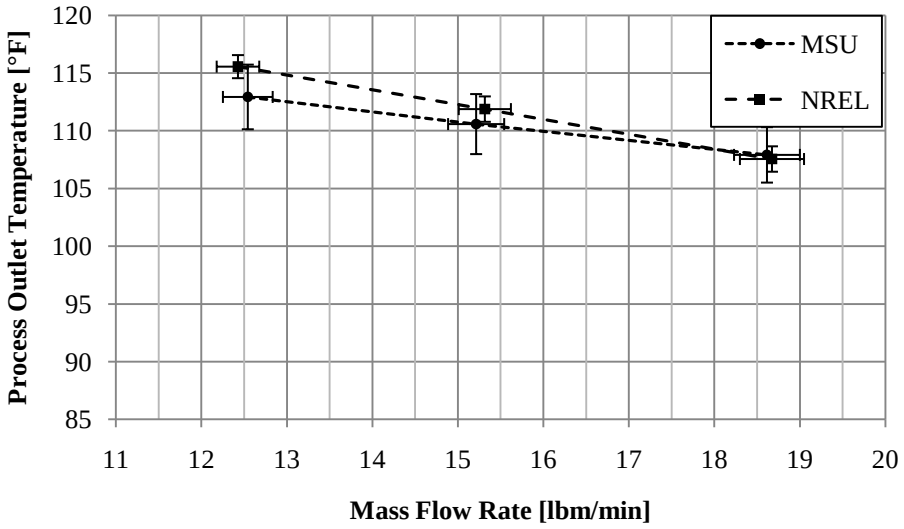

Figure 7.29

Process Outlet Temperature versus Mass Flow Rate of the Process Stream for Tests 3A, 3B, and 3C at MSU and NREL.

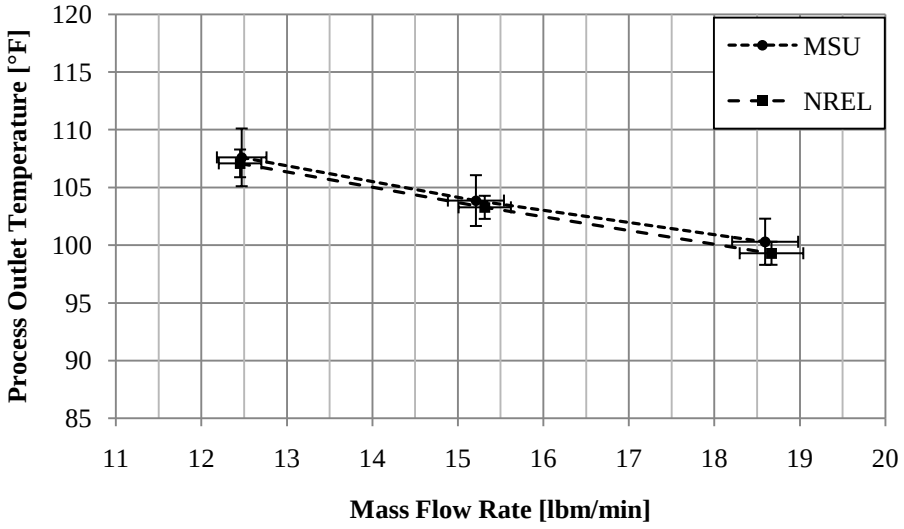

Figure 7.30

Process Outlet Temperature versus Mass Flow Rate of the Process Stream for Tests 4A, 4B, and 4C at MSU and NREL.

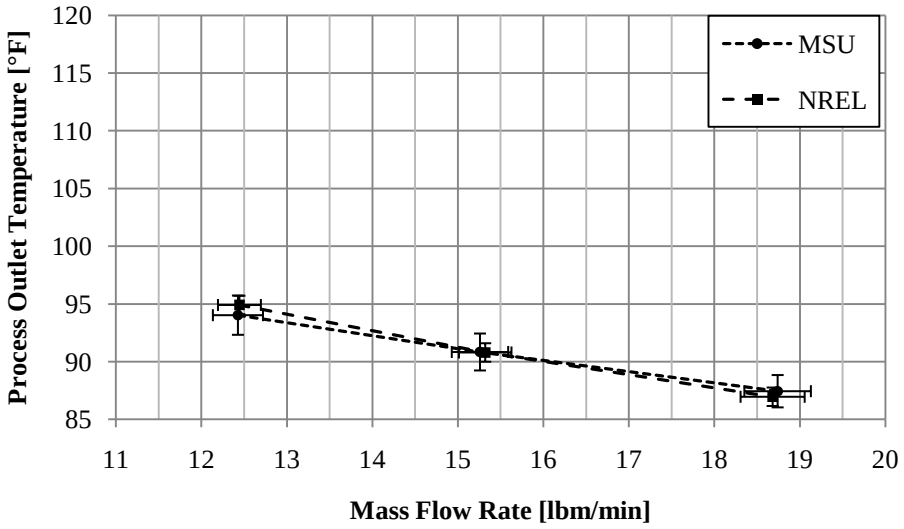

Figure 7.31

Process Outlet Temperature versus Mass Flow Rate of the Process Stream for Tests 5A, 5B, and 5C at MSU and NREL.

Table 7.3

Comparison of Process Outlet Temperature at MSU and NREL.

Test	MSU	NREL	Variation	
	[°F]		*[°F]*	*[%]*
1A	103.4	103.1	0.3	0.3
2A	105.8	105.5	0.4	0.3
3A	107.9	107.6	0.4	0.3
4A	100.3	99.3	1.0	1.0
5A	87.4	87.0	0.5	0.6
1B	107.9	110.5	-2.6	-2.4
2B	111.0	113.2	-2.2	-2.0
3B	112.9	115.6	-2.6	-2.3
4B	107.6	107.1	0.5	0.5
5B	94.0	94.9	-0.9	-0.9
1C	106.4	106.6	-0.1	-0.1
2C	108.3	109.0	-0.7	-0.7
3C	110.6	111.9	-1.3	-1.2
4C	103.9	103.3	0.6	0.6
5C	90.8	90.8	0.0	0.0

CHAPTER VIII

METHODOLOGIES

The content of this chapter is related to the methodologies that have been developed to estimate the performance of solid desiccant dehumidifiers at altitude from performance at standard conditions with the idea of selecting dehumidifiers to operate at altitude. The methodologies have been developed as a result of the analysis performed in Chapter VII. These methodologies can be used to predict the performance of a solid desiccant dehumidifier, as well as other related process associated with the design and operation of the system, as long as the performance at standard conditions is known.

Since certain design conditions should be kept constant when interpolating between standard and altitude conditions. Based on the analysis of the results, it was found that the following conditions must be kept constant when predicting performance. These design conditions should be known for both the process and regeneration streams, and should be the actual conditions (at local atmospheric pressure) for the particular location at altitude. They are:

- Process Inlet Mass Flow Rate
- Process Inlet Dry-Bulb Temperature
- Process Inlet Humidity Ratio
- Regeneration Inlet Mass Flow Rate

- Regeneration Inlet Dry-Bulb Temperature
- Regeneration Inlet Humidity Ratio

By keeping these six parameters constant, the methodologies can be followed in order to predict altitude performance of any solid desiccant dehumidifier, as long as the standard performance for the dehumidifier is available. Outlined below are the presented methodologies to predict the performance of solid desiccant dehumidifiers at altitude: moisture removal capacity, regenerations specific heat input, pressure drop through the wheel, and process stream temperature rise; as well as other design operation topics such as the use of ASHRAE design conditions, fan selection, and the conversion of field measurements at altitude to standard performance.

Moisture Removal Capacity

From the experimental data, it was found that the MRC fluctuates between sea-level and NREL's altitude (5,850 ft) around 4% to 5%, with the MRC decreasing with altitude. These variations are within the accuracies of both MSU and NREL. Therefore, due to (a) the small variation in MRC, (b) its comparison with the uncertainty associated with the experimental data, and (c) the fact that the results were obtained from a specific desiccant wheel with specific regeneration parameters, it seems to be unwise to propose a simple methodology that can be applied as a general methodology for selection of desiccant dehumidifiers at altitude. With this in mind, the change in MRC with respect to altitude may be considered negligible. Therefore, the MRC at altitude is estimated using the available standard software or performance curves for the desiccant wheel and

assumed to be equal. In practical applications, the common safety design factor used in engineering can be defined to take care of the small decrease of MRC with altitude.

In order to have an idea of the magnitude of the safety design factor, the following methodology is proposed to estimate the MRC at altitude based on the results. It should be recalled that the uncertainties of the MRC at MSU were above 6% and at NREL were above 3%.

From Chapter VII it was seen that the variation in MRC between MSU and NREL was about 5%, with the exception of Tests 5. It was shown that this variation may be mainly due to a difference in partial pressure of water vapor. Therefore, an estimation for the MRC at altitude was derived using the difference in partial pressures between the two altitudes. This equation can be seen in Equation (8.1).

$$MRC_z = \frac{MRC_0}{1+\Delta p_w} \tag{8.1}$$

where:

MRC_z = Estimated MRC at altitude, *[lbm/hr]*

MRC_0 = Rated MRC at Standard Conditions, *[lbm/hr]*

Δp_w = Difference in partial pressure between standard conditions and altitude, *[psi]*

Table 8.1 shows the results of Equation (8.1) for the experimental data. It can be seen that the prediction gives a variation that ranges between -2.4 and 1.2%, with the negative meaning that the actual performance is higher than the estimated performance. Although this could lead to oversizing, the uncertainty is quite low when considering the total uncertainty in the actual MRC measurements.

Table 8.1

Comparison of Actual and Estimated MRC at NREL.

Test	Actual	Estimated	Error	
	[lbm/hr]		*[lbm/hr]*	*[%]*
1A	5.03	5.09	0.06	1.1
2A	5.64	5.65	0.01	0.2
3A	6.23	6.19	-0.03	-0.5
4A	6.42	6.39	-0.03	-0.4
5A	5.50	5.40	-0.10	-1.8
1B	4.09	4.14	0.05	1.2
2B	4.56	4.58	0.01	0.3
3B	5.02	4.97	-0.06	-1.1
4B	5.10	5.10	0.00	0.1
5B	4.44	4.33	-0.11	-2.4
1C	4.55	4.58	0.03	0.6
2C	5.10	5.06	-0.04	-0.7
3C	5.71	5.66	-0.05	-0.8
4C	5.79	5.80	0.01	0.2
5C	5.02	4.96	-0.06	-1.2

Since this methodology is developed to deal with standard conditions, a general equation for the change in partial pressure is adapted [7, Chapter 1]. This is shown in Equation (8.2), where the inputs are the design conditions.

$$\Delta p_w = -\frac{w(125\, p_{atm} - 1837)}{125\, w + 544250} \tag{8.2}$$

where:

w = Design humidity ratio, *[Gr/lbm]*

p_{atm} = Atmospheric pressure at altitude, *[psi]* (Equation (6.1))

By using Equations (8.1) and (8.2), the MRC at altitude can be estimated. For Equation (8.2), as altitude approaches sea level, the variation in partial pressure goes to zero and $MRC_z = MRC_o$ in Equation 8.1. It should be noted that the uncertainties

involved with the MRC calculations are quite high and therefore, statistically speaking, the differences could be considered due strictly to biases in the measurement systems. However, based on the analysis of the results and the rationale of the properties of desiccants, it seems that Equation (8.1) is valid.

Regeneration Specific Heat Input

By definition, the RSHI is the ratio of the energy input of the regeneration heater to the MRC, as shown in Equation (2.2). Since the focus of the methodology is to examine the same dehumidification unit between sea-level and altitude, the method used for the regeneration heat should also remain the same. As discussed, the specific heat of air changes negligibly at altitudes less than 10,000 feet. With the mass flow rate and air temperatures at the inlet and exit of the heater constant, the energy input to the heater will also remain a constant. In order to apply this idea to Equation (2.2), the MRC at altitude must be applied. Applying MRC_z to Equation (2.2) yields Equation (8.3). For simplicity, Equation (8.3) is combined with Equation (8.1) to form Equation (8.4).

$$RSHI_z = \frac{Q}{MRC_z} \tag{8.3}$$

$$RSHI_z = (1 + \Delta p_w) RSHI_0 \tag{8.4}$$

where:

$RSHI_z$ = Estimated RSHI at altitude, *[BTU/lbm]*

$RSHI_0$ = Rated RSHI at Standard Conditions, *[BTU/lbm]*

Pressure Drop through the Wheel

The pressure drop was found to hold the most significant difference with respect to altitude. To propose a methodology some analysis of how pressure drop has been considered in previous studies is of great importance.

Pesaran and Heiden [10] suggested Equation (8.5) to estimate the pressure drop through the wheel for fully developed laminar flow assuming negligible entrance, exit, and acceleration effects.

$$\Delta P = \frac{1}{2}\frac{\dot{m}\,\mu\,\cancel{l}\,L}{\rho\,D_h^2\,A} = \frac{1}{2}\frac{\mu\,\cancel{l}\,L}{D_h^2}\,V \tag{8.5}$$

where:

$\cancel{l}$ = Geometric factor

Slayzak, *et al.* [15] used Equation (8.6) for laminar flow and Equation (8.7) for turbulent flow when analyzing the effect of altitude on pressure drop, with the assumption that the loss coefficient for turbulent entrance effects quantitatively follows this relationship.

$$\Delta P_{lam} = \rho\,\frac{64}{Re}\frac{L}{D_h}\frac{V^2}{2} = 32\,\frac{L}{D_h^2}\mu V \tag{8.6}$$

$$\Delta P_{turb} = \rho\,\frac{C}{Re^{0.25}}\frac{L}{D_h}\frac{V^2}{2} \tag{8.7}$$

Harshe, *et al.* [17] present Equation (8.8) as a general equation to describe the pressure drop through a desiccant wheel in their mathematical models. As can be noticed, *f* represents the friction factor which is a function of the inverse of Reynolds number. Therefore, the first term in Equation (8.8) has the same form as Equations (8.5) and (8.6).

$$\Delta P = \frac{2\, f\, \rho\, V^2 L}{D_h} + K \frac{1}{2} \rho\, V^2 \tag{8.8}$$

For all the equations Reynolds number can be defined as

$$Re = \frac{\rho\, V\, D_h}{\mu} = \frac{\dot{m}\, D_h}{\mu\, A} \tag{8.9}$$

Since all geometric parameter are fixed, by analyzing the previous equations it can be noticed that if the inlet conditions and the mass flow rate are kept constant between sea-level (standard conditions) and altitude, the pressure drop due to laminar, turbulent, entrance, and exit effect can be described by two terms, one depending on velocity and the other depending on the square of the velocity. Although air properties will change as the air moves through the desiccant wheel, the tests results suggest no significant variation in temperature between sea level and altitude. Therefore, effects due to variation of temperature can be neglected and only the effect of variation in density due to altitude becomes important.

Based on the previous discussion, the pressure drop (ΔP) through a honeycomb matrix as a function of actual face velocity (V) and density (ρ) can be well represented as a second order polynomial of the form

$$\Delta P(V) = C_l\, V + C_{k,t}\, \rho\, V^2 \tag{8.10}$$

where the coefficients C_l and $C_{k,t}$ are specific for each desiccant wheel, which account for geometric parameters of the desiccant wheel, thermophysical properties of the air, and units.

By knowing two different sets of actual face velocity and pressure drop, the coefficients C_l and $C_{k,t}$ can be found by simply solving the system of equations. When

keeping the mass flow rate constant, and with the coefficients known, the pressure drop at altitude (ΔP_z) can be calculated as

$$\Delta P_z(V_z) = C_l\, V_z + C_{k,t}\, \rho_z\, V_z^2 \tag{8.11}$$

where V_z and ρ_z are the actual face velocity and air density at altitude for the design mass flow rate, respectively.

Due to viscous effects of temperature, the coefficients C_l and $C_{k,t}$ must be found for process (low temperatures) and regeneration (high temperatures) air streams independently.

For simplicity, Equations (8.12) and (8.13) are provided to determine the coefficients as follows

$$C_l = \frac{\Delta P_1\, V_2^2 - \Delta P_2\, V_1^2}{(V_1\, V_2^2 - V_1^2\, V_2)} \tag{8.12}$$

$$C_{k,t} = \frac{\Delta P_2 - C_l\, V_2}{0.075\, V_2^2} \tag{8.13}$$

where subscripts 1 and 2 refer to the two sets of actual face velocity and pressure drop.

Tables 8.2 and 8.3 show the results applying Equations (8.10) through (8.13) for the process and regeneration streams, respectively. To obtain these results, the data from Tests A and B at MSU were used as Set 1 and Set 2, respectively. This method was repeated for each Test 1, 2, 3, 4, and 5, so that the data used for Sets 1 and 2 had the same temperature and humidity ratio as the inputs for altitude. It can be seen from the results of the estimation that the error for process ranges from -0.013 in WC (-2.6%) to 0.059 in WC (14.5%) for process with an average of 3.6%, and 0.005 in WC (1.0%) to 0.027 in WC (9.2%) for regeneration with an average of 4.1%. The error is evaluated as the variation between and predicted and actual pressure drops, but it should be kept in mind

that the actual data has an uncertainty associated with it. Without experimental uncertainty, the errors may be lower since the methodology is based on fundamental equations describing pressure drop.

The previously described equations (Polynomial Methodology) were used to validate the methodology with the experimental data. However, further analysis shows that the pressure drop can be computed using Equation (8.14) (Density Ratio Methodology). Equation (8.14) was derived using Equation (8.11) along with the definition of mass flow rate and the fact that the mass flow rate remains constant between sea-level and altitude. The derivation of this equation can be seen in Appendix B. By using Equation (8.14), the variations between the estimated pressure drops and actual pressure drops for NREL were computed again and are shown in Tables 8.4 and 8.5 for process and regeneration, respectively. By comparing the results of the two methodologies it can be noticed that the variations are negligible and can be attributed to uncertainties in the experimental data. Therefore, for simplicity, the Density Ratio Methodology should be used.

$$\Delta P_z = \frac{\rho_0}{\rho_z} \Delta P_0 \tag{8.14}$$

It should be noted that, when calculating the density at altitude, the actual atmospheric pressure should be used; however, although weather conditions may cause small variations with negligible effects compared with the uncertainty of the measurements, the standard barometric pressure found using Equation (6.1) can be used.

Since the methodology compares densities at the same temperature and humidity ratio, as defined by equations from ASHRAE [7, Chapter 1], the ratio of the densities can

be defined as the ratio of standard atmospheric pressures (Equation (6.1)). Therefore, Equation (8.15) is equivalent to Equation (8.14), with Z in feet.

$$\Delta P_z = \frac{1}{(1-6.8754\ x\ 10^{-6}\ Z)^{5.2559}} \Delta P_0 \tag{8.15}$$

Table 8.2

Comparison of Actual and Estimated Process Pressure Drop at NREL Using the Polynomial Methodology.

Test	**Actual**	**Estimated**	**Error**	
	[in WC]		*[in WC]*	*[%]*
1A	0.689	0.696	0.007	1.0
1B	0.475	0.465	-0.010	-2.1
1C	0.579	0.572	-0.007	-1.2
2A	0.707	0.700	-0.007	-1.0
2B	0.475	0.463	-0.013	-2.6
2C	0.582	0.572	-0.010	-1.8
3A	0.709	0.708	-0.002	-0.2
3B	0.476	0.473	-0.003	-0.7
3C	0.545	0.588	0.044	8.0
4A	0.675	0.713	0.038	5.6
4B	0.451	0.460	0.008	1.8
4C	0.561	0.574	0.013	2.4
5A	0.658	0.679	0.022	3.3
5B	0.409	0.468	0.059	14.5
5C	0.523	0.567	0.044	8.3

Table 8.3

Comparison of Actual and Estimated Regeneration Pressure Drop at NREL Using the Polynomial Methodology.

Test	Actual	Estimated	Error	
	[in WC]		*[in WC]*	*[%]*
1A	0.472	0.476	0.005	1.0
1B	0.309	0.318	0.009	2.8
1C	0.381	0.391	0.010	2.7
2A	0.463	0.476	0.013	2.8
2B	0.304	0.313	0.009	3.0
2C	0.382	0.388	0.006	1.7
3A	0.463	0.476	0.013	2.8
3B	0.301	0.313	0.012	4.1
3C	0.368	0.392	0.024	6.5
4A	0.456	0.467	0.011	2.4
4B	0.290	0.311	0.021	7.3
4C	0.368	0.383	0.015	4.0
5A	0.464	0.484	0.020	4.3
5B	0.292	0.319	0.027	9.2
5C	0.370	0.395	0.026	6.9

Table 8.4

Comparison of Actual and Estimated Process Pressure Drop at NREL Using the Density Ratio Methodology.

Test	**Actual**	**Estimated**	**Error**	
	[in WC]		*[in WC]*	*[%]*
1A	0.689	0.698	0.009	1.3
1B	0.475	0.467	-0.008	-1.6
1C	0.579	0.570	-0.009	-1.6
2A	0.707	0.698	-0.009	-1.3
2B	0.475	0.462	-0.013	-2.8
2C	0.582	0.566	-0.016	-2.7
3A	0.709	0.705	-0.004	-0.6
3B	0.476	0.477	0.001	0.2
3C	0.545	0.598	0.054	9.8
4A	0.675	0.709	0.034	5.1
4B	0.451	0.461	0.009	2.1
4C	0.561	0.568	0.007	1.3
5A	0.658	0.681	0.024	3.6
5B	0.409	0.467	0.058	14.3
5C	0.523	0.567	0.044	8.4

Table 8.5

Comparison of Actual and Estimated Regeneration Pressure Drop at NREL Using the Density Ratio Methodology.

Test	Actual	Estimated	Error	
	[in WC]		*[in WC]*	*[%]*
1A	0.472	0.477	0.005	1.1
1B	0.309	0.322	0.012	3.9
1C	0.381	0.385	0.004	1.1
2A	0.463	0.472	0.008	1.8
2B	0.304	0.313	0.008	2.8
2C	0.382	0.387	0.005	1.3
3A	0.463	0.476	0.014	3.0
3B	0.301	0.316	0.015	5.0
3C	0.368	0.388	0.020	5.5
4A	0.456	0.471	0.015	3.3
4B	0.290	0.312	0.022	7.6
4C	0.368	0.381	0.013	3.4
5A	0.464	0.484	0.020	4.3
5B	0.292	0.322	0.030	10.1
5C	0.370	0.391	0.021	5.7

Process Outlet Temperature

As discussed in Chapter VII, the process outlet temperature did not follow any specific trend between the two locations, and the variation was quite small, varying between -2.6°F (-2.4%) and 1.0°F (1.0%). Since the process temperature rise is due to the amount of water vapor adsorbed by the desiccant (latent heat) plus an additional amount of heat that is equal to between 5 and 25% of the latent heat [7, Chapter 32], it can be said that the process outlet temperature is directly related to the latent heat of water vapor and the specific desiccant material used. Since only one type of desiccant was tested, this fact alone makes it quite difficult to develop a simple and general

methodology to predict the change in outlet temperature at altitude. This reasoning, coupled with the small variations in the outlet temperatures, further shows that a general methodology cannot be used. Therefore, the change in process outlet temperature between standard conditions and altitude can be considered negligible. However, it should again be noted that at lower flow rates the outlet temperature at altitude was slightly higher, while at higher flow rates the outlet temperature at altitude was slightly lower, but with less magnitude than for the low flow rates.

Use of ASHRAE Design Conditions

Chapter 14 of the 2009ASHRAE Handbook – Fundamentals [7] provides climatic design conditions for 5,564 locations worldwide. This information includes, but is not limited to, latitude, longitude, elevation and annual percentiles for heating, cooling, evaporation, and dehumidification. The useful figures for this topic are the elevation and annual percentiles for dehumidification.

The dehumidification section provides information regarding the annual percentiles of 0.4 and 1.0 for the dew-point temperature, humidity ratio, and the mean coincident dry-bulb temperature. This is useful when selecting a desiccant unit to be used at altitude because the humidity ratio is calculated at the actual atmospheric pressure. Therefore, the humidity ratio reflects the actual partial pressure of water vapor, which is the driving force behind desiccant dehumidification.

In other words, the focus of this study has been to explain what variables must be kept constant when estimating performance at altitude from performance ratings at standard conditions. Chapter 14 gives information regarding the humidity ratio and

temperature of thousands of locations worldwide, with the information corresponding to the design conditions reflected in the methodologies. Therefore, this information can be useful in following the methodologies so that the proper humidity is used for the selection of desiccant equipment.

Since the method keeps constant the dry-bulb temperature and humidity ratio, the design conditions from Chapter 14 are the same to be used to estimate the performance at standard conditions. This standard condition performance is then used as the inputs to the proposed methodologies for MRC, RSHI, pressure drop, and process outlet temperature to estimate the performance at altitude.

Fan Selection

The first step in fan selection is defining the system pressure loss [3, Chapter 20]. This pressure loss is the total losses due to duct elements throughout the entire system that the fan will be operating in, which includes the pressure drop through the desiccant wheel. Generally, fan manufactures give information on how to select fans to operate at altitude. The additional information that must be taken into consideration is the variation in pressure drop through the wheel at altitude. However, additional information is provided in this section for completeness.

The fan laws provide a useful comparison between two fans. By considering a change in density on the speed, pressure, and power of a fan, the following equations can be used to compare the same fan between sea-level and altitude [21, 3, Chapter 20]. For a constant mass process, the speed of the fan must increase with altitude in order to move the same mass of air, as shown in Equation (8.16). This, in turn, increases the pressure

drop that the fan can overcome, as shown in Equation (8.17). However, the relationship between fan power and speed is a cubic relation, as shown in Equation (8.18). Therefore, it can be seen that more power will be needed to provide the higher speed to keep the mass flow rate constant; however the increase in speed will provide a higher pressure differential generated by the fan. Since the speed, pressure, and power at sea-level must be known to extrapolate this performance to altitude, the performance curves for the specific fan must be available. These performance curves will give more detail on how the magnitude of the change in speed will affect the fan power by considering the impact of the increase of pressure drop through the wheel compared with the increase of the pressure drop that the fan can overcome.

$$N_z = \frac{\rho_0}{\rho_z} N_0 \tag{8.16}$$

$$\Delta P_{\mathrm{f,z}} = \Delta P_{\mathrm{f,0}} \left(\frac{N_z}{N_0}\right)^2 \frac{\rho_z}{\rho_0} \tag{8.17}$$

$$W_z = W_0 \left(\frac{N_z}{N_0}\right)^3 \frac{\rho_z}{\rho_0} \tag{8.18}$$

where:

N = Fan speed, *[rpm]*

ΔP_f = Pressure change across fan, *[in WC]*

W = Fan power, *[hp]*

Method of Converting Field Measurements at Altitude to Standard Performance

When taking measurements in the field to determine the performance of a desiccant dehumidifier, sometimes it may be useful to convert this altitude performance to standard performance. In order to do this, the first thing to consider is what

measurements can be taken. The performance figures of merit are the MRC, RSHI, pressure drop through the wheel, and the process outlet temperature.

In order to obtain the MRC, the flow rate and humidity ratios must first be known. As discussed in Chapter IV, there are three methods of calculating the humidity ratio: relative humidity, wet-bulb temperature, and dew-point temperature. Any of these methods will work, however it is very important that the actual barometric pressure of the site be used when finding the humidity ratio. Since the flow rate can be directly measured, the only thing to keep in mind is that the actual density of the air at the location must be used when calculating the flow rate.

With this information known, the MRC_z can be calculated. To convert this calculation to standard performance, Equation (8.1) should be solved for MRC_0. As previously explained, this will give a reasonable estimate as to the magnitude of the safety design factor that is implemented in the unit at altitude.

Since the RSHI varies inversely proportional to the MRC, the method of converting the RSHI at altitude to RSHI at standard conditions is to solve Equation (8.3) for $RSHI_0$ and input the measurements at the altitude site.

For the pressure drop through the wheel, Equation (8.15) should be solved for ΔP_0 and the appropriate field measurements used to obtain the standard condition pressure drop.

Since the methodology for the process outlet temperature proposes that the change between standard conditions and altitude is negligible, there is nothing to be done

when converting the process outlet temperature from altitude to standard conditions. This measurement can be assumed the same at both locations.

The material presented in this Chapter describes the methodologies in detail to explain the rationality behind them, but a summary of the methodologies is presented in Appendix C.

CHAPTER IX

EASE OF USE CONFIRMATION

Activities

Activities developed for the evaluation of the proposed methodologies have been conducted at MSU. Different activities were given to graduate and undergraduate students, as well as engineers in the industry. These activities are shown in Appendix D. Based on analysis of the evaluation activities developed (results and participants' comments), adjustments were made to the methodologies to ensure simplicity, resulting in the final methodologies presented in Chapter VIII.

Step-by-Step Example of Methodologies

Shown below is a step-by-step example of how the methodologies can be used. The example was completed using design conditions for the Colorado Springs Municipal Airport as specified by Chapter 14 in the 2009 ASHRAE Handbook – Fundamentals [7] as well as specific information obtained from RotorSource's performance software, DSELECT [25]. A screenshot of DSELECT with the design conditions is shown in Figure 9.1.

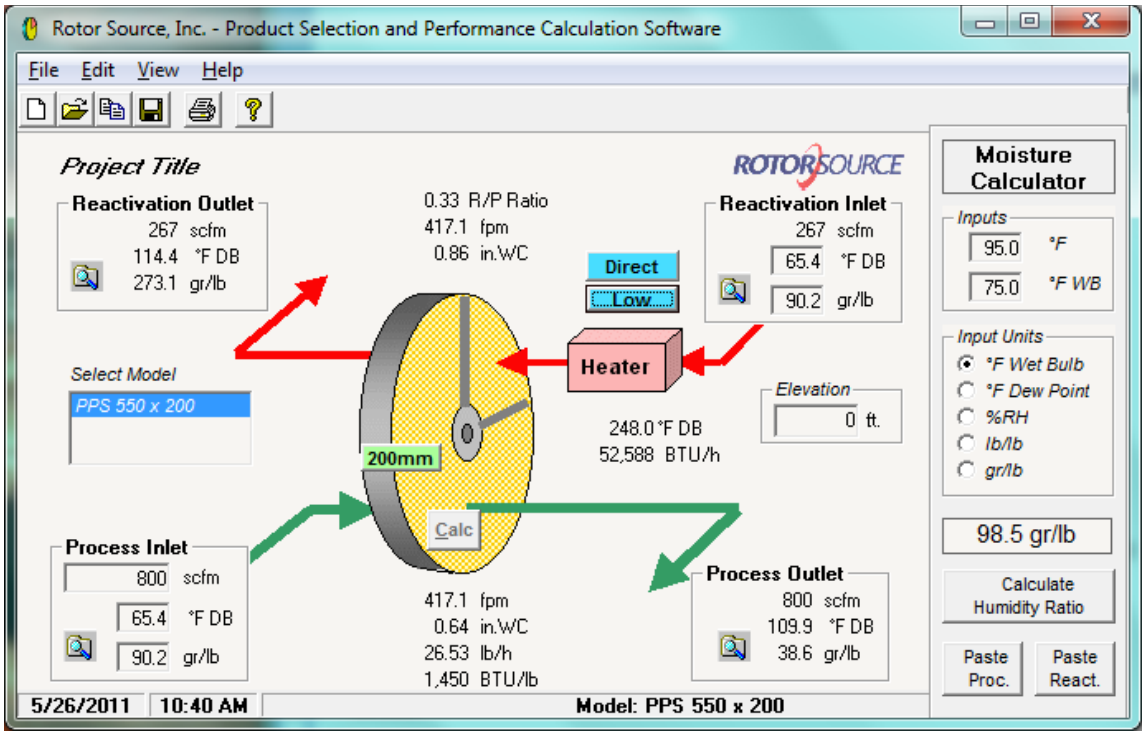

Figure 9.1

Screenshot of RotorSource Software, DSELECT.

Site: Colorado Springs Municipal Airport, Colorado Springs, CO
Altitude: 6,171 ft
Dehumidifier model: *PPS 550 x 200*

Process stream:

Dry Bulb Temperature: 65.4°F
Humidity Ratio: 90.2 Gr/lbm
Mass flow rate: 800 scfm (60 lbm/min)

Regeneration stream:

Dry Bulb Temperature: 65.4°F (before heater), heated to 248°F (Low, Indirect Heat)
Humidity Ratio: 90.2 Gr/lbm
Mass flow rate: (given by RotorSource software)

In order to follow the methodology, the following standard performance figures must be obtained from the selection software.

MRC_0 = 26.53 lbm/hr

$RSHI_0$ = 1,450 BTU/lbm

$\Delta P_{P,0}$ = 0.64 in WC

$\Delta P_{R,0}$ = 0.86 in WC

$T_{PO,0}$ = 109.9°F

Moisture Removal Capacity

For the design altitude, the barometric pressure is found using Equation (6.1).

$$p_{atm} = 14.696(1 - 6.8754 \times 10^{-6}(6{,}171\ ft))^{5.2559} = 11.701 \text{ psi}$$

Utilizing this atmospheric pressure as well as the design process inlet humidity ratio, Equation (8.2) is used to find the difference in partial pressure of water vapor.

$$\Delta p_w = -\frac{90.2(125(11.701) - 1837)}{125(90.2) + 544250} = 0.061 \text{ psi}$$

Finally, Equation (8.1) can be used to find the MRC at altitude.

$$MRC_z = \frac{26.53}{1 + 0.061} = \mathbf{25.01} \text{ lbm/hr}$$

Regeneration Specific Heat Input

To find the RSHI at altitude, Equation (8.4) must be used. With both inputs known, the equation can be used directly.

$$RSHI_z = (1 + 0.061)RSHI_0 = \mathbf{1{,}538} \text{ BTU/lbm}$$

Pressure Drop through the Wheel

With the standard condition pressure drops and altitude known, Equation (8.16) can be used to estimate the pressure drops at altitude.

$$\Delta P_{P,z} = \frac{1}{\left(1 - 6.8754\ x\ 10^{-6}(6{,}171)\right)^{5.2559}} 0.64 = \mathbf{0.80}\ \text{in WC}$$

$$\Delta P_{P,z} = \frac{1}{\left(1 - 6.8754\ x\ 10^{-6}(6{,}171)\right)^{5.2559}} 0.86 = \mathbf{1.08}\ \text{in WC}$$

Process Outlet Temperature

As defined by the methodology for the process outlet temperature, there is no variation between sea-level and altitude. Therefore

$$T_{PO,z} = T_{PO,0} = \mathbf{109.9}°\text{F}$$

CHAPTER X

TOOL

As shown in the step-by-step example in Chapter IX, the methodologies can include calculations that might not be readily available to some. Therefore, a general tool has been developed in Microsoft Excel to simplify the methodologies even further. A screenshot of the methodologies tool is shown in Figure 10.1. To utilize this tool, the required inputs are the design conditions (elevation, as well as inlet dry-bulb temperature and humidity ratio for process and regeneration streams) and the standard performance given by the manufacturer. This Excel tool has been adapted to HTML format in order that it can be available online to the general public.

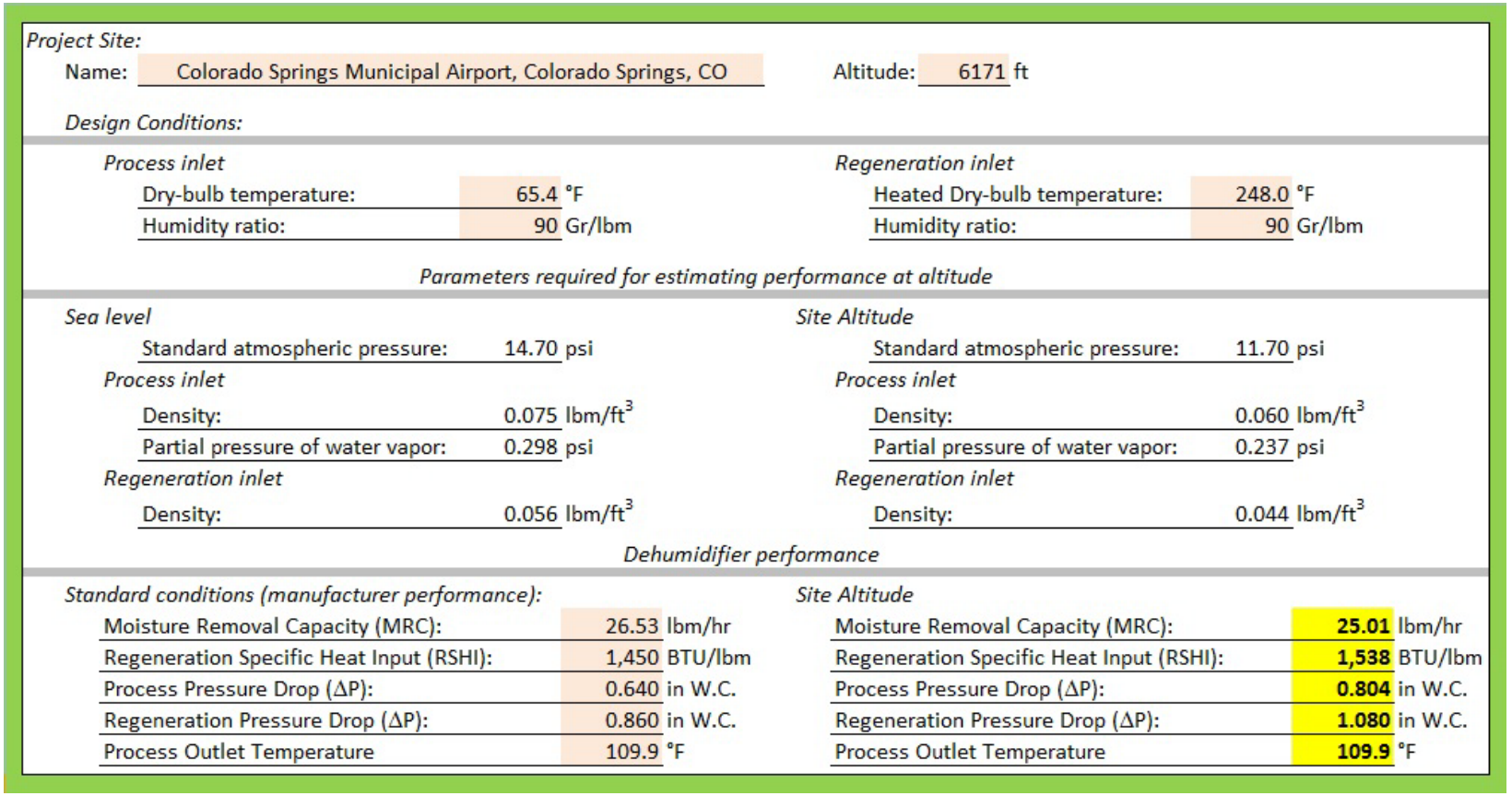

Project Site:

Name: Colorado Springs Municipal Airport, Colorado Springs, CO — Altitude: 6171 ft

Design Conditions:

Process inlet		*Regeneration inlet*	
Dry-bulb temperature:	65.4 °F	Heated Dry-bulb temperature:	248.0 °F
Humidity ratio:	90 Gr/lbm	Humidity ratio:	90 Gr/lbm

Parameters required for estimating performance at altitude

Sea level		*Site Altitude*	
Standard atmospheric pressure:	14.70 psi	Standard atmospheric pressure:	11.70 psi
Process inlet		*Process inlet*	
Density:	0.075 lbm/ft^3	Density:	0.060 lbm/ft^3
Partial pressure of water vapor:	0.298 psi	Partial pressure of water vapor:	0.237 psi
Regeneration inlet		*Regeneration inlet*	
Density:	0.056 lbm/ft^3	Density:	0.044 lbm/ft^3

Dehumidifier performance

Standard conditions (manufacturer performance):		*Site Altitude*	
Moisture Removal Capacity (MRC):	26.53 lbm/hr	Moisture Removal Capacity (MRC):	**25.01** lbm/hr
Regeneration Specific Heat Input (RSHI):	1,450 BTU/lbm	Regeneration Specific Heat Input (RSHI):	**1,538** BTU/lbm
Process Pressure Drop (ΔP):	0.640 in W.C.	Process Pressure Drop (ΔP):	**0.804** in W.C.
Regeneration Pressure Drop (ΔP):	0.860 in W.C.	Regeneration Pressure Drop (ΔP):	**1.080** in W.C.
Process Outlet Temperature	109.9 °F	Process Outlet Temperature	**109.9** °F

Figure 10.1

Screenshot of the Developed Tool for the Methodologies.

CHAPTER XI

CONCLUSIONS

Research was performed to develop a general methodology to be used for the selection of desiccant equipment at altitude. The research involved taking performance data from a test cassette with a diameter of 300 mm and a depth of 100 mm, a 50/50 wheel split, and a rotational speed of 14 rph, using set design inlet conditions. These conditions were developed based on information collected from different industry practices which concluded that by keeping the mass flow rate, inlet temperature, and inlet humidity ratio constant, the difference in performance between sea-level and altitude would be negligible.

The desiccant dehumidifier was tested by MSU and NREL, and the results of the tests were compared to find the relationship between the performance at sea-level and at altitude. The trends in the data were then adapted into the methodology for selecting desiccant equipment at altitude. The results of the tests showed that by keeping the mass flow rate, inlet temperature, and inlet humidity ratio constant between sea-level and altitude, the MRC varied by about 5%, the RSHI varied inversely proportional to the MRC, the process outlet temperature varied by about 1%, and the pressure drop through the wheel, which was the parameter most affected by altitude, varied proportional to the ratio of the atmospheric pressures between sea-level and altitude.

REFERENCES CITED

[1] Integrated Energy Systems. Available at: http://www.cogeneration.net/IntegratedEnergySystem.htm

[2] U.S. Department of Energy: ITP Industrial Distributed Energy: Thermally Activated Technologies. Available at: http://www1.eere.energy.gov/industry/distributedenergy/tat.html

[3] *2008 ASHRAE Handbook – HVAC Systems and Equipment*. American Society of Heating, Refrigeration, and Air-Conditioning Engineers, Inc.: Atlanta, GA.

[4] Houghton, D.J., Bishop, R.C., Lovins, A.B., Stickney, B.L., Newcomb, J.J., Davids, B.J. (1992) *State of the Art Technology Atlas: Space Cooling and Air Handling*. Boulder, Colorado: ESource, Inc.

[5] Howell, J. R., Peterson, J. L. (1986) *Preliminary Performance Evaluation of a Hybrid Vapor Compression/Liquid Desiccant Air Conditioning System*. ASME: Anaheim, California. Paper 86-WA/Sol. 9.

[6] Panaras, G., Mathioulakis, E., Belessiotis, V. (2007) *Achievable Working Range for Solid All-Desiccant Air-Conditioning Systems under Specific Space Comfort Requirements*. *Energy and Buildings* Vol. 39, No. 9, pp. 1055-1060.

[7] *2009 ASHRAE Handbook – Fundamentals*. American Society of Heating, Refrigeration, and Air-Conditioning Engineers, Inc.: Atlanta, GA.

[8] Bry-Air Dehumidification Applications Engineering Manual. Available at: http://www.bryair.com/download_pro.php?action=downloadfile&file=uploads/category_eng_manuals/MANU_B51BEB17894026EDApplication%20Engineering%20Manual_Final_2010.pdf

[9] Hamed, A.M., Khalil, A., Kabeel, A.E., Bassuoni, M.M., Elzahaby, A.M. (2005) *Performance Analysis of Dehumidification Rotating Wheel using Liquid Desiccant*. *Renewable Energy* Vol. 30, pp. 1689-1712.

[10] Pesaran, A.A., Heiden, R. (1994). *Influence of Altitude on the Performance of Desiccant-Cooling Systems*. *Energy* Vol. 19, No. 11, pp. 1165-1179.

[11] *1339-TRP, Selection of Desiccant Equipment at Altitude*. American Society of Heating, Refrigeration, and Air-Conditioning Engineers, Inc.: Atlanta, GA.

[12] Ruivo, C.R., Costa, J.J., Figueiredo, A.R. (2011) *Influence of the Atmospheric Pressure on the Mass Transfer Rate of Desiccant Wheels*. *International Journal of Refrigeration* Vol. 34, No. 3, pp. 707-718.

[13] Chung, J.D., Lee, D.Y. (2009) *Effect of Desiccant Isotherm on the Performance of Desiccant Wheel*. *International Journal of Refrigeration* Vol 32, pp. 720-726.

[14] *Method of Testing for Rating Desiccant Dehumidifiers Utilizing Heat for the Regeneration Process*. American Society of Heating, Refrigeration, and Air-Conditioning Engineers, Inc.: Atlanta, GA. ANSI/ASHRAE Standard 139-2007.

[15] Slayzak, S.J., Ryan, J.P., Jalalzadeh-Azar, A.A. (2002) *Measured Effect of Altitude on the Performance of a Regenerated Desiccant Matrix*. ASHRAE Transactions: Symposia. Vol. 108(2), pp. 556-562. (NREL Report No. 33844).

[16] Ruivo, C.R., Costa, J.J., Figueiredo, A.R. (2011). *Numerical Study of the Influence of the Atmospheric Pressure on the Heat and Mass Transfer Rates of Desiccant Wheels*. *International Journal of Heat and Mass Transfer* Vol. 54, pp. 1331-1339.

[17] Harshe, Y.M., Utikar, R.P., Ranade, V.V., Pahwa, D. (2005) *Modeling of Rotary Desiccant Wheels*. *Chemical Engineering & Technology* Vol. 28, No. 12, pp. 1473-1479.

[18] Schultz, C.C. (2006) *Engineering for High Altitudes*. *Engineered Systems*, pp. 26-33.

[19] Hodge, B.K.., Taylor, R.P. (1999) *Analysis and Design of Energy Systems*. Upper Saddle River, NJ: Prentice Hall. Print.

[20] Wen, T., Tian, J., Lu, T.J., Queheillalt, D.T., Wadley, H.N.G. (2006) *Forced Convection in Metallic Honeycomb Structures*. *International Journal of Heat and Mass Transfer* Vol. 49, pp. 3313-3324.

[21] Belady, C.L. (1996) *Design Considerations for Air Cooling Electronic Systems in High Altitude Conditions*. *IEEE Transactions on Components, Packaging, and Manufacturing Technology – Part A* Vol. 19, No. 4, pp. 495-500.

[22] Tretiak, C.S., Abdallah, N.B. (2009) *Sorption and Desorption Characteristics of a Packed Bed of Clay-$CaCl_2$ Desiccant Particles*. *Solar Energy* Vol. 83, pp. 1861-1870.

[23] Niu, J.L., Zhang, L.Z. (2002) *Heat Transfer and Friction Coefficients in Corrugated Ducts Confined by Sinusoidal and Arc Curves*. *International Journal of Heat and Mass Transfer* Vol. 45, pp. 571-578.

[24] NovelAire Technologies
http://www.novelaire.com

[25] RotorSource
http://www.rotorsource.com

[26] Munters Corporation
http://www.munters.com

[27] Desiccant Rotors International
http://www.drirotors.com

[28] Teige, P. (6 Aug. 2010). Email Interview.

[29] Slayzak, S.J., Ryan, J.P. (2000). *Desiccant Dehumidification Wheel Test Guide*. National Renewable Energy Laboratory: Golden, Colorado. NREL/TP-550-26131.

[30] Slayzak, S.J., Ryan, J.P. (1998) *Instrument Uncertainty Effect on Calculation of Absolute Humidity Using Dewpoint, Wet-Bulb, and Relative Humidity Sensors*. Prepared for: Solar 98: Renewable Energy for the Americas Conference: Albuquerque, New Mexico. NREL/CP-550-24523.

[31] Coleman, H.W., Steele, W.G. (2009) Experimentation, Validation, and Uncertainty Analysis for Engineers. Hoboken, NJ: John Wiley & Sons. Print.

APPENDIX A

MATHCAD WORKSHEET FOR UNCERTAINTY ANALYSIS

Relative Humidity Method

Definitions

Grains per pound

$$Gr := \frac{lbm}{7000}$$

Conversion from Fahrenheit to Rankine

$$F(T) := \overrightarrow{[(T + 459.67)\cdot R]}$$

Full-Scale of the pressure transducer used for flow rates

$$FS := 0.25$$

Constant used in the flow rate equation

$$C_V := 1096.5$$

Specific enthalpy of water vapor

$$h_{fg} := 970\frac{BTU}{lbm}$$

Specific heat of air

$$c_p := 0.24\cdot\frac{BTU}{lbm}$$

Gas constant for dry air

$$R_{da} := 53.35\frac{ft\cdot lbf}{lbm\cdot R}$$

Inputs

Uncertainties

$$ac_{pz} := 0$$

$$u_{Tpi} := 0.18\Delta°F$$

$$u_{Tpo} := 0.18\Delta°F$$

$$u_{\phi po} := 1\%$$

$$u_{\Delta Ppo} := \overrightarrow{(0.5\%\cdot FS)}$$

$u_{\phi pi} := (1 \;\; 1 \;\; 1 \;\; 1.5 \;\; 1.5 \;\; 1 \;\; 1 \;\; 1 \;\; 1.5 \;\; 1.5 \;\; 1 \;\; 1 \;\; 1 \;\; 1.5 \;\; 1.5)^{T}$ %

*The different numbers represent the different uncertainties associated with high relative humidity.

Data

Barometric pressure:

$$p_z := \begin{pmatrix} 14.77 \\ 14.63 \\ 14.63 \\ 14.77 \\ 14.75 \\ 14.69 \\ 14.72 \\ 14.66 \\ 14.50 \\ 14.77 \\ 14.63 \\ 14.63 \\ 14.66 \\ 14.65 \\ 14.73 \end{pmatrix} \text{psi} \qquad u_{pz} := \overrightarrow{\left(ac_{pz} \cdot p_z\right)}$$

Process inlet temperature and relative humidity:

$$T_{pi} := \begin{pmatrix} 75.0 \\ 74.9 \\ 75.1 \\ 65.1 \\ 55.1 \\ 75.0 \\ 75.0 \\ 75.0 \\ 65.0 \\ 55.2 \\ 75.1 \\ 75.0 \\ 74.9 \\ 65.0 \\ 55.2 \end{pmatrix} \qquad \phi_{pi} := \begin{pmatrix} 61.4 \\ 70.5 \\ 80.2 \\ 98.6 \\ 98.5 \\ 60.5 \\ 70.4 \\ 81.4 \\ 97.7 \\ 97.9 \\ 60.3 \\ 70.2 \\ 80.9 \\ 98.5 \\ 97.1 \end{pmatrix} \%$$

Process outlet temperature and relative humidity: Flow Rate:

$$T_{po} := \begin{pmatrix} 103.4 \\ 105.8 \\ 107.9 \\ 100.3 \\ 87.4 \\ 107.9 \\ 111.0 \\ 112.9 \\ 107.6 \\ 94.0 \\ 106.4 \\ 108.3 \\ 110.6 \\ 103.9 \\ 90.8 \end{pmatrix} \qquad \phi_{po} := \begin{pmatrix} 14.7 \\ 16.0 \\ 17.7 \\ 17.1 \\ 14.9 \\ 10.6 \\ 11.8 \\ 13.7 \\ 11.5 \\ 9.0 \\ 12.1 \\ 13.9 \\ 15.2 \\ 14.0 \\ 11.0 \end{pmatrix} \% \qquad Acfmpo := \begin{pmatrix} 265.4 \\ 267.9 \\ 269.0 \\ 262.4 \\ 258.2 \\ 179.8 \\ 179.2 \\ 182.4 \\ 181.4 \\ 172.9 \\ 218.4 \\ 219.3 \\ 220.3 \\ 217.6 \\ 211.7 \end{pmatrix} \cdot cfm$$

Calculations

Saturation Pressure

$C_8 := -1.0440397 \times 10^4$ $\qquad C_{11} := 1.2890360 \cdot 10^{-5}$

$C_9 := -1.1294650 \cdot 10^1$ $\qquad C_{12} := -2.4780681 \cdot 10^{-9}$

$C_{10} := -2.7022355 \cdot 10^{-2}$ $\qquad C_{13} := 6.5459673$

$$p_{ws}(TR) := e^{\left[\frac{C_8}{TR} + C_9 + C_{10} \cdot TR + C_{11} \cdot (TR)^2 + C_{12} \cdot (TR)^3 + C_{13} \cdot \ln(TR)\right]} psi$$

Uncertainty

$$u_{pws}(TR, u_{TR}) := \sqrt{\left[\left(\frac{d}{dTR} p_{ws}(TR)\right) \cdot u_{TR}\right]^2}$$

Process Inlet

$$p_{ws.pi} := \overrightarrow{p_{ws}\left(\frac{F(T_{pi})}{R}\right)}$$

$$u_{pws.pi} := \overrightarrow{u_{pws}\left[\frac{F(T_{pi})}{R}, \frac{u_{Tpi}}{(\Delta°F)}\right]}$$

Process Outlet

$$p_{ws.po} := \overrightarrow{p_{ws}\left(\frac{F(T_{po})}{R}\right)}$$

$$u_{pws.po} := \overrightarrow{u_{pws}\left[\frac{F(T_{po})}{R}, \frac{u_{Tpo}}{(\Delta°F)}\right]}$$

Humidity Ratio

$$w(\phi, p_z, p_{ws}) := \left(\overrightarrow{0.621945 \cdot \frac{\phi \cdot p_{ws}}{p_z - \phi \cdot p_{ws}}}\right) \frac{lbm}{lbm}$$

Uncertainty

$$u_w(\phi, p_z, p_{ws}, u_\phi, u_{pz}, u_{pws}) := \left[\overrightarrow{\left[\begin{array}{l}\left(\frac{d}{d\phi} w(\phi, p_z, p_{ws}) \cdot u_\phi\right)^2 \ldots \\ + \left(\frac{d}{dp_z} w(\phi, p_z, p_{ws}) \cdot u_{pz}\right)^2 \ldots \\ + \left(\frac{d}{dp_{ws}} w(\phi, p_z, p_{ws}) \cdot u_{pws}\right)^2\end{array}\right]}\right]^{0.5}$$

Process Inlet

$$G_{pi} := \overrightarrow{w(\phi_{pi}, p_z, p_{ws.pi})}$$

$$u_{Gpi} := \overrightarrow{u_w\left(\phi_{pi}, p_z, p_{ws.pi}, u_{\phi pi}, u_{pz}, u_{pws.pi}\right)}$$

Process Outlet

$$G_{po} := \overrightarrow{w\left(\phi_{po}, p_z, p_{ws.po}\right)}$$

$$u_{Gpo} := \overrightarrow{u_w\left(\phi_{po}, p_z, p_{ws.po}, u_{\phi po}, u_{pz}, u_{pws.po}\right)}$$

Grain Depression

$$\Delta G\left(G_i, G_o\right) := G_i - G_o$$

$$u_{\Delta G}\left(G_i, G_o, u_{Gi}, u_{Go}\right) := \left[\left(\frac{d}{dG_i}\Delta G\left(G_i, G_o\right)\cdot u_{Gi}\right)^2 + \left(\frac{d}{dG_o}\Delta G\left(G_i, G_o\right)\cdot u_{Go}\right)^2\right]^{0.5}$$

$$\Delta GPP := \Delta G\left(G_{pi}, G_{po}\right)$$

$$u_{\Delta GPP} := \overrightarrow{u_{\Delta G}\left(G_{pi}, G_{po}, u_{Gpi}, u_{Gpo}\right)}$$

Density

$$\rho\left(\phi, p_z, p_{ws}, t\right) := \left(\frac{p_z}{R_{da}\cdot t}\cdot\frac{1 + w\left(\phi, p_z, p_{ws}\right)}{1 + 1.608\cdot w\left(\phi, p_z, p_{ws}\right)}\right)$$

Uncertainty

$$u_\rho\left(\phi, p_z, p_{ws}, t, u_\phi, u_{pws}, u_t, u_{pz}\right) := \left[\begin{array}{l}\left(\frac{d}{d\phi}\rho\left(\phi, p_z, p_{ws}, t\right)\cdot u_\phi\right)^2 \ldots \\ +\left(\frac{d}{dp_z}\rho\left(\phi, p_z, p_{ws}, t\right)\cdot u_{pz}\right)^2 \ldots \\ +\left(\frac{d}{dp_{ws}}\rho\left(\phi, p_z, p_{ws}, t\right)\cdot u_{pws}\right)^2 \ldots \\ +\left(\frac{d}{dt}\rho\left(\phi, p_z, p_{ws}, t\right)\cdot u_t\right)^2\end{array}\right]^{0.5}$$

Process In

$$\rho_{pi} := \overrightarrow{\rho\left(\phi_{pi}, p_z, p_{ws.pi}, F\left(T_{pi}\right)\right)}$$

$$u_{\rho.pi} := \overrightarrow{u_\rho\left(\phi_{pi}, p_z, p_{ws.pi}, F\left(T_{pi}\right), u_{\phi pi}, u_{pws.pi}, u_{Tpi}, u_{pz}\right)}$$

Process Out

$$\rho_{po} := \overrightarrow{\rho\left(\phi_{po}, p_z, p_{ws.po}, F\left(T_{po}\right)\right)}$$

$$u_{\rho.po} := \overrightarrow{u_\rho\left(\phi_{po}, p_z, p_{ws.po}, F\left(T_{po}\right), u_{\phi po}, u_{pws.po}, u_{Tpo}, u_{pz}\right)}$$

Pressure Drop for Velocity

Interior area of the flow meter

$$Area := \frac{\pi \cdot (5.88in)^2}{4} = 0.189 \cdot ft^2$$

Flow meter equation solved for differential pressure

$$\Delta P_{po} := \left[\overrightarrow{\frac{8.3173069225569314461e\text{-}7 \cdot \left(\frac{Acfmpo}{cfm}\right)^2 \cdot \frac{\rho_{po}}{\frac{lbm}{ft^3}}}{\left(\frac{Area}{ft^2}\right)^2}}\right]$$

Velocity

$$V\left(C, \Delta P, \rho\rho\right) := \left(\overrightarrow{C \cdot \sqrt{\frac{\Delta P}{\frac{\rho\rho}{\frac{lbm}{ft^3}}}} \cdot \frac{ft}{min}}\right)$$

Uncertainty

$$u_V(C, \Delta P, \rho, u_{\Delta P}, u_\rho) := \left[\left[\left(\frac{d}{d\Delta P} \frac{V(C, \Delta P, \rho)}{\frac{ft}{min}} \cdot u_{\Delta P} \right)^2 + \left(\frac{d}{d\rho} \frac{V(C, \Delta P, \rho)}{\frac{ft}{min}} \cdot u_\rho \right)^2 \right]^{0.5} \right] \cdot \frac{ft}{min}$$

$$u_{V_{po}} := u_V(C_V, \Delta P_{po}, \rho_{po}, u_{\Delta Ppo}, u_{\rho.po})$$

Process Out

$$V_{po} := V(C_V, \Delta P_{po}, \rho_{po})$$

This uncertainty incorporates the 2% given by the manufacturer, as well as the uncertainty due to the measurement systems.

$$u_{V_{po}} := \sqrt{u_V^2 + (2\% \cdot V_{po})^2}$$

Volumetric Flow Rate

$$ACFM(Vel, Area) := Area \cdot Vel$$

$$u_{ACFM}(Vel, Area) := \left(\frac{d}{dVel} ACFM(Vel, Area) \cdot u_V \right)$$

$$u_{Acfmp} := u_{ACFM}(V_{po}, Area)$$

Mass Flow Rate

$$mfr(acfm, \rho) := (acfm \cdot \rho)$$

Uncertainty

$$u_{mfr}(acfm, u_{cfm}, \rho, u_{\rho}) := \left[\overrightarrow{\left[\left(\frac{d}{dcfm} mfr(acfm, \rho)\cdot u_{cfm}\right)^2 + \left(\frac{d}{d\rho} mfr(acfm, \rho)\cdot u_{\rho}\right)^2\right]}\right]^{0.5}$$

$$mfr := mfr(Acfmpo, \rho_{po})$$

Mass flow rate based on process outlet measurements

$$u_{mfr} := \overrightarrow{u_{mfr}(Acfmpo, u_{Acfmp}, \rho_{po}, u_{\rho.po})}$$

Moisture Removal Capacity (MRC)

$$mrc(mfr, \Delta G) := \overrightarrow{(mfr\cdot\Delta G)}$$

Uncertainty

$$u_{mrc}(mfr, u_{mfr}, \Delta G, u_{\Delta G}) := \left[\overrightarrow{\left[\left(\frac{d}{dmfr} mrc(mfr, \Delta G)\cdot u_{mfr}\right)^2 \ldots + \left(\frac{d}{d\Delta G} mrc(mfr, \Delta G)\cdot u_{\Delta G}\right)^2\right]}\right]^{0.5}$$

$$MRC := \overrightarrow{mrc(mfr, \Delta GPP)}$$

$$u_{MRC} := \overrightarrow{u_{mrc}(mfr, u_{mfr}, \Delta GPP, u_{\Delta GPP})}$$

Process Outlet Temperature

Assuming the temperature rise is strictly due to the latent heat of evaporation

$$Q(mfr, \Delta W) := mfr\cdot h_{fg}\cdot\Delta W$$

$$Q_{\Delta GPP} := \overrightarrow{Q(mfr, \Delta GPP)}$$

Uncertainty

$$u_Q(mfr, \Delta W, u_m, u_{\Delta W}) := \left[\left(\frac{d}{dmfr} Q(mfr, \Delta W)\cdot u_m\right)^2 + \left(\frac{d}{d\Delta W} Q(mfr, \Delta W)\cdot u_{\Delta W}\right)^2\right]^{0.5}$$

$$u_{Q\Delta GPP} := \overrightarrow{u_Q(mfr, \Delta GPP, u_{mfr}, u_{\Delta GPP})}$$

$$T_o(Q, mfr, T_i) := \frac{Q}{mfr\cdot c_p} + T_i$$

$$T_{po.est} := \overrightarrow{T_o(Q_{\Delta GPP}, mfr, T_{pi})}$$

$$u_{To}(Q, mfr, T_i, u_Q, u_m, u_{Ti}) := \left[\left(\frac{d}{dQ} T_o(Q, mfr, T_i)\cdot u_Q\right)^2 + \left(\frac{d}{dmfr} T_o(Q, mfr, T_i)\cdot u_m\right)^2 \ldots + \left(\frac{d}{dT_i} T_o(Q, mfr, T_i)\cdot u_{Ti}\right)^2\right]^{0.5}$$

Estimated process temperature out

$$u_{Tpo.est} := \overrightarrow{u_{To}\left(Q_{\Delta GPP}, mfr, T_{pi}, u_{Q\Delta GPP}, u_{mfr}, \frac{u_{Tpi}}{\Delta °F}\right)}$$

Results

Calculation **Uncertainties**

Process Inlet Humidity Ratio

G_{pi} =	u_{Gpi} =	$\frac{u_{Gpi}}{G_{pi}}$ =
79.253	1.4	1.768
91.823	1.44	1.573
105.48	1.5	1.418
91.032	1.53	1.68
63.383	1.07	1.682
78.503	1.41	1.791
91.429	1.44	1.575
106.508	1.49	1.401
91.572	1.55	1.693
63.137	1.07	1.69
78.833	1.42	1.796
91.737	1.45	1.579
105.476	1.49	1.408
91.373	1.54	1.682
62.786	1.07	1.702

$\cdot \frac{Gr}{lbm}$ $\cdot \frac{Gr}{lbm}$ $\cdot \%$

Process Outlet Humidity Ratio

G_{po} =	u_{Gpo} =	$\frac{u_{Gpo}}{G_{po}}$ =
46.065	3.177	6.896
54.442	3.458	6.351
64.188	3.696	5.758
48.876	2.903	5.939
28.502	1.932	6.78
38.057	3.627	9.531
46.34	3.976	8.581
57.188	4.24	7.413
41.497	3.649	8.795
21.099	2.359	11.179
41.783	3.493	8.361
50.844	3.71	7.298
59.425	3.975	6.689
44.88	3.248	7.237
23.424	2.145	9.157

$\cdot \frac{Gr}{lbm}$ $\cdot \frac{Gr}{lbm}$ $\cdot \%$

Grain Depression

$\Delta GPP = \begin{bmatrix} 33.188 \\ 37.381 \\ 41.292 \\ 42.156 \\ 34.881 \\ 40.447 \\ 45.089 \\ 49.319 \\ 50.075 \\ 42.038 \\ 37.05 \\ 40.892 \\ 46.051 \\ 46.493 \\ 39.362 \end{bmatrix} \cdot \frac{Gr}{lbm}$

$u_{\Delta GPP} = \begin{bmatrix} 3.472 \\ 3.747 \\ 3.987 \\ 3.281 \\ 2.207 \\ 3.89 \\ 4.229 \\ 4.495 \\ 3.965 \\ 2.589 \\ 3.769 \\ 3.983 \\ 4.244 \\ 3.593 \\ 2.396 \end{bmatrix} \cdot \frac{Gr}{lbm}$

$\frac{u_{\Delta GPP}}{\Delta GPP} = \begin{bmatrix} 10.461 \\ 10.024 \\ 9.655 \\ 7.783 \\ 6.327 \\ 9.618 \\ 9.379 \\ 9.113 \\ 7.919 \\ 6.158 \\ 10.174 \\ 9.74 \\ 9.215 \\ 7.728 \\ 6.088 \end{bmatrix} \cdot \%$

Mass Flow Rate

$mfr = \begin{bmatrix} 18.716 \\ 18.621 \\ 18.613 \\ 18.603 \\ 18.744 \\ 12.52 \\ 12.427 \\ 12.544 \\ 12.471 \\ 12.427 \\ 15.181 \\ 15.18 \\ 15.208 \\ 15.209 \\ 15.259 \end{bmatrix} \cdot \frac{lbm}{min}$

$u_{mfr} = \begin{bmatrix} 0.388 \\ 0.386 \\ 0.385 \\ 0.386 \\ 0.389 \\ 0.291 \\ 0.29 \\ 0.291 \\ 0.29 \\ 0.293 \\ 0.327 \\ 0.327 \\ 0.328 \\ 0.328 \\ 0.33 \end{bmatrix} \cdot \frac{lbm}{min}$

$\frac{u_{mfr}}{mfr} = \begin{bmatrix} 2.072 \\ 2.071 \\ 2.071 \\ 2.074 \\ 2.075 \\ 2.326 \\ 2.333 \\ 2.317 \\ 2.323 \\ 2.356 \\ 2.157 \\ 2.156 \\ 2.154 \\ 2.157 \\ 2.165 \end{bmatrix} \cdot \%$

Moisture Removal Capacity

$MRC =$ (lbm/hr)

5.324
5.966
6.588
6.722
5.604
4.34
4.803
5.303
5.353
4.478
4.821
5.321
6.003
6.061
5.148

$u_{MRC} =$ (lbm/hr)

0.568
0.611
0.651
0.541
0.373
0.429
0.464
0.499
0.442
0.295
0.501
0.531
0.568
0.486
0.333

$\frac{u_{MRC}}{MRC} =$ (%)

10.664
10.236
9.875
8.054
6.659
9.895
9.665
9.403
8.252
6.593
10.4
9.976
9.463
8.023
6.462

Process Temperature Out

$T_{po.est} =$

94.2
96.5
98.9
89.4
75.2
98.4
101
103.5
93.9
79.5
96.5
98.6
101.5
91.8
77.9

$u_{Tpo.est} =$

2.089
2.261
2.412
2.032
1.416
2.381
2.595
2.764
2.485
1.709
2.279
2.416
2.587
2.238
1.559

$\frac{u_{Tpo.est}}{T_{po.est}} =$ (%)

2.219
2.344
2.438
2.272
1.882
2.421
2.568
2.671
2.646
2.15
2.362
2.45
2.549
2.436
2.001

Dew-Point Temperature Method

Definitions

Grains per pound

$$Gr := \frac{lbm}{7000}$$

Conversion from Fahrenheit to Rankine

$$F(T) := \overrightarrow{[(T + 459.67)\cdot R]}$$

Specific enthalpy of water vapor

$$h_{fg} := 970\frac{BTU}{lbm}$$

Specific heat of dry air

$$c_p := 0.24\cdot\frac{BTU}{lbm}$$

Gas constant for dry air

$$R_{da} := 53.35\frac{ft\cdot lbf}{lbm\cdot R}$$

Inputs

Uncertainties

$ac_{pz} := 0\%$

$u_{Tpi} := 0.3\Delta°F$

$u_{Tpo} := 0.3\Delta°F$

$u_{Tdp.i} := 0.3\Delta°F$

$u_{Tdp.o} := 0.3\Delta°F$

$ac_f := 2\%$

Data

Barometric pressure:

$$p_z := \begin{pmatrix} 12.0 \\ 12.0 \\ 12.0 \\ 12.0 \\ 11.8 \\ 12.0 \\ 12.0 \\ 12.0 \\ 11.8 \\ 12.0 \\ 12.0 \\ 11.8 \\ 12.0 \\ 11.8 \end{pmatrix} \text{psi} \qquad u_{pz} := \overrightarrow{(ac_{pz} \cdot p_z)}$$

Process inlet dry-bulb and dew-point temperatures:

$$T_{pi} := \begin{pmatrix} 75.00354286 \\ 75.00457143 \\ 75.00405714 \\ 65.0012 \\ 54.99628571 \\ 74.97422857 \\ 75.01022857 \\ 75.00148571 \\ 64.99965714 \\ 55.09502857 \\ 74.99017143 \\ 74.99737143 \\ 75.00611429 \\ 64.99708571 \\ 55.00142857 \end{pmatrix} \qquad T_{dp.i} := \begin{pmatrix} 55.022 \\ 59.10594286 \\ 62.98982857 \\ 59.1224 \\ 48.96515429 \\ 55.04874286 \\ 59.13011429 \\ 63.06337143 \\ 59.03085714 \\ 49.31214286 \\ 54.93611429 \\ 59.07971429 \\ 62.84428571 \\ 59.12651429 \\ 49.05957714 \end{pmatrix}$$

Process outlet dry-bulb and dew-point temperatures:

$$T_{po} := \begin{pmatrix} 103.1149143 \\ 105.4677714 \\ 107.5537143 \\ 99.28914286 \\ 86.9612 \\ 110.4928571 \\ 113.2329714 \\ 115.5549714 \\ 107.0749143 \\ 94.91154286 \\ 106.5755429 \\ 109.0024571 \\ 111.8768 \\ 103.2671429 \\ 90.79725714 \end{pmatrix} \qquad T_{dp.o} := \begin{pmatrix} 41.6336 \\ 46.15180571 \\ 50.51711429 \\ 43.85562286 \\ 29.66596571 \\ 37.73012 \\ 42.48577143 \\ 47.17842286 \\ 39.69721143 \\ 24.53210857 \\ 39.72364571 \\ 44.40272 \\ 48.63066286 \\ 41.837 \\ 26.88671429 \end{pmatrix}$$

Flow Rate:

$$Acfmp := \begin{pmatrix} 326 \\ 328 \\ 330 \\ 325 \\ 320 \\ 220 \\ 221 \\ 222 \\ 220 \\ 217 \\ 269 \\ 270 \\ 275 \\ 268 \\ 265 \end{pmatrix} \cdot \text{cfm} \qquad u_{Acfmp} := \overrightarrow{(Acfmp \cdot ac_f)}$$

Calculations

Saturation Pressure

$C_8 := -1.0440397 \times 10^4$ $\quad C_{11} := 1.2890360 \cdot 10^{-5}$

$C_9 := -1.1294650 \cdot 10^1$ $\quad C_{12} := -2.4780681 \cdot 10^{-9}$

$C_{10} := -2.7022355 \cdot 10^{-2}$ $\quad C_{13} := 6.5459673$

$$p_{ws}(TR) := e^{\left[\frac{C_8}{TR} + C_9 + C_{10} \cdot TR + C_{11} \cdot (TR)^2 + C_{12} \cdot (TR)^3 + C_{13} \cdot \ln(TR)\right]} \text{psi}$$

Uncertainty

$$u_{pws}(TR, u_{TR}) := \sqrt{\left[\left(\frac{d}{dTR} p_{ws}(TR)\right) \cdot u_{TR}\right]^2}$$

Process Inlet at Dry-Bulb Temperature

$$p_{ws.pi} := p_{ws}\left(\frac{F(T_{pi})}{R}\right)$$

$$u_{pws.pi} := u_{pws}\left[\frac{F(T_{pi})}{R}, \frac{u_{Tpi}}{(\Delta°F)}\right]$$

Process Outlet at Dry-Bulb Temperature

$$p_{ws.po} := p_{ws}\left(\frac{F(T_{po})}{R}\right)$$

$$u_{pws.po} := u_{pws}\left[\frac{F(T_{po})}{R}, \frac{u_{Tpo}}{(\Delta°F)}\right]$$

Process Inlet at Dew-Point Temperature

$$p_{ws.dp.pi} := p_{ws}\left(\frac{F(T_{dp.i})}{R}\right)$$

$$u_{pws.dp.pi} := u_{pws}\left(\frac{F(T_{dp.i})}{R}, \frac{u_{Tdp.i}}{\Delta°F}\right)$$

Process Outlet at Dew-Point Temperature

$$p_{ws.dp.po} := p_{ws}\left(\frac{F(T_{dp.o})}{R}\right)$$

$$u_{pws.dp.po} := u_{pws}\left(\frac{F(T_{dp.o})}{R}, \frac{u_{Tdp.o}}{\Delta°F}\right)$$

Humidity Ratio At Saturation At T_{dp}

$$w_s(p_{ws}, p_z) := \overrightarrow{\left(0.621945 \cdot \frac{p_{ws}}{p_z - p_{ws}}\right)} \cdot \frac{lbm}{lbm}$$

Uncertainty

$$u_{ws}(p_{ws}, p_z, u_{pws}, u_{pz}) := \left[\overrightarrow{\left[\left[\frac{d}{dp_{ws}}(w_s(p_{ws}, p_z)) \cdot u_{pws}\right]^2 + \left(\frac{d}{dp_z} w_s(p_{ws}, p_z) \cdot u_{pz}\right)^2\right]}\right]^{0.5}$$

Process Inlet

$$w_{s.pi} := \overrightarrow{w_s(p_{ws.dp.pi}, p_z)}$$

$$u_{ws.pi} := \overrightarrow{u_{ws}(p_{ws.dp.pi}, p_z, u_{pws.dp.pi}, u_{pz})}$$

Process Outlet

$$w_{s.po} := w_s(p_{ws.dp.po}, p_z)$$

$$u_{ws.po} := \overrightarrow{u_{ws}(p_{ws.dp.po}, p_z, u_{pws.dp.po}, u_{pz})}$$

Humidity Ratio

$$w(T_{dp}, w_s) := \frac{\overrightarrow{(1093 - 0.556 \cdot T_{dp}) \cdot w_s - 0.240 \cdot (T_{dp} - T_{dp})}}{1093 + 0.444 \cdot T_{dp} - T_{dp}} \cdot \frac{lbm}{lbm}$$

Uncertainty

$$u_w(T_{dp}, w_s, u_{Tdp}, u_{ws}) := \left[\overrightarrow{\left[\left(\frac{d}{dT_{dp}} w(T_{dp}, w_s)\cdot u_{Tdp}\right)^2 \ldots + \left(\frac{d}{dw_s} w(T_{dp}, w_s)\cdot u_{ws}\right)^2\right]}\right]^{0.5}$$

Process Inlet

$$G_{pi} := w\left(\frac{F(T_{dp.i})}{R} - 459.67, w_{s.pi}\right)$$

$$u_{Gpi} := \overrightarrow{u_w\left(\frac{F(T_{dp.i})}{R} - 459.67, w_{s.pi}, \frac{u_{Tdp.i}}{\Delta°F}, u_{ws.pi}\right)}$$

Process Outlet

$$G_{po} := w\left(\frac{F(T_{dp.o})}{R} - 459.67, w_{s.po}\right)$$

$$u_{Gpo} := \overrightarrow{u_w\left(\frac{F(T_{dp.o})}{R} - 459.67, w_{s.po}, \frac{u_{Tdp.o}}{\Delta°F}, u_{ws.po}\right)}$$

Grain Depression

$$\Delta GPP(G_{pi}, G_{po}) := G_{pi} - G_{po}$$

$$u_{\Delta GPP}(G_{pi}, u_{Gpi}, G_{po}, u_{Gpo}) := \left[\begin{array}{l}\left(\frac{d}{dG_{pi}} \Delta GPP(G_{pi}, G_{po})\cdot u_{Gpi}\right)^2 \ldots \\ + \left(\frac{d}{dG_{po}} \Delta GPP(G_{pi}, G_{po})\cdot u_{Gpo}\right)^2\end{array}\right]^{0.5}$$

$$\Delta GPP := \overrightarrow{\Delta GPP(G_{pi}, G_{po})}$$

$$u_{\Delta GPP} := \overrightarrow{u_{\Delta GPP}(G_{pi}, u_{Gpi}, G_{po}, u_{Gpo})}$$

Density

$$\rho(p_z, t, w) := \overrightarrow{\left(\frac{p_z}{R_{da} \cdot t} \cdot \frac{1 + w}{1 + 1.608 \cdot w}\right)}$$

Uncertainty

$$u_\rho(p_z, t, w, u_{pz}, u_t, u_w) := \left[\overrightarrow{\left[\left(\frac{d}{dp_z}\rho(p_z, t, w) \cdot u_{pz}\right)^2 + \left(\frac{d}{dt}\rho(p_z, t, w) \cdot u_t\right)^2 + \left(\frac{d}{dw}\rho(p_z, t, w) \cdot u_w\right)^2\right]}\right]^{0.5}$$

Process Inlet

$$\rho_{pi} := \rho(p_z, F(T_{pi}), G_{pi})$$

$$u_{\rho.pi} := \overrightarrow{u_\rho(p_z, F(T_{pi}), G_{pi}, u_{pz}, u_{Tpi}, u_{Gpi})}$$

Process Outlet

$$\rho_{po} := \rho(p_z, F(T_{po}), G_{po})$$

$$u_{\rho.po} := \overrightarrow{u_\rho(p_z, F(T_{po}), G_{po}, u_{pz}, u_{Tpo}, u_{Gpo})}$$

Mass flow rate

$$mfr(cfm, \rho) := \overrightarrow{(cfm \cdot \rho)}$$

Uncertainty

$$u_{mfr}(cfm, u_{cfm}, \rho, u_\rho) := \left[\overrightarrow{\left[\left(\frac{d}{dcfm}mfr(cfm, \rho) \cdot u_{cfm}\right)^2 + \left(\frac{d}{d\rho}mfr(cfm, \rho) \cdot u_\rho\right)^2\right]}\right]^{0.5}$$

Process Outlet

$$\underset{\sim}{mfr} := \overrightarrow{mfr(Acfmp, \rho_{po})}$$

$$u_{mfr} := \overrightarrow{u_{mfr}\left(Acfmp, u_{Acfmp}, \rho_{po}, u_{\rho.po}\right)}$$

Moisture Removal Capacity (MRC)

$$mrc(mfr, \Delta w) := \overrightarrow{(mfr \cdot \Delta w)}$$

Uncertainty

$$u_{mrc}\left(mfr, u_{mfr}, \Delta w, u_{\Delta w}\right) := \left[\overrightarrow{\left[\left(\frac{d}{dmfr} mrc(mfr, \Delta w) \cdot u_{mfr}\right)^2 \ldots + \left(\frac{d}{d\Delta w} mrc(mfr, \Delta w) \cdot u_{\Delta w}\right)^2\right]}\right]^{0.5}$$

$$MRC := \overrightarrow{mrc(mfr, \Delta GPP)}$$

$$u_{MRC} := \overrightarrow{u_{mrc}\left(mfr, u_{mfr}, \Delta GPP, u_{\Delta GPP}\right)}$$

Process Outlet Temperature

Assuming the temperature rise is strictly due to the latent heat of evaporation

$$Q(mfr, \Delta W) := mfr \cdot h_{fg} \cdot \Delta W$$

$$Q_{\Delta GPP} := \overrightarrow{Q(mfr, \Delta GPP)}$$

Uncertainty

$$u_Q\left(mfr, \Delta W, u_m, u_{\Delta W}\right) := \left[\left(\frac{d}{dmfr} Q(mfr, \Delta W) \cdot u_m\right)^2 + \left(\frac{d}{d\Delta W} Q(mfr, \Delta W) \cdot u_{\Delta W}\right)^2\right]^{0.5}$$

$$u_{Q\Delta GPP} := \overrightarrow{u_Q\left(mfr, \Delta GPP, u_{mfr}, u_{\Delta GPP}\right)}$$

$$T_o\left(Q, mfr, T_i\right) := \frac{Q}{mfr \cdot c_p} + T_i$$

$$T_{po.est} := \overrightarrow{T_o\left(Q_{\Delta GPP}, mfr, T_{pi}\right)}$$

$$u_{To}\left(Q, mfr, T_i, u_Q, u_m, u_{Ti}\right) := \left[\left(\frac{d}{dQ} T_o\left(Q, mfr, T_i\right)\cdot u_Q\right)^2 + \left(\frac{d}{dmfr} T_o\left(Q, mfr, T_i\right)\cdot u_m\right)^2 \ldots + \left(\frac{d}{dT_i} T_o\left(Q, mfr, T_i\right)\cdot u_{Ti}\right)^2\right]^{0.5}$$

Estimated process temperature out

$$u_{Tpo.est} := \overrightarrow{u_{To}\left(Q_{\Delta GPP}, mfr, T_{pi}, u_{Q\Delta GPP}, u_{mfr}, \frac{u_{Tpi}}{\Delta °F}\right)}$$

Results

Calculation **Uncertainties**

Process Inlet Humidity Ratio

G_{pi} =			u_{Gpi} =			$\frac{u_{Gpi}}{G_{pi}}$ =		
	79.152			0.88			1.112	
	91.984			1.008			1.096	
	105.898			1.144			1.081	
	92.04			1.008			1.095	
	64.155			0.73			1.138	
	79.23			0.881			1.112	
	92.066			1.009			1.095	
	106.179	$\cdot\frac{Gr}{lbm}$		1.147	$\cdot\frac{Gr}{lbm}$		1.08	$\cdot\%$
	91.732			1.005			1.096	
	65.005			0.739			1.137	
	78.9			0.878			1.112	
	91.896			1.007			1.096	
	107.174			1.159			1.082	
	92.054			1.008			1.095	
	64.385			0.733			1.138	

Process Outlet Humidity Ratio

$G_{po} =$

47.564
56.653
66.883
51.856
29.956
40.788
49.17
58.923
44.086
24.204
44.132
52.964
63.346
47.943
26.706

$\cdot \frac{Gr}{lbm}$

$u_{Gpo} =$

0.557
0.652
0.757
0.602
0.369
0.486
0.574
0.675
0.521
0.305
0.521
0.614
0.722
0.561
0.333

$\cdot \frac{Gr}{lbm}$

$\frac{u_{Gpo}}{G_{po}} =$

1.172
1.151
1.131
1.161
1.232
1.191
1.168
1.146
1.181
1.26
1.181
1.159
1.14
1.171
1.247

$\cdot \%$

Grain Depression

$\Delta GPP =$

31.588
35.332
39.015
40.184
34.199
38.442
42.895
47.256
47.647
40.801
34.768
38.932
43.828
44.111
37.679

$\cdot \frac{Gr}{lbm}$

$u_{\Delta GPP} =$

1.042
1.2
1.372
1.174
0.818
1.006
1.161
1.331
1.132
0.799
1.021
1.179
1.366
1.154
0.805

$\cdot \frac{Gr}{lbm}$

$\frac{u_{\Delta GPP}}{\Delta GPP} =$

3.298
3.397
3.516
2.923
2.393
2.617
2.705
2.817
2.376
1.959
2.936
3.029
3.116
2.616
2.136

$\cdot \%$

Mass Flow Rate

mfr	u_{mfr}	$\frac{u_{mfr}}{mfr}$
18.686	0.374	2.001
18.707	0.374	2.001
18.736	0.375	2.001
18.749	0.375	2.001
18.597	0.372	2.001
12.454	0.249	2.001
12.442	0.249	2.001
12.437	0.249	2.001
12.525	0.251	2.001
12.436	0.249	2.001
15.329	0.307	2.001
15.308	0.306	2.001
15.242	0.305	2.001
15.356	0.307	2.001
15.298	0.306	2.001
$\cdot\frac{lbm}{min}$	$\cdot\frac{lbm}{min}$	$\cdot\%$

Moisture Removal Capacity

MRC	u_{MRC}	$\frac{u_{MRC}}{MRC}$
5.059	0.195	3.858
5.665	0.223	3.942
6.266	0.253	4.046
6.458	0.229	3.542
5.451	0.17	3.119
4.104	0.135	3.294
4.575	0.154	3.365
5.038	0.174	3.455
5.115	0.159	3.106
4.349	0.122	2.8
4.568	0.162	3.553
5.108	0.185	3.63
5.726	0.212	3.703
5.806	0.191	3.294
4.941	0.145	2.927
$\cdot\frac{lbm}{hr}$	$\cdot\frac{lbm}{hr}$	$\cdot\%$

Process Temperature Out

$T_{po.est}$ =
93.2
95.4
97.5
88.2
74.7
97.2
99.8
102.3
92.5
78.7
95.1
97.5
100.3
90.5
76.8

$u_{Tpo.est}$ =
0.847
0.95
1.06
0.99
0.791
0.907
1.015
1.13
1.06
0.864
0.872
0.979
1.107
1.026
0.828

$\frac{u_{Tpo.est}}{T_{po.est}}$ =	·%
0.909	
0.996	
1.087	
1.123	
1.058	
0.933	
1.017	
1.105	
1.146	
1.099	
0.917	
1.004	
1.103	
1.134	
1.078	

APPENDIX B

DERIVATION OF PRESSURE DROP METHODOLOGY

The following derivation follows the procedure used to obtain Equation (8.14) from Equations (8.10) and (8.11).

Starting with the equations for pressure drop at sea-level (B-1) and altitude (B-2)

$$\Delta P_0 = C_l V_0 + C_{k,t}\rho_0 V_0^2 \tag{B-1}$$

$$\Delta P_z = C_l V_z + C_{k,t}\rho_z V_z^2 \tag{B-2}$$

and the fact that the mass flow rates at sea-level and altitude are equal

$$\dot{m}_0 = \dot{m}_z \tag{B-3}$$

$$\rho_0 V_0 A = \rho_z V_z A \tag{B-4}$$

$$V_z = \frac{\rho_0}{\rho_z} V_0 \tag{B-5}$$

Equation (B-5) can be substituted into Equation (B-2) and simplified to yield Equation (B-8).

$$\Delta P_z = C_l \left(\frac{\rho_0}{\rho_z} V_0\right) + C_{k,t}\rho_z \left(\frac{\rho_0}{\rho_z} V_0\right)^2 \tag{B-6}$$

$$\Delta P_z = \frac{\rho_0}{\rho_z} C_l V_0 + \frac{\rho_0}{\rho_z} C_{k,t}\rho_0 {V_0}^2 \tag{B-7}$$

$$\Delta P_z = \frac{\rho_0}{\rho_z} \left(C_l V_0 + C_{k,t}\rho_0 {V_0}^2\right) \tag{B-8}$$

It can be seen that the terms in parenthesis in Equation (B-8) are equal to Equation (B-1). Substituting Equation (B-1) into Equation (B-8) yields Equation (B-9), which is the same as Equation (8.14).

$$\boxed{\boldsymbol{\Delta P_z = \frac{\rho_0}{\rho_z} \Delta P_0}} \tag{B-9}$$

APPENDIX C

SUMMARY OF METHODOLOGIES

This appendix includes a short summary of each methodology. When following the methodologies, it is important to keep in mind the six design conditions that must remain a constant between sea-level and altitude:

- Process Inlet Mass Flow Rate
- Process Inlet Dry-Bulb Temperature
- Process Inlet Humidity Ratio
- Regeneration Inlet Mass Flow Rate
- Regeneration Inlet Dry-Bulb Temperature
- Regeneration Inlet Humidity Ratio

Also, it is necessary that sea-level performance data is available for the desiccant unit under inspection. This sea-level performance data includes the MRC, RSHI, pressure drop through the wheel for process and regeneration, and the process temperature out. It should be noted that each manufacturers' performance material is different. In the event that the volumetric flow rate or face velocity is needed, it is necessary to use the density calculated at the standard atmospheric pressure at altitude when converting from mass flow rate.

In order to follow the methodology, a few preliminary calculations must be made. These variables are applied directly to the equations for the estimations at altitude. First, the standard atmospheric pressure at the specific altitude is needed. The standard atmospheric pressure is given by Equation (C-1).

$$p_{atm} = 14.696(1 - 6.8754 \times 10^{-6} Z)^{5.2559} \quad \text{(C-1)}$$

where:

p_{atm} = Standard atmospheric pressure at altitude, *[psi]*

Z = Altitude, *[ft]*

The second variable that is needed to complete the methodology is the difference in the partial pressure of water vapor between sea-level and altitude for the specified process inlet humidity ratio, given by Equation (C-2).

$$\Delta p_w = -\frac{w(125p_{atm}-1837)}{125w+544250} \quad \text{(C-2)}$$

where:

Δp_w = Difference in partial pressure between sea-level and altitude, *[psi]*

w = Design process inlet humidity ratio, *[Gr/lbm]*

With the sea-level performance known and the two preliminary calculations completed, the methodology can now be followed simply by utilizing the equations below.

Moisture Removal Capacity

$$MRC_z = \frac{MRC_0}{1+\Delta p_w} \quad \text{(C-3)}$$

where:

MRC_0 = MRC at sea-level, *[lbm/hr]*

MRC_z = Estimated MRC at altitude, *[lbm/hr]*

Regeneration Specific Heat Input

$$RSHI_z = (1 + \Delta p_w)RSHI_0 \quad \text{(C-4)}$$

where:

$RSHI_0$ = RSHI at sea-level, *[BTU/lbm]*

$RSHI_z$ = Estimated RSHI at altitude, *[BTU/lbm]*

Pressure Drop through the Wheel

$$\Delta P_z = \frac{\rho_0}{\rho_z}\Delta P_0 \quad \text{(C-5a)}$$

$$\Delta P_z = \frac{1}{(1-6.8754\,x\,10^{-6}Z)^{5.2559}}\Delta P_0 \quad \text{(C-5b)}$$

where:

ρ_0 = Density at sea-level, *[lbm/ft^3]*

ρ_z = Density at altitude, *[lbm/ft^3]*

ΔP_0 = Pressure drop through the wheel at sea-level, *[in WC]*

ΔP_z = Pressure drop through the wheel at altitude, *[in WC]*

Note: Equation (C-5) must be used separately for process and regeneration pressure drops.

Process Outlet Temperature

There is not a significant change in the process outlet temperature between sea-level and altitude. Therefore, the process outlet temperature at sea-level is taken as equal to the process outlet temperature at altitude.

Use of ASHRAE Design Conditions

Chapter 14 of the 2009 ASHRAE Handbook – Fundamentals [7] provides climatic design conditions for 5,564 locations worldwide. These design conditions include elevation and annual percentiles for dehumidification, both of which are particularly useful when selecting a desiccant dehumidifier for altitude. This is because

the humidity ratios given are calculated at the atmospheric pressure of the elevation. The humidity ratio and mean coincident dry-bulb temperature given for each location should be used as the design conditions when selecting a desiccant dehumidifier.

Fan Selection

Since system pressure loss is the key factor in fan selection, special attention must be paid to how the pressure drop through the wheel changes with altitude. Generally, fan manufacturers give information on how to select fans to operate at altitude. Following the guidelines set by the manufacturer and taking into consideration the increased pressure losses through the wheel due to altitude will ensure proper fan selection for the system in question.

Method of Converting Field Measurements at Altitude to Standard Performance

In order to convert field measurements at altitude to standard performance, the methodologies must be followed in the reverse order. First, the altitude performance must be known for each measurement listed in the methodology: MRC, RSHI, pressure drop through the wheel, and process temperature out. Also, the preliminary calculations listed in Equations (C-1) and (C-2) must be performed in the same manner as previously discussed. Finally, each equation for the individual methodologies (Equations (C-3) to (C-5)) must be solved for the sea-level condition. By applying the measured altitude performance variables to these new equations, the estimated standard performance can be obtained.

APPENDIX D

ACTIVITIES FOR EASE OF USE CONFIRMATION

Below are shown the four activities given to various students and manufacturers in order to confirm the simplicity of the methodologies.

Undergraduate Student Activity

SOLID DESICCANT DEHUMIDIFIER SELECTION AT ALTITUDE

As a part of the ASHRAE research project 1339-TRP, "Selection of Desiccant Equipment at Altitude", Mississippi State University and the National Renewable Energy Laboratory have collaborated together in collecting performance data for a selected desiccant dehumidifier. The results of these tests have been used to develop a simple methodology that can be applied to any desiccant dehumidification unit in order to predict its performance at any altitude. In order to do this, the performance at standard conditions (sea-level) must be used. Since these performance parameters are readily available from any manufacturer, the methodology can be easily used.

Part of the project is the Ease of Use Confirmation. In this task, we need feedback on the methodology that we have developed in order to ensure that it is straightforward and easy to use. We have asked you to come today to use our methodology to predict the pressure drop at a given altitude for specific conditions. Your feedback will greatly help us to see if the methodology is simple enough to follow. This is very useful information because you most likely have little to no background in the dehumidification field.

Please, follow methodology and fill in the blank spaces in the tables provided to apply the methodology. For your convenience, an Excel spreadsheet has been provided to help to find the densities for the specific air conditions and barometric pressure at the process and regeneration inlets.

Methodology for Pressure Drop through the Wheel

Pressure drop (ΔP) through a honeycomb matrix as a function of actual face velocity (V) and density (ρ) can be well represented as a second order polynomial of the form

$$\Delta P(V) = C_l\, V + C_{k,t}\, \rho\, V^2 \tag{1}$$

where the coefficients C_l and $C_{k,t}$ are specific for each desiccant wheel, which account for geometric parameters of the desiccant wheel, thermophysical properties of the air, and units.

By knowing two different sets of actual face velocity and pressure drop, the coefficients C_l and $C_{k,t}$ can be found by simply solving the system of equations. When keeping the mass flow rate constant, and with the coefficients known, the pressure drop at altitude (ΔP_z) can be calculated as

$$\Delta P_z(V_z) = C_l\, V_z + C_{k,t}\, \rho_z\, V_z^2 \tag{2}$$

where V_z and ρ_z are the actual face velocity and air density at altitude for the design mass flow rate, respectively.

Due to viscous effects of temperature, coefficients C_l and $C_{k,t}$ must be found for process (low temperatures) and regeneration (high temperatures) sides independently.

For simplicity, Equations (3) and (4) have been provided so that the coefficients can be solved for directly

$$C_l = \frac{\Delta P_1\, V_2^2 - \Delta P_2\, V_1^2}{(V_1\, V_2^2 - V_1^2\, V_2)} \tag{3}$$

$$C_{k,t} = \frac{\Delta P_2 - C_l\, V_2}{0.075\, V_2^2} \tag{4}$$

where subscript 1 and 2 refer to the two sets of actual face velocity and pressure drop obtained as described below.

Set 1:

- Mass flow rate equal to the design mass flow rate.
- Velocity equal to the actual face velocity for the design mass flow rate and air density computed at standard barometric pressure for sea level (14.7 psi). $[\dot{m} = A\, V\, \rho]$
- Pressure drop equal to the pressure drop given by manufacturer's performance data at standard conditions for the design mass flow rate.

Set 2:

- Mass flow rate computed as

$$\dot{m}_2 = \dot{m}_1\, \frac{0.075}{\rho_z} \tag{6}$$

  where $\dot{m}_1$ is the design mass flow rate (mass flow rate of Set 1), and ρ_z is the air density at altitude for the design conditions.

- Velocity equal to the actual face velocity for the mass flow rate obtained using Equation (6) and air density computed at standard barometric pressure for sea level (14.7 psi). $[\dot{m} = A\, V\, \rho]$.

- Pressure drop equal to the pressure drop given by manufacturer's performance data at standard conditions for $\dot{m}_2$.

A step-by-step procedure on how to apply the methodology is given at the end of this document.

Activity for the Evaluation of the Methodology

Estimate the pressure drop through a desiccant wheel at the process and regeneration sides for the giving design conditions. The desiccant wheel surface area of the process and regeneration sides is 0.415 ft^2.

Design conditions:

- Altitude: 5675 ft (barometric pressure 12.0 psi)

- Process inlet:
  Mass flow rate: 18.7 lbm/min
  Temperature: 75 °F
  Humidity ratio: 92 gr/lbm

- Regeneration inlet:
  Mass flow rate: 9.3 lbm/min
  Temperature: 200 °F
  Humidity ratio: 129 gr/lbm

To facilitate the completion of the activity the following set of tables are given to be fill out. Information on the desiccant wheel performance at standard conditions will be provided as it is requested.

PROCESS SIDE

Table 1A. Coefficients for Equation (2)

	Actual Face Velocity	**Pressure Drop ΔP**	**Coefficients**	
	[fpm]	*[in. w.c.]*	C_l	$C_{k,t}$
Set 1				
Set 2				

Table 2A. Prediction of Pressure Drop at Altitude for the Design Conditions

Mass Flow Rate	**Air Density**	**Actual Face Velocity**	**Pressure Drop ΔP**
[lbm/min]	*[lbm/ft^3]*	*[fpm]*	*[in. w.c.]*

REGENERATION SIDE

Table 1B. Coefficients for Equation (2)

	Actual Face Velocity	Pressure Drop ΔP	Coefficients	
	[fpm]	*[in. w.c.]*	C_l	$C_{k,t}$
Set 1				
Set 2				

Table 2B. Prediction of Pressure Drop at Altitude for the Design Conditions

Mass Flow Rate	Air Density	Actual Face Velocity	Pressure Drop ΔP
[lbm/min]	*[lbm/ft^3]*	*[fpm]*	*[in. w.c.]*

1. On a scale from 1 to 10, with one being the hardest and 10 being the simplest, please rate the simplicity of the methodology. Also, please comment on the reason for your rating.

2. Do you have any suggestions that can make this methodology easier to follow? Please elaborate on your comment.

Step-by-Step Procedure to Apply the Methodology for Pressure Drop

Since standard conditions can be used to size the desiccant wheel to operate at altitude, it is assumed that a desiccant wheel has been selected for the application. Therefore, the surface area for the process and regeneration sides are known, and software or performance curves are available. Notice that the following step-by-step procedure must be applied for process and regeneration sides independently.

Units: mass flow rate [lbm/min], density [lbm/ft^3], velocity [fpm], pressure drop [in w.c.], and area [ft^2].

Defining Set 1 to find coefficients C_l and $C_{k,t}$

1. Compute the air density with the design inlet conditions (temperature and humidity ratio) and barometric pressure of 14.7 psi.

2. Compute the actual face velocity using the design mass flow rate, the air density at barometric pressure of 14.7 psi (step 1), and the surface are of the desiccant wheel [$\dot{m} = A\ V\ \rho$].

   Note: since for most of the cases the density to be computed in step 1 will not have a significant variation with respect to the standard density (0.075 lbm/ft^3), for the process side steps 1 and 2 can be avoided and the standard face velocity can be used as actual face velocity.

3. Using manufacturer's performance data find the pressure drop at standard conditions for the design mass flow rate.

Defining Set 2 to find coefficients C_l and $C_{k,t}$

4. Compute the air density at altitude (ρ_z) using the design inlet conditions (temperature and humidity ratio) and the barometric pressure for the altitude of the site.

5. Define a new mass flow rate as

$$\dot{m}_2 = \dot{m}_1 \frac{0.075}{\rho_z}$$

   where $\dot{m}_1$ is the design mass flow rate, 0.075 lbm/ft^3 is the standard density, and ρ_z is the air density at altitude for the design conditions (step 4).

6. Compute the actual face velocity using $\dot{m}_2$, the computed density at standard barometric pressure of 14.7 psi (step 1), and the surface area of the desiccant wheel [$\dot{m} = A\ V\ \rho$].
   Note: be sure to use the density from step 1 and not from step 4.

7. Using manufacturer's performance data find the pressure drop at standard conditions for $\dot{m}_2$.

Finding coefficients C_l and $C_{k,t}$

8. Using the actual face velocity and pressure drop from Set 1 (velocity - step 2 and pressure drop - step 3) and Set 2 (velocity - step 6 and pressure drop - step 7), find the coefficients C_l and $C_{k,t}$ as

$$C_l = \frac{\Delta P_1\ V_2^2 - \Delta P_2\ V_1^2}{(V_1\ V_2^2 - V_1^2\ V_2)}$$

$$C_{k,t} = \frac{\Delta P_2 - C_l V_2}{0.075 V_2^2}$$

Actual face velocity at altitude

9. Using the air density at altitude (step 4) and the design mass flow rate compute the actual face velocity at altitude $[\dot{m} = A V \rho]$.

Pressure drop at altitude

10. Using the actual face velocity at altitude V_z (step 9), the air density at altitude (step 4), and the coefficients C_l and $C_{k,t}$ (step 8) compute the pressure drop at altitude as

$$\Delta P_z(V_z) = C_l V_z + C_{k,t} \rho_z V_z^2$$

Graduate Student Activity #1

Methodology for Pressure Drop through the Wheel

Pressure drop (ΔP) through a honeycomb matrix as a function of actual face velocity (V) and density (ρ) can be well represented as a second order polynomial of the form

$$\Delta P(V) = C_l\, \rho\, V^2 + C_{k,t}\, V \tag{1}$$

where the coefficients C_l and $C_{k,t}$ are specific for each desiccant wheel, which account for geometric parameters of the desiccant wheel and thermophysical properties of the air.

By knowing two different sets of actual face velocity and pressure drop, the coefficients C_l and $C_{k,t}$ can be found by simply solving the system of equations. When keeping the mass flow rate constant, and with the coefficients known, the pressure drop at altitude (ΔP_z) can be calculated as

$$\Delta P_z(V_z) = C_l\, \rho_z\, V_z^2 + C_{k,t}\, V_z \tag{2}$$

where V_z and ρ_z are the actual face velocity and air density at altitude for the design mass flow rate, respectively.

Due to viscous effects of temperature, coefficients C_l and $C_{k,t}$ must be found for process (low temperatures) and regeneration (high temperatures) independently.

For simplicity, Equations (3) and (4) have been provided so that the coefficients can be solved for directly

$$C_l = \frac{V_1\, \Delta P_2 - V_2\, \Delta P_1}{0.075\, (V_1\, V_2^2 - V_1^2\, V_2)} \tag{3}$$

$$C_{k,t} = \frac{\Delta P_1 - 0.075\, C_l\, V_1^2}{V_1} \tag{4}$$

where subscript 1 and 2 refer to the two sets of actual face velocity and pressure drop obtained as described below.

Set 1:

- Mass flow rate equal to the design mass flow rate.
- Velocity equal to the actual face velocity for the design mass flow rate and air density computed at standard barometric pressure for sea level (14.7 psi). $[\dot{m} = A\, V\, \rho]$
- Pressure drop equal to the pressure drop given by manufacturer's performance data at standard conditions for the design mass flow rate.

Set 2:

- Mass flow rate computed as

$$\dot{m}_2 = \dot{m}_1\, \frac{0.075}{\rho_z} \tag{6}$$

where $\dot{m}_1$ is the design mass flow rate (mass flow rate of Set 1), and ρ_z is the air density at altitude for the design conditions.

- Velocity equal to the actual face velocity for the mass flow rate obtained using Equation (6) and air density computed at standard barometric pressure for sea level (14.7 psi). [$\dot{m} = A\ V\ \rho$].
- Pressure drop equal to the pressure drop given by manufacturer's performance data at standard conditions for $\dot{m}_2$.

A step-by-step procedure on how to apply the methodology is given at the end of this document.

Activity for the Evaluation of the Methodology

Estimate the pressure drop through a desiccant wheel at the process and regeneration sides for the giving design conditions. The desiccant wheel surface area of the process and regeneration sides is 0.415 ft^2.

Design conditions:

- Altitude: 5675 ft (barometric pressure 12.0 psi)

- Process inlet:
  Mass flow rate: 18.7 lbm/min
  Temperature: 75 °F
  Humidity ratio: 92 gr/lbm

- Regeneration inlet:
  Mass flow rate: 9.3 lbm/min
  Temperature: 200 °F
  Humidity ratio: 129 gr/lbm

Information on densities and desiccant wheel performance at standard conditions will be provided as it is requested.

Step-by-Step Procedure to Apply the Methodology for Pressure Drop

Since standard conditions can be used to size the desiccant wheel to operate at altitude, it is assumed that a desiccant wheel has been selected for the application. Therefore, the surface area for the process and regeneration sides are known, and software or performance curves are available. Notice that the following step-by-step procedure must be applied for process and regeneration sides independently.

Defining Set 1 to find coefficients C_l and $C_{k,t}$

1. Compute the air density with the inlet conditions (temperature and humidity ratio) and barometric pressure of 14.7 psi.

2. Compute the actual face velocity using the design mass flow rate, the computed density (step 1), and the surface are of the desiccant wheel [$\dot{m} = A\ V\ \rho$].

Note: since for most of the cases the density to be computed in step 1 will not have a significant variation with respect to the standard density (0.075 lbm/ft^3), for the process side steps 1 and 2 can be avoided and the standard face velocity can be used as actual face velocity.

3. Using manufacturer's performance data find the pressure drop at standard conditions for the design mass flow rate.

Defining Set 2 to find coefficients C_l and $C_{k,t}$

4. Compute the air density at altitude (ρ_z) using the inlet conditions (temperature and humidity ratio) and the barometric pressure for the altitude of the site.

5. Define a new mass flow rate using Equation (6) $\left[\dot{m}_2 = \dot{m}_1 \frac{0.075}{\rho_z}\right]$.

6. Compute the actual face velocity using $\dot{m}_2$, the computed density at standard barometric pressure of 14.7 psi (step 1), and the surface area of the desiccant wheel [$\dot{m} = A\ V\ \rho$].

7. Using manufacturer's performance data find the pressure drop at standard conditions for $\dot{m}_2$.

Finding coefficients C_l and $C_{k,t}$

8. Using the actual face velocities and pressure drop from Set 1 and Set 2, find coefficients C_l and $C_{k,t}$ using Equations (3) and (4).

Actual face velocity at altitude

9. Using the air density at altitude (step 4) and the design mass flow rate compute the actual face velocity at altitude.

Pressure drop at altitude

10. Apply Equation (2) using the actual face velocity at altitude (step 9) and the coefficients C_l and $C_{k,t}$ (step 8).

Graduate Student Activity #2

For this activity there were six different design conditions evaluated: three different locations with two desiccant wheels for each location. The locations are outlined below, and the design conditions were taken from Chapter 14 of the 2009 ASHRAE Handbook – Fundamentals [7] for the annual 1% for dehumidification.

- Colorado Springs Municipal Airport, Colorado Springs, CO
- Casper/Natrona County International Airport, Casper, WY
- Amarillo International Airport, Amarillo, TX

The software provided by RotorSource [25] (DSELECT) was used for the activity. The two models and flow rates used were the *PPS 550 x 200*, 800 scfm (60 lbm/min) and the *PPS 770 x 400*, 2000 scfm (150 lbm/min).

Shown below is one example of the activity.

SOLID DESICCANT DEHUMIDIFIER SELECTION AT ALTITUDE

As a part of the ASHRAE research project 1339-TRP, "Selection of Desiccant Equipment at Altitude", Mississippi State University and the National Renewable Energy Laboratory have collaborated together in collecting performance data for a selected desiccant dehumidifier. The results of these tests have been used to develop simple methodologies that can be applied to any desiccant dehumidification unit in order to predict its performance at any altitude. In order to do this, the performance at standard conditions (sea-level) must be used. Since these performance parameters are readily available from any manufacturer, the methodologies can be easily used.

Part of the project is the task "Ease of Use Confirmation." In this task, we need to verify that the developed methodology is straightforward and easy to use. Therefore, for this activity we are asking you to apply the methodologies developed to estimate the performance of solid desiccant dehumidifiers. You will find the methodologies in Appendix A. The system and design conditions are given, and when required, the performance at standard conditions can be obtained from the software described in Appendix B. To simplify the computations of density and partial pressure of water vapor required to make some calculations, an Excel file is provided.

System:

A general desiccant system is sketched in the figure below. The system will be used to dehumidify outside air (ventilation air) with design conditions obtained from Chapter 14 of the 2009 ASHRAE Handbook – Fundamentals. These design conditions are outlined below. The model of the dehumidifier used for these design conditions is the *PPS 550 x 200*, where the 550 defines the diameter of the wheel (mm) and the 200 defines the thickness (depth) of the wheel (mm).

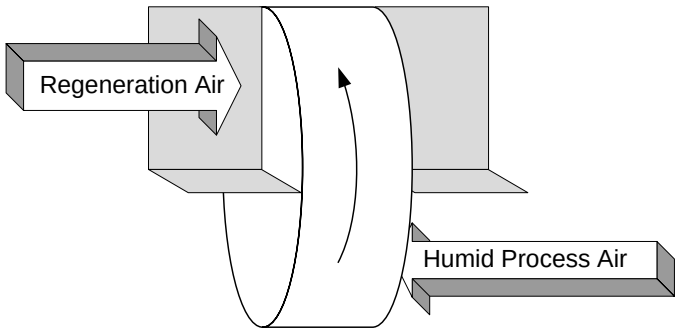

Design Conditions:

Site: Colorado Springs Municipal Airport, Colorado Springs, CO
Altitude: 6,171 ft
Dehumidifier model: *PPS 550 x 200*

Process stream:
Dry Bulb Temperature: 65.4°F
Humidity Ratio: 90.2 Gr/lbm[1]
Volume flow rate: 800 scfm (60 lbm/min)

Regeneration stream:
Dry Bulb Temperature: 65.4°F (before heater), heated to 248°F (Low, Indirect Heat)
Humidity Ratio: 90.2 Gr/lbm
Volume flow rate: (given by RotorSource software)

Results

Complete the following table to present your results and attach to this document all material that justifies your results (sheets with computations, print out of software used, etc.)

Moisture Removal Capacity			lbm/hr
Regeneration Specific Heat Input			BTU/lbm
Process Stream Temperature Rise			°F
Pressure Drop through the Wheel	Process		in W.C.
	Regeneration		

[1] The conversion of grains to pounds of water vapor is 7000 Gr = 1 lbm.

Comments

Please comment on the methodologies. We would like to know if you consider that the methodologies are simple enough to follow, particularly for the MRC and pressure drop through the wheel.

Participant: _____

Affiliation: _____

Thank you very much for your participation!

APPENDIX A

Methodologies

Moisture Removal Capacity

The moisture capacity of a desiccant is a direct function of the partial pressure of water vapor in the air. Therefore, an estimation for the MRC at altitude was derived using the difference in partial pressures between standard conditions and altitude. This equation can be seen in Equation (1).

$$MRC_z = \frac{MRC_0}{1+\Delta p_w} \tag{1}$$

where:

MRC_z	=	Estimated MRC at altitude, *[lbm/hr]*
MRC_0	=	Rated MRC at Standard Conditions, *[lbm/hr]*
Δp_w	=	Difference in partial pressure between standard conditions and altitude, *[psi]*

Regeneration Specific Heat Input

By definition, RSHI is the ratio of the energy supplied for regeneration to the MRC. By understanding that the energy supplied for regeneration will remain constant over different altitudes as long as the mass flow rate and raise in temperature remain constant, it can be seen that the RSHI will change inversely proportional to the change in MRC. This can be done by applying the methodology used for the MRC to the equation for RSHI. The resulting RSHI at altitude can be seen in Equation (2).

$$RSHI_z = (1 + \Delta p_w) RSHI_0 \tag{2}$$

where:

$RSHI_z$	=	Estimated RSHI at altitude, *[BTU/lbm]*
$RSHI_0$	=	Rated RSHI at Standard Conditions, *[BTU/lbm]*
Δp_w	=	Difference in partial pressure between standard conditions and altitude, *[psi]*

Process Stream Temperature Rise

Due to the effects of air properties on the heat and mass transfer, a simple methodology could not be developed without the use of complex mathematical models. Also, experimental results show that the difference in process outlet temperature between sea-level and altitude is quite low. Therefore, the change in process outlet temperature between standard conditions and altitude can be considered negligible.

Pressure Drop through the Wheel

The pressure drop (ΔP) through a honeycomb matrix is known to be a function of density and actual face velocity. Based on our analysis, since the actual velocity is calculated based on the ratio of the densities, and the only thing in the density calculation that change is the atmospheric pressure, the pressure drop at altitude can be estimated based on the ratio of the atmospheric pressures, as shown in Equation (3):

$$\Delta P_z = \Delta P_0 \frac{\rho_o}{\rho_z} \tag{3}$$

where ΔP_0 is the pressure drop found at standard conditions, ρ_o is the density computed at the inlet temperature and humidity ratio with the standard atmospheric pressure (14.7 psi), and ρ_z is the density computed at the inlet conditions but at the barometric pressure of the site (altitude). Since the regeneration temperature is quite high, it is important to compute $\rho_o$at the regeneration inlet conditions and not at the standard density of 0.075 lbm/ft^3.

APPENDIX B

RotorSource Software Information

RotorSource Software Download Link:
http://www.nature-cool.com/RS/DSelect371.zip

In order to run this software, the required inputs are:

- Model (Wheel Size)
  - Wheel Depth
- Process Inlet Conditions
  - Standard Volumetric Flow Rate, *[scfm]*
  - Dry-Bulb Temperature, *[°F]*
  - Humidity Ratio, *[Gr/lbm]*
- Reactivation Inlet
  - Dry-Bulb Temperature, *[°F]*
  - Humidity Ratio, *[Gr/lbm]*
  - Indirect/Direct Heat
  - Low (248°F), Medium (284°F), or High (320°F) Heat

Once these inputs have been considered, the **Calc** button can be pressed to obtain the results.

The outputs of importance are the MRC, RSHI, pressure drops through the wheel, and process outlet temperature. The MRC is given under the diagram of the wheel, and shows units of **lb/h**. The RSHI is directly below the MRC, with units of **BTU/lb**. Directly above the MRC is the Process Pressure Drop, with units of **in. WC**. Above the diagram of the wheel is the Regeneration Pressure Drop, also with units of **in. WC**. The Process Outlet Temperature is given in the area designated **Process Outlet**, and has units of **°F DB**.

SOLID DESICCANT DEHUMIDIFIER SELECTION AT ALTITUDE

As part of the ASHRAE research project 1339-TRP, "Selection of Desiccant Equipment at Altitude," Mississippi State University (MSU) would like to ask for your participation in the validation and ease of use confirmation of the developed methodology. The objective of the research project is to develop a simple methodology for the selection of solid desiccant dehumidifiers to operate at altitude using the manufacturer's performance data at standard conditions. The methodology has been developed based on experimental data obtained from tests conducted at MSU and the National Renewable Energy Laboratory (NREL).

For your participation we are asking you to predict the performance of a desiccant wheel at standard conditions and for an altitude of 5,675 ft:

- using your proprietary methodology
- using the developed methodology.

Figure 1 illustrates the schematic of the dehumidifier used in the tests. It has dimensions of 320 mm in diameter and 100 mm in width, a process/regeneration ratio of 0.5, a rotational speed of 14 rpm, and area of 0.415 ft^2. However, for the performance predictions, although a similar wheel may be helpful to verify the experimental results, the proposed methodology should apply to any desiccant wheel.

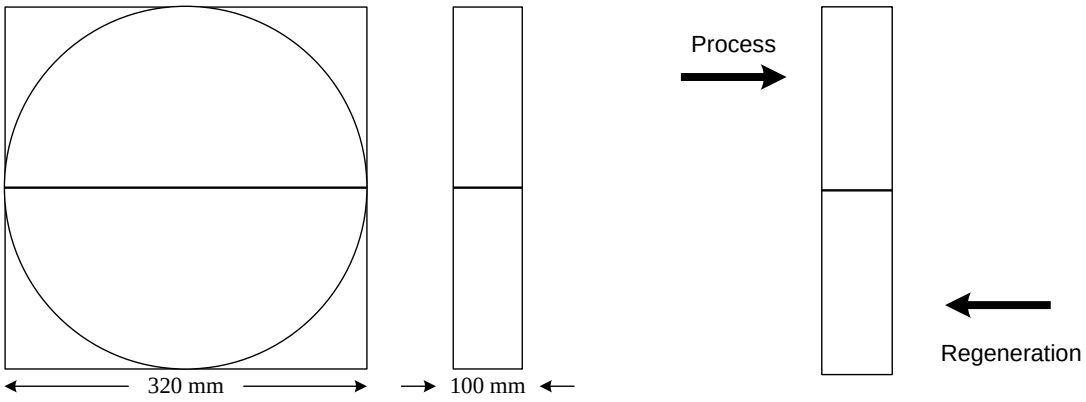

Figure 1: Desiccant Wheel Size and Flow Configuration.

The design inlet air conditions to predict the performance are given in Table 1. For your consideration we have prepared tables to record your results. The results at standard conditions can be recorded on Table 2, while the results at altitude using your proprietary methodology and the methodology developed by MSU can be recorded in Tables 3 and 4, respectively.

Table 1: Design Conditions at 5675 ft Altitude.

Conditions		Temperature	Humidity Ratio	Mass Flow
		[°F – db]	*[gr/lbm]*	*[lbm/min]*
1A	P	75.0	79	18.7
2A	P	75.0	92	18.7
3A	P	75.0	106	18.7
4A	P	65.0	92	18.7
5A	P	55.0	64	18.7
1A-5A	R	200.0	129	9.3
1B	P	75.0	79	12.5
2B	P	75.0	92	12.5
3B	P	75.0	106	12.5
4B	P	65.0	92	12.5
5B	P	55.0	64	12.5
1B-5B	R	200.0	129	6.2
1C	P	75.0	79	15.2
2C	P	75.0	92	15.2
3C	P	75.0	106	15.2
4C	P	65.0	92	15.2
5C	P	55.0	64	15.2
1C-5C	R	200.0	129	7.6

P: Process
R: Regeneration

Table 2: Results Using Standard Conditions.

Test ID	Altitude	Process Out		MRC	Wheel Pressure Drop	
		Humidity Ratio	Temperature		Process	Regen.
	[ft]	*[gr/lbm]*	*[°F]*	*[lbm/hr]*	*[in w.c.]*	*[in w.c.]*
1A	**0**					
2A	**0**					
3A	**0**					
4A	**0**					
5A	**0**					
1B	**0**					
2B	**0**					
3B	**0**					
4B	**0**					
5B	**0**					
1C	**0**					
2C	**0**					
3C	**0**					
4C	**0**					
5C	**0**					

Table 3: Results for Altitude Using Manufacturer's Methodology.

Test ID	Altitude	Process Out		MRC	Wheel Pressure Drop	
		Humidity Ratio	Temperature		Process	Regen.
	[ft]	*[gr/lbm]*	*[°F]*	*[lbm/hr]*	*[in w.c.]*	*[in w.c.]*
1A	**5675**					
2A	**5675**					
3A	**5675**					
4A	**5675**					
5A	**5675**					
1B	**5675**					
2B	**5675**					
3B	**5675**					
4B	**5675**					
5B	**5675**					
1C	**5675**					
2C	**5675**					
3C	**5675**					
4C	**5675**					
5C	**5675**					

Methodology Developed by MSU as Part of the ASHRAE Project 1339-TRP

This methodology has been developed to aid end users and design engineers alike in selecting desiccant dehumidifiers for use at altitude (non-standard conditions). In order to select a desiccant dehumidifier, the entering conditions of the air for both the process and regeneration air streams must be known. When using this methodology, the following parameters must be known for the location (altitude), and these are kept constant when determining the standard performance:

- Process Inlet Mass Flow Rate
- Process Inlet Dry-Bulb Temperature
- Process Inlet Humidity Ratio
- Regeneration Inlet Mass Flow Rate
- Regeneration Inlet Dry-Bulb Temperature
- Regeneration Inlet Humidity Ratio

By keeping these six parameters constant, this methodology can be followed in order to predict altitude performance of any solid desiccant dehumidifier, as long as the standard performance for the dehumidifier is available.

1. Moisture Removal Capacity (MRC)

From the experimental data, it was found that the MRC fluctuates between sea-level and NREL's altitude (5,765 ft) around 4% to 5%, with the MRC decreasing with altitude. Since the moisture capacity of a desiccant is a direct function of the partial pressure of water vapor in the air, an estimation for the MRC at altitude was derived using the difference in partial pressures between standard conditions and altitude. This equation can be seen in Equation (1).

$$MRC_z = \frac{MRC_0}{1+\frac{\Delta p_w}{psi}} \tag{1}$$

where:

MRC_z	=	Estimated MRC at altitude, *[lbm/hr]*
MRC_0	=	Rated MRC at Standard Conditions, *[lbm/hr]*
Δp_w	=	Difference in partial pressure between standard conditions and altitude, *[psi]*

2. Regeneration Specific Heat Input (RSHI)

By definition, RSHI is the ratio of the energy supplied for regeneration to the MRC. By understanding that the energy supplied for regeneration will remain constant over different altitudes as long as the mass flow rate and raise in temperature remain constant, it can be seen that the RSHI will change inversely proportional to the change in MRC. This can be done by applying the methodology used for the MRC to the equation for RSHI. The resulting RSHI at altitude can be seen in Equation (2).

$$RSHI_z = \left(1 + \frac{\Delta p_w}{psi}\right) RSHI_0 \tag{2}$$

where:

$RSHI_z$	=	Estimated RSHI at altitude, *[BTU/lbm]*
$RSHI_0$	=	Rated RSHI at Standard Conditions, *[BTU/lbm]*

3. Pressure Drop Through the Wheel

The pressure drop (ΔP) through a honeycomb matrix is known to be a function of density and actual face velocity. Based on our analysis, since the actual velocity is calculated based on the ratio of the

densities, and the only thing in the density calculation that change is the atmospheric pressure, the pressure drop at altitude can be estimated based on the ratio of the atmospheric pressures, as shown in Equation (3):

$$\Delta P_z = \Delta P_0 \frac{\rho_o}{\rho_z} \tag{3}$$

where ΔP_0 is the pressure drop found at standard conditions, ρ_o is the density computed at the inlet temperature and humidity ratio with the standard atmospheric pressure (14.7 psi), and ρ_z is the density computed at the inlet conditions but at the barometric pressure of the site (altitude). Since the regeneration temperature is quite high with respect to the temperature at standard conditions, it is important to compute ρ_o at the regeneration inlet conditions and not use the standard density of 0.075 lbm/ft^3.

4. Process Outlet Dry-Bulb Temperature

The variation in temperature in a dehumidification process is mainly due to the latent heat of vaporization from the mass transfer process; in other words, it is associated with the grain depression through the wheel. Due to the effects of air properties on the heat and mass transfer, a simple methodology could not be developed without the use of complex mathematical models. Also, experimental results show that the difference in process outlet temperature between sea-level and altitude is quite low, with a maximum variation of the process outlet temperature between both locations being around 2.5%. Therefore, the change in process outlet temperature between standard conditions and altitude can be considered negligible.

Feedback

After completing Table 4, it will be very helpful if you can provide some comments that may help improving the proposed methodology. (Please, feel free to use additional pages as needed).

Table 4: Results for Altitude Using MSU's Methodology.

Test ID	Altitude	Atmospheric Velocity		Process Out		MRC	Wheel Pressure Drop	
		Process	Regen.	Humidity Ratio	Temperature		Process	Regen.
	[ft]	*[Afpm]*	*[Afpm]*	*[gr/lbm]*	*[°F]*	*[lbm/hr]*	*[in w.c.]*	*[in w.c.]*
1A	**5675**							
2A	**5675**							
3A	**5675**							
4A	**5675**							
5A	**5675**							
1B	**5675**							
2B	**5675**							
3B	**5675**							
4B	**5675**							
5B	**5675**							
1C	**5675**							
2C	**5675**							
3C	**5675**							
4C	**5675**							
5C	**5675**							